Hydrogen-producing ability and its ecophysiological roles in vibrios

(ビブリオ属細菌の水素生産能とその生理生態学的役割)

北海道大学大学院水産科学院

海洋応用生命科学専攻

Graduate School of Fisheries Sciences

Division of Marine Life Science

松村　佑太

Yuta Matsumura

2018 (平成 30 年)

CONTENTS

CHAPTER I
General introduction

Increasing global energy demand is the biggest problem consisting of environmental, economical, and political issues. Despite the impressive growth in alternative energy sources, most global energy demand is still covered by fossil fuels. Global energy demand is predicted to grow at an average rate of 1.2% from 2008 to 2035, and the total energy supply will be at least double around 2050 [International Energy Agency, World Energy outlook 2013. http://www.worldenergyoutlook.org/pressmedia/recentpresentations/LondonNovember12.pdf]. However, the reserve-production ratio of fossil fuels, such as oil, natural gas, and coal are predicted to be 52.5, 54.1 and 110 years, respectively [BP Statistical Review of World Energy June 2015. http://www.bp.com/content/dam/bp/pdf/energy-economics/statistical-review-2015 /bp-statistical-review-of-world-energy-2015-full-report.pdf]. In addition, fossil fuels produce carbon dioxide, one of the primary greenhouse gases (GHG) during combustion. Therefore, fossil fuels are not a viable option in solving the world's energy problems.

Renewable energy, such as hydro-, wind-, and solar-power, geothermal heat, and biofuels has been rapidly introduced across the world in the 21st century with a view to reducing GHG emissions and increasing energy security. Among these renewable energy sources, hydrogen (H_2) energy appears to be a major primary energy source because of its unique advantages. H_2 possess a high energy contents of 122 kJ/g, which is 2.75 times greater than hydrocarbon fuels [Kapdan and Kargi, 2006], and the only byproduct from its combustion is pure water. In addition, H_2 can be directly used to produce electricity through fuel cells. Until now, H_2 have been used in the industrial processes to hydrogenate heavy oil, foods, and ammonia for fertilizer [Energy Information Administration, The Impact of Increased Use of Hydrogen on Petroleum Consumption and Carbon Dioxide Emissions 2008. https://www.eia.gov/analysis/requests/2008/sroiaf(2008)04.pdf]. Furthermore, H_2 is an ideal electron donor in the reduction of oxidized water pollutants such as nitrate, perchlorate, and selenite [Rittmann *et al*., 2007]. In contrast to the attractive advantages of H_2 as energy carrier and industrial feedstock, 96% of H_2 produced in the world comes from fossil fuels including 48% from natural gas stream reforming, 30% from naphtha/oil reforming in the chemical industry, and 18% from coal gasification [Abánades *et al*., 2013]. Therefore, there is great possibility that renewable resources such as biomass can be used for H_2 production.

H_2 produced via biological processes such as fermentation, photosynthesis, and microbial fuel cells, has been recognized as a renewable and carbon-neutral energy source in the future.

Among these methods, fermentative H_2 production has predominantly attracted a lot of interest because of the magnitude order of H_2 production rate compared to other methods, the applicability of wide range and complex forms of organic substrates, and its simple system construction [Sinha *et al*., 2011]. In our laboratory, brown macroalgae (seaweed) has been used as an ideal resource for biofuel production because of its high sugar content without lignin. The sugars in brown macroalgae mainly consist of alginate, mannitol, laminaran, and fucoidan [Obluchinskaya, 2008], and these sugars can be released easily by simple operations such as milling or crushing. Among these sugars, mannitol is the primary storage compound produced by photosynthesis and can account for 20-30% dry weight in some *Laminaria* species [Zubia *et al*., 2008; Rousvoal *et al*., 2011]. In addition, it is proposed that seaweed has further advantages as a biomass resource; 1) higher mass productivity (13.1 kg dry weight/m^2/7 months) than sugar cane (6.1–9.5 kg fresh weight/m^2/year) [Kraan, 2013] and 2) lower requirements of nutrients and fresh water [Horn *et al*., 2000a]. Although utilization of alginate is a major challenge especially for ethanol production due to the issue of redox balance, previous studies reported that this has been already achieved by alginate-metabolizing bacteria and metabolic engineering [Hashimoto *et al*., 2010; Wargacki *et al*., 2012].

To achieve successful energy production via fermentation, acquisition or development of suitable microbial biocatalysts is the primary issues. However, high sodium (Na^+) concentration had negative effects on the H_2 productivity of *Enterobacter aerogenes* and *Clostridium* species [Kim *et al*., 2009; Lee *et al*., 2012; Tanisho, 2011]. In screenings of effective biofuel producers from seaweed carbohydrates even under saline conditions, we succeeded in isolating H_2-producing bacteria from the gut of sea hare (*Aplysia kurodai*) [Sawabe *et al*., 2013]. The bacterial strain was determined as novel species assigned to the genus *Vibrio* on the basis of polyphasic taxonomic approaches. The family *Vibrionaceae* currently comprises of a total of more than 170 species with valid nomenclature [Association of Vibrio Biologists website, http://www.vibriobiology.net/]. Although the H_2 production phenotype has so far been experimentally confirmed in at least 11 species of vibrios with valid nomenclature, the H_2 productivity, the gene regulation and the ecophysiological role of H_2 production in vibrios have not been fully described yet. In this study, the author attempts to reveal the H_2 production ability and its mechanism in *Vibrio tritonius* AM2.

In CHAPTER II, I examine the availability of marine vibrios for H_2 production from seaweed biomass. To evaluate the H_2 production ability of *V. tritonius* AM2, the culture condition was optimized regarding culture pH and temperature with glucose or mannitol as carbon sources. Furthermore, we tried to conduct 3 L scale-batch culture experiments using powdered brown

macroalgae under the pre-determined optimum conditions. Fortunately, the H_2 producing ability of *V. tritonius* AM2 was high enough to conduct deeper studies in elucidating the H_2-producing mechanism in marine vibrios. The genetic organization responsible for H_2 production and the transcriptional pattern is described in CHAPTER III. We sequenced and analyzed the *V. tritonius* genome. Interestingly, the *V. tritonius* genome was found to encode unique genes cluster responsible for H_2 production. In CHAPTER V, to understand the H_2 production mechanism of *V. tritonius* from genomic and transcriptomic insight, we further investigate the H_2 producing ability of vibrios. We newly obtained draft genome sequences of the other H_2 producing *Vibrio* species. Comparative genomics was performed with the aim of finding the important genetic factors regulating H_2 producing ability. Furthermore, the genome sequencing of marine vibrios provides an opportunity to understand the ecophysiological role of H_2 production in vibrios.

CHAPTER II

Enhanced hydrogen production in a newly described heterotrophic marine bacterium, *Vibrio tritonius* AM2, from seaweed as a feedstock

ABSTRACT

In order to achieve more stable H_2 production from non-food feedstock, stable feedstock preparations of marine biomass and development of an efficient H_2 system using marine bacteria under saline conditions are two important key technologies that need to be developed. *V. tritonius* AM2 isolated from a gut of a marine invertebrate was cultured under various conditions in marine broth (at initial 2.25% (w/v) NaCl) supplemented with mannitol, a seaweed carbohydrate, to evaluate its hydrogen productivity. The maximum molar yield of H_2 was recorded as 1.7 mol H_2/mol mannitol at pH 6 and 37°C. The mannitol-grown cells showed a higher yield of H_2 than the glucose-grown cells in the pH range 5.5-7.5. Compared to glucose, mannitol was considered to be a more suitable substrate for H_2 production of the strain AM2. Fermentation product profiling indicated that the strain AM2 use the formate hydrogen lyase for H_2 production. Furthermore, the strain AM2 was able to produce H_2 from powdered brown macroalgae containing 31.1% dry weight of mannitol. The molar yield of H_2 reached 1.6 mol H_2/mol mannitol contained in the seaweed feedstock. In conclusion, the strain AM2 was found to have the ability for high-yield H_2 production from mannitol even under saline conditions.

INTRODUCTION

The World Energy Outlook 2013 [International Energy Agency, World Energy outlook 2013. http://www.worldenergyoutlook.org/pressmedia/recentpresentations/LondonNovember12.pdf] summarized that the orientation of global energy sectors is currently shifting drastically resulting in many major importers becoming exporters and the former exporter countries are now becoming leading centers of global demand growth. Apparently, there is an urgent need for a quest of alternative global energy sources to abrogate the dependence on finite fossil fuels which are also implicated in environment pollution and climatic change. H_2 is cited as one potential candidate with several socio-economic, technological and environmental benefits [Das, 2009]. It is known to offer a major advantage over hydrocarbon fuels as its combustion yields a comparatively higher energy of 2.75 times (122 kJ/g) without the emission of CO_2 and can be directly used to power fuel cells [Kapdan and Kargi, 2006; Lee *et al*., 2010]. This extremely clean valuable energy carrier also serves as an important feedstock in some industries, useful in detoxifying a wide range of water pollutants and is largely used in fertilizers and petroleum

industries [Kapdan and Kargi, 2006; Lee *et al*., 2010; Kotay and Das, 2008].

Rising energy cost scenarios in many countries have accelerated research being done locally and/or internationally to find an energy boost to their economies. Lucrative H_2 fuel alternative is predicted to be a notable contributor to the total energy market providing up to 10% by 2025 [Armor, 1999] and a preferable choice of domestic energy resource to be used in all economic sectors and regions of the world [Kotay and Das, 2008]. H_2 and oxygen are electrochemically recombined in fuel cells to deliver clean electricity and heat efficiently. Thus, it is unavoidable to notice that demand on hydrogen as energy source is closely linked to an encouraging trend of fuel cell technology. Considering the fuel cell industry alone, roughly 30,000 fuel cells systems were shipped from the United State with monetary revenues expected to reach USD785 million in 2012 [U.S. Department of Energy, 2012 Fuel cell technologies market report. file:///E:/PhD/2012_market_report.pdf]. Both the US Department of Energy and Fuel Cells Commercialization Conference Japan reported development in multidisciplinary researches has significantly reduced production costs which in turn lead to greater profitability.

However, acquiring a sustainable alternative energy source is a daunting task. Currently, the establishment of a H_2 energy economy cannot be fully realized in a sustainable way. Despite its attractive advantages, conventional technologies of H_2 production are still heavily dependent on reformation of fossil fuels and most processes require intensive energy with high temperatures (>850°C) [Kapdan and Kargi, 2006]. This means in practice that the majority of H_2 production is not conducted in a renewable and environmentally friendly way which contradicts the initial purpose of its application. Development of renewable technologies is becoming the bottleneck in many conventional methods of H_2 production including the most sustainable approach of steam reforming and electrolysis [Kapdan and Kargi, 2006; Armor, 1999; Kim, 2003]. For instance, electrolysis approach suffers from two drawbacks i.e. only approximately 65% of the energy is efficiently captured using the latest technologies, and, high electrical capacity is needed for the process to occur [Hallenbeck, 2009].

Currently, biological processes seem to be the best alternative which utilizes both renewable feedstock and energy [Kim *et al*., 2009]. Biological H_2 production via fermentation is attracting a lot of interest predominantly because the magnitude of H_2 production rate is larger than those achieved by other methods, the applicability of a wide range and complex forms of organic substrates, and the simple system construction [Lee *et al*., 2010; Sinha and Pandey, 2011]. Simultaneously, rapid advances in biofuel industries are greatly advancing the demand for alternative feedstocks which is more likely to be sustainable economically and environmentally. In 2008, 87 gigaliters of liquid biofuels were produced from crops planted for food production

such as corn and sugarcane [Somerville *et a*l., 2010]. The amount of liquid biofuels increased further in 2010 and has directly affected the choices of various feedstocks across different regions of the world [Gasparatos *et al*., 2013] to meet the demands and soothe public concerns over the "food vs fuel" issue. The choices were widened and include cellulosic biomass from agricultural residues or the food industry, carbohydrate rich industrial wastewater and wastewater sludge [Kapdan and Kargi, 2006]. With the same rationale in mind, macroalgae has been in the spotlight as an ideal biomass feedstock for bioH_2 production [Takeda *et al*., 2011; Wargacki *et al*., 2012; Enquist-Newman *et al*., 2013].

Brown macroalgae in particular, possess several advantageous features that can complement the global needs in both food and energy production [Takeda *et al*., 2011; Wargacki *et al*., 2012; Enquist-Newman *et al*., 2013]. Obviously, their marine based cultivation has an edge over any terrestrial biofuel crops in terms of not competing directly for arable land, high rate of productivity [Horn *et al*., 2000a] and it does not require freshwater or fertilizer. Additionally, their lack of lignin, low cellulose and lipid content has made the sugar extraction feasible by simple biorefinery processes such as milling, leaching and crushing [Wargacki *et al*., 2012; Enquist-Newman *et al*., 2013]. Also, high carbohydrate and sugar contents underpin their successful conversion to various gas and liquid fuels. Brown macroalgae have a complex composition and breakdown of all components points to efficient H_2 production. However, the composition of brown macroalgae varies considerably between species, seasonal changes and habitat [Horn *et al*., 2000a]. Generally, alginate forms the major structural complex of brown macroalgae and its utilization, previously recognized as the greatest challenge on biological ethanol production, has already been achieved using the metabolically engineered *Escherichia coli* [Enquist-Newman *et al*., 2013] and alginate-metabolizing *Sphingomonas* sp. [Wargacki *et al*., 2012]. Alternatively, mannitol which is also the most abundant storage component can be extracted from milled macroalgae relatively easier than alginate [Horn *et al*., 2000]. This primary stored sugar can account for 20-30% of the dry weight in some *Laminaria* species [Zubia *et al*., 2008; Rousvoal *et al*., 2011; Wang *et al*., 2013] and has been successfully used for bioethanol production [Horn *et al*., 2000a; Wang *et al*., 2013; Horn *et al*., 2000b].

The backbone of a successful fermentative process is the acquisition of good host microorganisms [Das, 2009]. At present, high sodium (Na^+) concentration that has been reported to adversely affected the H_2 productivity of *Enterobacter aerogenes* and *Clostridium* species [Kim *et al*., 2009; Lee *et al*., 2012; Tanisho, 2011] and mannitol which is not readily fermented [Horn *et al*., 2000b] require a more dynamic strain for efficient H_2 production. In a recent screening of effective H_2 producers from seaweed carbohydrates under saline conditions, a

newly described facultative anaerobic marine bacterium, *V. tritonius* AM2, was isolated from the gut of sea hare (*Aplysia kurodai*) [Sawabe *et al*., 2013; Gomez-Gil *et al*., 2014]. Batch culture experiments without pH control showed that H_2 production was observed on the glucose- and mannitol-grown cells, but unfortunately the strain AM2 does not use alginate as a substrate. Since vibrios are phylogenetically related to *Enterobacteriaceae* [Ruimy *et al*., 1994; Gomez-Gil *et al*., 2014], such as *E. coli* and *En. aerogenes*, it is interesting to compare their metabolic pathways, with particular interest in the H_2-producing pathway. H_2 production of the enterobacteria is commonly achieved by formate hydrogen lyase (FHL) producing H_2 and carbon dioxide (CO_2) through formate oxidation [Axley *et al*., 1990; Böck and Sawers, 1996; Sawers, 1994; Sawers, 2004].

The majority of studies on fermentative H_2 production have been on *Clostridium* [Taguchi *et al*., 1996; Levin *et al*., 2006] as a representative of strict anaerobes, and *E. coli* [Yoshida *et al*., 2006; Maeda *et al*., 2007] and *En. aerogenes* [Tanisho, 2011; Nakashimada *et al*., 2002] representing the facultative anaerobes. Research focusing on H_2-producing marine vibrios has not yet been undertaken. Therefore, research on H_2 producer marine vibrios living in environments rich in seaweed carbohydrates under saline conditions is noteworthy. Herein, the author reports unexpectedly higher H_2 productivity of marine vibrio from glucose and mannitol even under saline conditions. Furthermore, 3 L scale-batch culture experiments with the aim of practical H_2 production were conducted using powdered brown macroalgae (*Saccharina sculpera*) as feedstock under pre-determined optimum conditions. The ability of *V. tritonius* AM2 utilizing marine biomass under their indigenous environment to produce H_2 has opened up a novel and promising approach to meet increasing energy needs with a view to replacing the current use of fossil fuels.

MATERIALS AND METHODS

Bacterial strain and culture conditions

V. tritonius AM2 was used in this study. The strain AM2 was cultured in marine broth (5% (w/v) polypeptone, 1% (w/v) yeast extract, 100 mM MOPS (Dojindo, Kumamoto, Japan), and 75% (v/v) artificial seawater composed of 30 g/L NaCl, 0.7 g/L KCl, 5.3 g/L $MgSO_4 \cdot 7H_2O$, 10.8 g/L $MgCl_2 \cdot 6H_2O$, and 1.3 g/L $CaSO_4 \cdot 2H_2O$) and/or marine agar (marine broth containing 1.5% agar). Initially, the strain was precultured aerobically in marine broth to achieve a cell density of 1.0±0.1 OD_{620} at 25°C with shaking at 130 rpm (NR-80, TAITEC, Saitama, Japan). The culture condition remained similar throughout the study unless otherwise stated. Later, 1 mL of the preculture strain was added to a 100 mL marine broth containing 5% (w/v) glucose or 5% (w/v)

mannitol which was prepared in a glass bottle reactor. Batch fermentation culture was then conducted using a magnetic stirrer (RO 10 power IKAMAG, IKA, Staufensee, Germany) with gentle mixing. The pH of the culture was maintained at pH 5.5, 6, 6.5 or 7.5 using pH controller (DT-1023P, ABLE, Tokyo, Japan) equipped with an autoclavable electrode (FermProbe pH electrodes, Broadley-James Corp., Branford, USA) by adding 5 N NaOH or HCl. The effects of pH on H_2 production were determined in three replicated cultures. The temperatures of the culture were set at 25°C, 30°C, 37°C and 42°C, respectively, to determine the H_2 production speed. The control culture was made without addition of any sugars in the marine broth.

Assays

The volume of H_2 produced during fermentation was measured upon capture in an aluminum bag using water displacement and gas chromatography (GC8A or GC2014, Shimadzu, Kyoto, Japan) with a thermal conductivity detector and Shincarbon ST column (Shinwa Chemical Industries Ltd., Kyoto, Japan). Extracellular ethanol, formate, acetate and lactate were measured by enzymatic measurement using a F-kit (Roche Diagnostics, Mannheim, Germany). Ethanol produced from seaweed was also measured by enzymatic measurement [Cornell and Veech, 1983] using F-kit and gas chromatography with flame ionization detector and HP-B ALC capillary column (Agilent, California, USA) and He as a carrier gas. Glucose and mannitol concentrations in the medium were measured using phenol-sulfuric acid method [Dubois *et al*., 1956] and HPLC with TSKgel Amide-80 (TOSOH, Tokyo, Japan), respectively. Cell density of the culture was measured as an optical density (OD) at 620 nm using spectrophotometer (Ultrospec 2000, Pharmacia, Sweden). Molar yields of fermentative products including H_2 were analyzed using one-way analysis of variance (ANOVA) with Tukey-Kramer test for multiple comparisons. Probability of less than 5% (P<0.05) was considered statistically significant.

H_2 production from seaweed feedstock by *Vibrio tritonius* AM2

A batch culture experiment using seaweed material as feedstock was also performed to evaluate H_2 productivity of the strain AM2. The powdered brown macroalgae (*Saccharina sculpera*; 30.5% (w/w) alginate, 31.1% (w/w) mannitol, 8.4% (w/w) protein, 1.6% (w/w) lipid, 5.0% (w/w) fiber, 18.9% (w/w) total ash and 4.5% (w/w) others) was kindly provided by Dr. Akihiko Fukushi (Hokkaido Research Organization, Fisheries Research Department, Kushiro Fisheries Research Institute, Kushiro, Japan). In this batch culture experiment, the strain AM2 was cultured in 3 L marine broth adding 300 g of the powdered brown macroalgae using a 5 L jar fermenter (MBE 500ME, Eyela, Tokyo, Japan). The culture was conducted by adding 30 mL of

preculture of strain AM2 which gave 1.0±0.1 OD_{620} cell turbidity.

RESULTS

Effects of pH on cell growth and H_2 production in *Vibrio tritonius* AM2

The H_2 production profiles of strain AM2 were determined using glucose and mannitol (Fig. 1-1). The growth of mannitol-grown cells was always lower than that of glucose-grown cells. The growth of the strain AM2 was higher at pH 7.5 than under slightly acidic conditions (Fig. 1-1A). *V. tritonius* AM2 produced H_2 from glucose and mannitol in the pH range of 5.5-7.5 at 30°C (Fig. 1-1B). The volume of H_2 production at pH 6 from both the glucose- and the mannitol-grown cells peaked at levels of 319 and 285 mmol/L reactor volume (Fig. 1-1B), respectively, but these decreased to 40 to 50% of the maximum values at pH 5.5. At pH 7.5, faint H_2 production was observed. The volumetric H_2 production from mannitol was higher than that from glucose at pH 6.5 and pH 7.5, but showed the opposite results below pH 6 (Fig. 1B).

Calculation of the molar yields of H_2 on both substrates revealed different pictures, when compared to the volume of H_2 production in the strain AM2 (Fig. 1-2). The molar yields of H_2 on mannitol were greater than those on glucose with a statistical significance (P<0.05) at pH range 5.5-6.5, and the culture at pH 5.5 and 6.0 gave the maximum molar yield on both substrates; 1.2 mol H_2/mol glucose and 1.4 mol H_2/mol mannitol. On the other hand, pH dependency on the molar yields of formate, which is a precursor of H_2 on the FHL pathway, showed that there was a countertrend to that of H_2 on both glucose and mannitol (Fig. 1-2).

Effects of temperature on H_2 productivity of *Vibrio tritonius* AM2

To determine the optimum temperature for H_2 production, H_2 production rates of the strain AM2 were measured at pH 6 and the temperature range of 25°C to 42°C (Fig. 1-1C). The results showed that H_2 production rates strongly depended on the temperature of the culture; the maximum production rates of H_2 were observed at 37°C in both the substrate-grown cells showing the production rate of 9.5 and 8.0 mmol/h/L from glucose and mannitol, respectively (Fig. 1-1C). The maximum production rates of H_2 at 37°C on glucose and mannitol were 1.5 and 1.2 times higher than those at 30°C, respectively, and the H_2 production rates from glucose were higher than those from mannitol in the all temperature ranges examined. At 25°C, the difference between glucose and mannitol was the largest. In the culture on glucose at 42°C, the observed volume of H_2 production was faint and lower than at 25°C, and H_2 production stopped after 34.5 hours (data not shown). Finally, at pH 6 and 37°C, the molar yields of H_2 of the strain AM2 reached 1.5 mol H_2/mol glucose and 1.7 mol H_2/mol mannitol in batch culture.

Effects of substrates and pH on fermentative products of *Vibrio tritonius* AM2

Molar yields of fermentation products (sum of H_2 and formate, ethanol, acetate and lactate) produced by the strain AM2 were compared in the pH range of 5.5-7.5 (Table 1-1). The sum molar yields of H_2 and formate which were nearly equal to molar yield of total formate generated by PFL were rather stable at all pH levels examined, except for the glucose-grown cells at pH 5.5. The sum of H_2 and formate yields on mannitol was higher than that on glucose (P<0.05) at pH 5.5, whereas they were not significantly different at pH 6-7.5.

Mannitol-grown cells showed that molar yields of ethanol were significantly higher than those of acetate at all pH levels examined, whereas the glucose-grown cells showed that the molar yields of ethanol were not much different to that of acetate. On the other hand, faint molar yields of lactate were shown on both substrates.

H_2 production from seaweed feedstock by *Vibrio tritonius* AM2

Batch culture experiment for H_2 production from seaweed feedstock was carried out in a 5 L jar fermenter, with 3 L working volume (Fig. 1-3). The culture condition was maintained at pH 6 and 37°C. Agitation was set at 600 rpm. Mannitol consumption was started after inoculation of the strain AM2 into the medium, and continued for 72 hours until all mannitol was completely consumed. The volume of H_2 production reached 254 mmol/L reactor volume. The maximum production rate of H_2 was maintained at the time range of 24-32 hours after inoculation, and reached 8.7 mmol/h/L reactor volume. The molar yield of H_2 was 1.6 mole H_2/mole mannitol, which corresponded to 94% yield under the same conditions with mannitol supplemented culture with 100 mL working volume. Ethanol production was also observed, and the final concentration reached 10.9 g/L and the molar yield of ethanol reached 1.4 mole ethanol/mole mannitol.

DISCUSSION

H_2 is a potentially promising clean energy source for use in the future. To produce H_2 economically, we must develop not only the infrastructure for the use of H_2 based energy, electricity, and transportation but also a stable H_2 supply system including biocatalysts and a stable feedstock production. As marine biomass is one of the candidates to fulfill the criteria for creating a sustainable bioenergy production system, the authors have evaluated the potential of H_2 production in a newly described marine vibrio which is capable of fermenting seaweed carbohydrates under saline conditions.

The H_2 productivity of the newly isolated marine bacterium *V. tritonius* AM2 was examined with a view to optimizing its ability. H_2 production and the cell growth of the strain AM2 is

dependent on pH of the medium. The volume of H_2 produced by the strain AM2 increased at pH 6.0-7.5, whereas the cell density showed a countertrend to H_2 production (Fig. 1-1AB). Therefore, the pH-dependent H_2 production is thought not to be caused by the cell mass but rather the self-ability of strain AM2 to produce H_2, such as gene expression or enzymatic activities responsible for H_2 production.

High salt concentration inhibits H_2 production due to preventing cell activity [Kim *et al*., 2009; Lee *et al*., 2012]. Molar yield and production rate of H_2 by *En. aerogenes* (1.6 mol H_2/mol mannitol in maximum) markedly decreased to 1.2 and 0.8 mol H_2/mol mannitol under 2 and 3% (v/w) NaCl, respectively [Tanisho, 2011]. There have only been few reports about H_2 production under marine conditions, such as *Bacillus* sp. B2 [Liu and Wang, 2012]. The maximum molar yield of H_2 was obtained at pH 6 and 37°C, and under these conditions the strain AM2 achieved 1.7 mol H_2/mol mannitol (initial 2.25% (w/v) NaCl). To our knowledge, the maximum molar yield of H_2 by strain AM2 was higher than that of any other wild-type strains of facultative anaerobes under saline conditions.

The effects of NaCl concentration towards H_2 production of the strain AM2 was not evaluated in detail in this study. Under aerobic conditions, the strain AM2 is capable of growing at 0.5-8% (w/v) NaCl, and the optimum is 3% (w/v) (data not shown). As the fermentation to produce H_2 occurred under anaerobic or microaerobic conditions, electron flow in the cell may be changed under aerobic conditions. Therefore, further studies are needed on the effects of NaCl on H_2 production of the strain AM2.

To enhance molar yield of H_2, carbon flux on the upstream pathway of formate and acetyl-CoA is an important factor. Based on the fermentation pathway, especially described in *E. coli*, disruption of lactate- and succinate-producing pathways enhance the molar yield of H_2. Inactivation of both *ldhA* gene (lactate dehydrogenase gene) and *frdBC* gene (fumarate reductase genes) enhanced the molar yields of H_2 from 1.08 to 1.82 mol H_2/mol glucose in *E. coli* [Alam and Clark, 1989; Yoshida *et al*., 2006]. The molar yield of lactate produced from pyruvate displayed remarkably low values at all pH levels examined on the strain AM2 (Table 1-1), although the succinate production was not studied here. Therefore, one of the factors in achieving high-yield H_2 production by the strain AM2 may be the faint lactate production.

Formate is a precursor of H_2 produced by FHL in most H_2-producing facultative anaerobes. Formate is either excreted from the cell through the formate channel (FocA) or decomposes to CO_2 and H_2 by FHL in enterobacteria [Axley *et al*., 1990; Sawers, 1994; Sawers, 2004]. In the strain AM2, the molar yields of H_2 and formate showed a countertrend toward pH of the medium (Fig. 2), and the sum molar yields of H_2 and formate, which is nearly equal to that of total

formate produced by PFL, were also stable in the pH range of 6-7.5 (Table 1-1). These production dynamics of H_2 and formate depending on pH levels showed that the strain AM2 used mainly FHL, and produced H_2 by oxidation of formate under slightly acidic conditions (pH 5.5 and 6).

The H_2-producing pathway from mannitol is elucidated by determining the balance of fermentative products at various pH levels of the medium. Mannitol, which is a more reduced form of hexose, can generate excess molecules of NADH during glycolysis compared to glucose [Böck and Sawers, 1996]. Generally, excess reducing equivalents, such as NADH, were used for the production of lactate, succinate, ethanol and 2.3-butanediol [Böck and Sawers, 1996; Alam and Clark, 1989]. In the strain AM2, the molar yield of ethanol on mannitol-grown cells showed higher values than those on glucose-grown cells, and that of acetate showed a countertrend (Fig. 1-2 and Table 1-1). The shift of carbon flux from ethanol to acetate also suggested that the mannitol-grown AM2 cells might be in the physiologically reduced condition. The molar yields of H_2 also showed similar trends to those of ethanol against pH of the medium (Fig. 1-2). In most facultative anaerobes which use only the FHL pathway, NADH is unlikely to be used for H_2 production [Nakashimada *et al*., 2002]. However, enhanced H_2 yield of the mannitol-grown cells suggested that there might be some effects preventing H_2 production, such as the reduce equivalents and the carbon flux on mannitol metabolism in the strain.

To understand carbon flux during H_2 production, the sum of H_2 and formate yields was compared between glucose- and mannitol-grown cells at each pH of the medium. The sums yield of H_2 and formate on glucose were significantly lower than that on mannitol ($P<0.05$) at pH 5.5, whereas there were no significant differences between the glucose- and mannitol-grown cells at pH 6.0-7.5. Such results suggested that the carbon flux of strain AM2 during glucose metabolism at pH 5.5 might be less efficient compared to other culture conditions examined. In other words, the mannitol-grown cells which stably showed high sum yields of H_2 and formate might indicate an efficient mannitol metabolism by the strain AM2. However, the amounts of mannitol consumed were lower than glucose at pH 5.5 and 6. On the other hand, both substrates added (5% (w/v)) were consumed completely at pH 6.5 and 7.5, when the gas production stopped (data not shown). These results indicated that there was a difference between the efficiency between H_2 production and sugar consumption of mannitol-grown cells. Therefore, more detailed analysis must focus on the metabolic and genetic control and/or feedback to understand the entire mannitol metabolism of strain AM2.

Finally, we succeeded in achieving practical H_2 production from powdered seaweed feedstock using a jar fermenter under pre-optimized culture conditions (Fig. 1-3). Our batch

culture experiments showed the advantage of strain AM2 as a high-yield H_2 producer from mannitol which is the primary reserve compound of brown macroalgae under saline conditions. The batch culture experiment was carried out in a 5 L jar fermenter, and 3 L marine broth was added to 300 g powder of brown macroalgae (*Saccharina sculpera*) containing 31.1 % (w/w). After 72 hours of cultivation, all mannitol contained in the seaweed feedstock was completely consumed (Fig. 1-3). The results revealed that the use of seaweed feedstock for fermentation can be realized by simple pretreatment, such as powderization. When seaweed feedstock was used as a substrate, nevertheless the molar yields of H_2 and ethanol cannot be compared directly to the values observed in the *in vitro* culture with pure mannitol as a substrate, the strain AM2 achieved 80% of the theoretical molar yield of H_2 in facultative anaerobes. The gap in yields might be caused by scale-up of the working volume (data not shown) or by fermentation inhibition due to various compounds contained in seaweed feedstock.

Recently, we found an interesting report that high saline concentration not only inhibits fermentative H_2 production but also can cause selective pressure on the structure of the bacterial community in the natural environment. The family of *Vibrionaceae* becomes the dominant species under moderate halophilic condition [Pierra *et al*., 2014]. Our findings also can support the data.

These batch culture experiments also showed two further challenges in H_2 production from seaweed feedstock using the strain AM2. One is the rather low H_2 production rate of the strain AM2 compared to the H_2 production of the enterobacteria, such as *E. coli* [Yoshida *et al*., 2006] and *En. aerogenes* [Rachman *et al*., 1997; Tanisho, 2011]. Improvement of culture methods is both effective and realistic for increasing the H_2 productivity [Tanisho, 2011]. Designing of gene disrupted strains or overexpression of genes responsible for H_2 production are also effective [Yoshida *et al*., 2006]. Therefore, the establishment of a continuous culture system is essential for technical advances in securing its establishment. The other is the fermentative residues mainly contained alginate which is not consumed by the strain AM2. We found that the strain AM2 was capable of converting formate directly to H_2 (unpublished data). Therefore, we need to improve the H_2 productivity from both the cultivation system and the metabolic engineering of strain AM2.

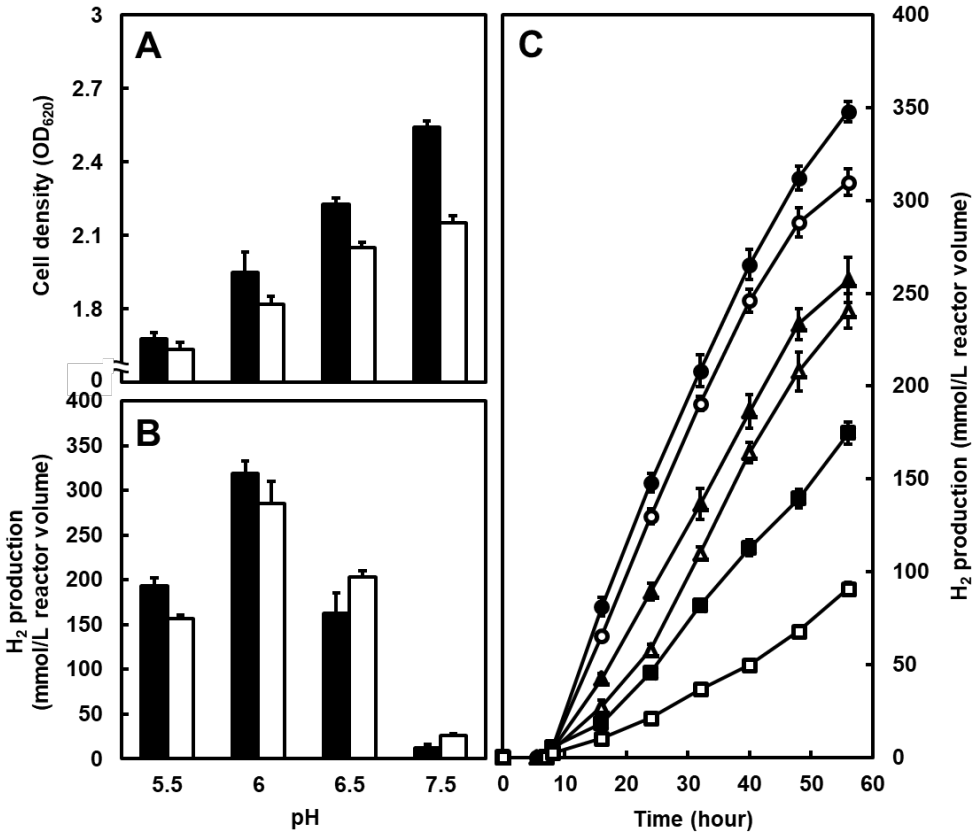

Fig. 1-1. Hydrogen production profiles of *Vibrio tritonius* AM2. Effects of pH on cell growth (A) and hydrogen production (B), and effects of temperature on hydrogen production (C) of *Vibrio tritonius* AM2 in batch culture. A and B: closed bar, on glucose; open bar, on mannitol. Symbols: ●, glucose at 37°C; ○, mannitol at 37°C; ▲, glucose at 30°C; △, mannitol at 30°C; ■, glucose at 25°C; □, mannitol at 25°C. Culture condition was set at 30°C (A and B), and pH 6 (C). n=3, error bars represent SD.

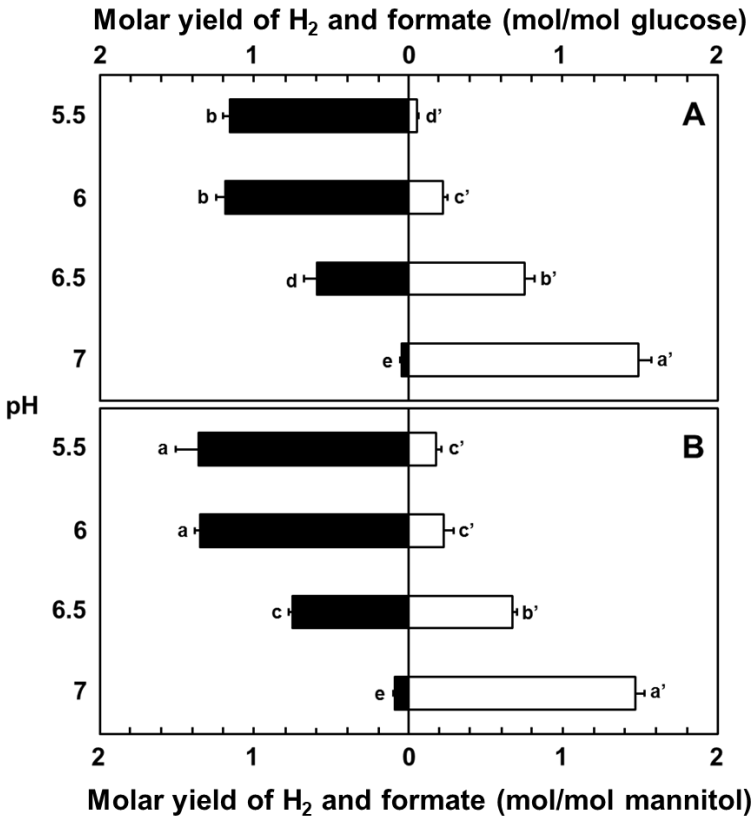

Fig. 1-2. Effects of pH on molar yields of hydrogen and formate produced by *Vibrio tritonius* AM2. Glucose (A) and mannitol (B) were used as substrates, respectively. Closed bar, molar yields of hydrogen; open bar: molar yields of formate. Culture condition: temperature of the medium maintained at 30°C. n=3, error bars represent SD. Statistically significance (P<0.05) is indicated by letters.

Table 1-1. Fermentation product profiles

pH	Molar yields (mol/mol substrate) Substrates							
	Glucose				Mannitol			
	H_2+Formate	Ethanol	Acetate	Lactate	H_2+Formate	Ethanol	Acetate	Lactate
5.5	1.22±0.04	0.66±0.12	0.64±0.1	0.06±0.01	1.53±0.11	0.85±0.13	0.31±0.03	0.04±0.00
6	1.42±0.1	0.57±0.03	0.67±0.03	0.06±0.00	1.58±0.07	0.92±0.07	0.39±0.02	0.06±0.01
6.5	1.37±0.06	0.82±0.09	0.75±0.07	0.06±0.00	1.41±0.00	1.12±0.05	0.37±0.02	0.05±0.00
7.5	1.54±0.07	0.77±0.04	0.71±0.07	0.01±0.00	1.56±0.05	1.11±0.04	0.28±0.08	0.02±0.01

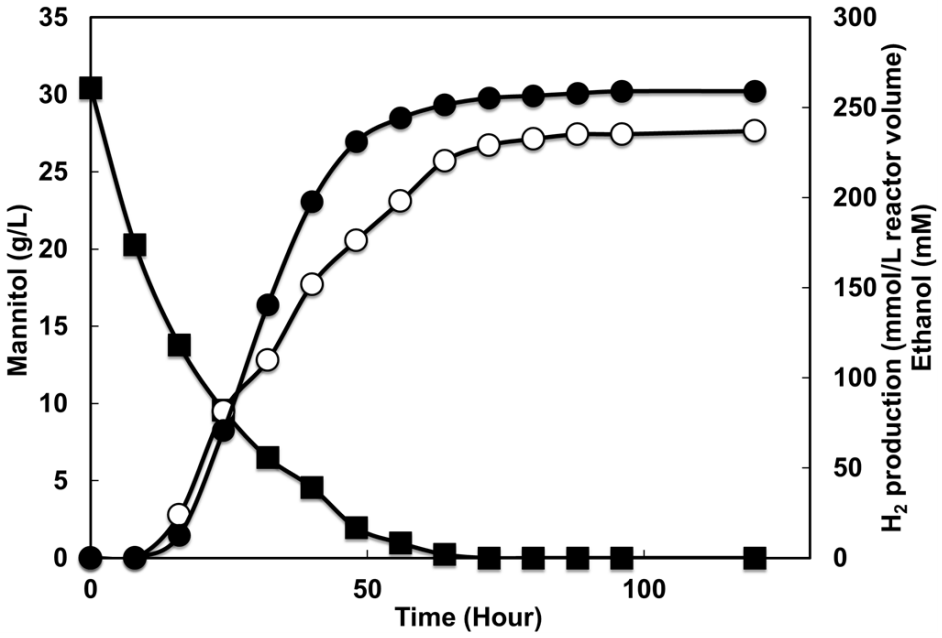

Fig. 1-3. Practical hydrogen and ethanol production from seaweed feedstock by *Vibrio tritonius* AM2 in 3 L batch culture. Culture conditions: pH and temperature of the medium maintained at pH 6 and 37°C, respectively. Symbols: ●, hydrogen production; ○, ethanol production; ■, mannitol concentration.

CHAPTER III

Molecular characterization and transcriptional analysis of a gene cluster responsible for hydrogen evolution in *Vibrio tritonius* AM2

ABSTRUCT

V. tritonius AM2 represents high-yield H_2 production (1.7 mol H_2/mol mannitol) even under saline conditions (initial 2.25% (w/v) NaCl). However, the molecular mechanism of the efficient H_2 production has never been studied in the genus *Vibrio*. The aim of this study was to identify genes responsible for the hydrogen evolution of *V. tritonius* and the gene expression pattern. Complete genome analysis revealed an existence of a single 24 kb gene cluster consisting of 21 genes, which are essential in forming energy-conserving FHL containing 11 Hyf-type proteins in the large chromosome of the strain AM2. In a gene (designated as *hyfG* gene) encoding a large subunit of hydrogenase, typical motifs coordinating [NiFe] center at the active site were conserved, which means that the *V. tritonius* hydrogenase is regarded as a [NiFe]-hydrogenase. Moreover, transcriptional expression analysis also revealed that the expression level of the *hyfG* gene increased upon pH decrease, this trend was correlated to the pH-dependent hydrogen production of the strain AM2. Accordingly, we can conclude that the *V. tritonius* Hyf-type protein is the key enzyme in H_2 production under acidic conditions. Interestingly, the 24 kb gene cluster was likely to be transcribed in a single transcript during efficient H_2 production state.

INTRODUCTION

H_2 produced via biological processes such as fermentation and photosynthesis, has been recognized as a potential renewable and carbon-neutral energy source in the future. Biological production of H_2 is commonly achieved using hydrogenase (or nitrogenase), which catalyzes both functions in evolution and oxidation of H_2, representing the following in the simple chemical reaction: $2H^+ + 2e^- \rightleftarrows H_2$ [Vignais *et al*., 2001; Vignais *et al*., 2004]. Currently, hydrogenases can be classified into [NiFe]-hydrogenases, [FeFe]-hydrogenases, and [Fe]-hydrogenases based on the distinctive functional core containing catalytic metal center [Vignais *et al*., 2004; Nicolet and Lemon, 2000]. The [NiFe]-hydrogenases are widely distributed in microorganisms belonging to the domains of Bacteria and Archaea, and have been the most extensively studied. The [NiFe]-hydrogenases which contribute to H_2 metabolism in bacteria are further classified into four groups based on the full sequence alignments of the large and small subunits [Vignais *et al*., 2004; Vignais and Billoud, 2007]. Among the four groups of the [NiFe]-hydrogenases, group 4, which is defined as H_2-evolving, energy-conserving, and

membrane-associated hydrogenase, plays an important role in the disposal of excess reducing equivalents [Nakashimada *et al*., 2002], acidic resistance [Noguchi *et al*., 2008], and energy-conservation [Andrews *et al*., 1997; Sapra *et al*., 2003; Kulkarni *et al*., 2009].

E. coli possesses two types of FHL which consists of the [NiFe]-hydrogenase and Fdh-H as a major H_2-evolving structural protein complex; one is FHL-1 consisting of a Hyc complex of hydrogenase-3 (*hyc* operon) and the other is proposed as FHL-2 consisting of a Hyf complex of hydrogenase-4 (*hyf* operon) [Andrews *et al*., 1997; Axley *et al*., 1990; Sawers, 1994]. These catalytic subunits of the [NiFe]-hydrogenases are classified in the above mentioned group 4, on the basis of amino acid sequences of the large and small subunits [Vignais *et al*., 2001; Vignais *et al*., 2004]. *E. coli* FHL-1 (including Hyc complex) plays an important role in circumventing the critical acidification of the cytoplasm due to the accumulation of formate (p*K*a=3.75) which is produced by pyruvate formate lyase (PFL), when pH of the medium drops below 6.8 [Sawers, 2005]. The major structural differences are found in the possible integral proteins between the Hyc and Hyf complex; the Hyf complex is composed of three additional integral membrane components which might perform the function of proton translocation [Andrews *et al*., 1997]. Up to now, however, no Hyf-derived hydrogenase or formate dehydrogenase activity has been detected, and no Ni-containing protein corresponding to HyfG containing the large subunit of Hyf complex have been observed [Skibinski *et al*., 2002], nevertheless structural similarity to complex I has been discussed [Marreiros *et al*., 2013].

V. tritonius AM2, isolated from a gut of a sea hare (*Aplysia kurodai*), is a facultative anaerobe which produces H_2 via formate oxidation [Sawabe *et al*., 2013]. *V. tritonius* represents high-yield H_2 production (1.7 mol H_2/mol mannitol) even under saline conditions [Matsumura *et al*., 2014]. Vibrios are phylogenetically related to *Enterobacteriaceae* [Ruimy *et al*., 1994] and genes related to form FHL are found in the complete genome data of *Vibrio furnissii* NCTC 11218 [Lux *et al*., 2011]. Therefore, it is expected that *V. tritonius* genome data also indicate the presence of the genes responsible for the formation of FHL.

The property of H_2 production in the genus *Vibrio* is believed to be atypical; this means that details on biochemistry, genetics, genomics, and molecular biology involving transcriptional regulation of the H_2 production mechanism have not been identified yet. Fortunately, as mentioned above, H_2 productivity of *V. tritonius* is high enough to conduct deeper studies in elucidating the H_2-producing mechanism in marine vibrios [Matsumura *et al*., 2014]. In this study, the authors focused on the genetic characteristics and the transcriptional patterns of the genes responsible for the H_2 evolution in *V. tritonius*. The results will also contribute not only to improvements in H_2 productivity in *V. tritonius* but also in the understanding of the H_2

metabolism and the evolutionary framework of the maintenance in genus *Vibrio*.

MATERIALS AND METHODS

Bacterial strain and culture condition

In preculture and batch culture experiments, *V. tritonius* AM2 was grown in a synthetic medium containing 200 mM NaCl, 50 mM $MgSO_4 \cdot 7H_2O$, 10 mM KCl, 10 mM $CaCl_2 \cdot 2H_2O$, 20 mM glucose, 19 mM NH_4Cl, 0.33 mM K_2HPO_4, 50 mM MES and 0.2% (v/v) trace metal solution; 5 mM $NiCl_2$, 1.6 mM ferric citrate, 1 mM $Na_2Mo_4 \cdot 2H_2O$ and 1 mM Na_2SeO_3. The preculture was performed aerobically to achieve 0.6±0.05 OD_{620} cell density with shaking at 130 rpm at pH 7 and 37°C. The batch culture was conducted by adding 1 mL of the preculture, and was stirred with a magnetic stirrer (RO 10 power IKAMAG, IKA, Staufensee, Germany). pH and temperature of the medium were maintained at pH 5.5, 6, 6.5 or 7 using pH controller (DT-1023P, ABLE, Tokyo, Japan) with an electrode (FermProbe pH electrodes, Broadley-James Corp., Irvine, USA) by adding 5 N NaOH or HCl, and 37°C respectively.

Assays

The volume of H_2 production was measured by analyzing the H_2 composition of head space of the bottles using gas chromatography (GC2014, Shimadzu, Kyoto, Japan) with a thermal conductivity detector and Shincarbon ST (Shinwa Chemical Industries Ltd., Kyoto, Japan). Dry cell weight (DCW) was calculated by measuring optical density (OD) at 620 nm; 1 OD_{620} was estimated as 0.41 g DCW/L. Data of H_2 production were analyzed using one-way analysis of variance (ANOVA) with Tukey-Kramer test for multiple comparisons. Probability of less than 5% ($P<0.05$) was considered statistically significant.

Genome analysis

The whole genome sequence of the strain AM2 was obtained using 454 GS FLX Titanium sequencer (Roche Diagnostics, Branford, USA) and the sequence reads were assembled using the Newbler software version 2.3 or later. Gaps were filled manually by Sanger sequencing. Illumina reads obtained by MiSeq sequencer (Illumina, San Diego, USA) were used only for sequence error correction. Identification of protein-coding sequences (CDSs) was carried out using the Microbial Genome Annotation Pipeline (MiGAP; http://www.migap.org/) [Sugawara *et al*., 2009] and Glimmer [Delcher *et al*., 1999]. Gene analysis was performed using In Silico Molecular Cloning software (In silico biology, Inc., Yokohama, Japan). Amino acid sequence alignments of hydrogenase subunits were conducted using CLUSTAL X2 program [Larkin *et al*.,

2007; Thompson *et al*., 1994]. Molecular characterization of genes responsible for H_2 production was conducted using InterPro database [Hunter *et al*., 2011]. Nucleotide sequence of the terminator region was predicted using ARNold finding terminators [Naville *et al*., 2011]. Transmembrane helices were predicted using SOSUI program [Hirokawa *et al*., 1998]. Protein localization was predicted using PSORTb 3.0 [Yu *et al*., 2010].

Total RNA extraction and real-time quantitative PCR

Total RNA was extracted from cells grown in a synthetic medium described above to mid-logarithmic phase at pH 6 using TRIzol LS Reagent (Life Technologies, Carlsbad, USA). The total RNA was treated using RNase-free DNase (Promega, Madison, USA) to remove any residual DNA, and was further purified using the RNeasy Mini kit (Qiagen, Hilden, Germany). The purified total RNA was reverse transcribed to first-strand cDNA using SuperScript™ III Reverse Transcriptase (RT) and random 6-mer (Life Technologies, Carlsbad, USA) at 46°C for 3 hours. The cDNA was used for transcriptional unit analysis and real-time quantitative PCR (qPCR).

V. tritonius hyfG gene was selected as a target gene of interest and *proS* and *pyrH* genes as reference genes for the qPCR. Primer for the qPCR was designed using Primer Express Software (Life Technologies, Carlsbad, USA). SYBR Green PCR platform and ΔΔCt method using One-Step real time PCR machine (Life Technologies, Carlsbad, USA) were used. The PCR cycle conditions consisted of 95°C for 10 min., followed by 40 cycles of 95°C for 15 sec. and 60°C for 1 min. All expression levels are presented here relative to those at pH 7.

Transcriptional unit analysis

The first strand cDNA, which corresponds to a 24 kb region of FHL-Hyp gene cluster of the strain AM2, was synthesized using the same protocol as described in the above section, but using gene specific primers. The conditions for the RT consisted of 55°C for 90 min. and 70°C for 15 min. Using the first strand cDNA as a template, PCR was performed with primer pairs that are able to amplify intergenic regions of the FHL-Hyp gene cluster of the strain AM2 using GoTaq Green Master Mix (Promega, Madison, USA). The PCR cycle consisted of 95°C for 2 min. for an initial denaturation, and 30 cycles of 95°C for 1 min (denaturation), 55°C for 1 min. (annealing) and 72°C for 1 min. (extension). Genomic DNA of the strain AM2 extracted using Wizard Genomic DNA Purification Kit (Promega, Madison, USA) was used for a positive control reaction. A negative control reaction was performed without RT as total RNA template.

All primers used in this study are listed in Table S1. The PCR product was analyzed by 1.0% agarose gel electrophoresis in 0.5x TBE buffer.

RESULTS

Identification of *Vibrio tritonius* FHL-Hyp gene cluster in the large chromosome

The gap-closed whole genome information on *V. tritonius* AM2 consisted of two circular forms with 3,434,724 bp for the large chromosome (Chr. 1) and 1,787,202 bp for the smaller second one (Chr. 2). G+C% of the Chr. 1 and Chr. 2 were 43.96 and 43.78, respectively. A total of 34 rRNA genes were found on the Chr. 1 but not on the Chr. 2. Total CDSs of the Chr. 1 and Chr. 2 might be around 3,000 and 1,600, respectively. Possible chromosome replication regions (*oriC* region) were estimated by OriC finder [Gao and Zhang, 2008]. The region of Chr. 1 was also identified by co-localizing *gidA*, *mioC*-like FMN-binding protein gene, *dnaA*, *dnaN*, *recF* and *gyrB* [Heidelberg *et al*., 2000; Egan and Waldor, 2003]. The genes encoding plasmid partitioning proteins (ParAB) were also located at the *oriC* region of the Chr. 1. The region of Chr. 2 was identified by the structural similarities, of which *parAB* and *rctB* genes were co-localizing, but less similarities in the *rctA* gene sequence of *Vibrio cholerae* [Heidelberg *et al*., 2000; Egan and Waldor, 2003]. A 5' inter-genetic region of *rctB* of the strain AM2 possessed an AT rich region showing high similarity against those of *V. cholera* and *Vibrio parahaemolyticus* Chr. 2.

From the genome data of *V. tritonius*, only two possible genes corresponding to large and small subunit of hydrogenase were found. By further observation of the flanking region around the possible hydrogenase genes, a single gene cluster with the total length of 24 kb which could be responsible for the H_2 production appeared on 481,700-505,700 bp region on the Chr. 1 of *V. tritonius* (Fig. 2-1A). Using both BLAST and InterPro Scan search, which aims to find proteins possessing well known conserved domains and/or structures, the genome region of *V. tritonius* was identified as a gene cluster including 21 genes required for the formation of FHL (Fig. 2-1A and Table 2-1). We found a similarity in the gene products of *V. tritonius* and those of *E. coli* K-12 W3110, but not only in the amino acid identity ranged from 32-68% but also the gene arrangement was unlikely to match those of *hyc* and *hyf* operon of *E. coli* (Fig. 2-1A). We also found more similarity against the putative gene cluster responsible for forming FHL of *V. furnissii* than that of *E. coli*, but at least three genes corresponding to *hyfDEF* genes of *V. tritonius* and *E. coli* absent in the putative gene cluster responsible for the H_2 production in *V. furnissii* (Table 2-1). Finally, we identified the gene cluster retained by *V. tritonius* as FHL-Hyp gene cluster. The gene arrangement consisted of a hydrogenase complex in the FHL-Hyp gene

cluster was likely to be similar to *hyf* operon of *E. coli*, so these genes were named as *Vt-hyfABCDEFGHIJ* and *hycI*, respectively, but *E. coli hyf* (*Ec-hyf*) operon does not have *hycI*, *fdhF*, and *hyp* homologue genes in the franking region.

Properties of the predicted gene products of *hyf*-like operon in *Vibrio tritonius*

Vt-HyfA (21.6 kDa) was predicted to contain four conserved motifs, each containing four cysteine residues corresponding to four [4Fe4S] clusters (Fig. 2-2). The 16Fe ferredoxins generally function as electron-accepting/donating components in oxido-reduction pathways [Andrews *et al*., 1997]. The motifs are also found in *Ec*-HycE, which plays a role in electron transport between Fdh-H and Hyc complex [Sauter *et al*., 1992].

Vt-HyfB (72.6 kDa), *Vt*-HyfD (51.2 kDa) and *Vt*-HyfF (56.6 kDa) were predicted as transmembrane proteins belonging to the protein family, *Oxidored_q1* (PF00361), in which NADH-ubiquinone/plastoquinone (complex I) are classified. The molecular function of the proteins belonging to this family was predicted to be proton translocation across cytoplasmic membrane coupled to ATP synthesis. *Vt*-HyfBDF showed high amino acid sequence homology (>56% in average) to *Ec*-HyfBDF.

Vt-HyfC (34.4 kDa) and *Vt*-HyfE (23.7 kDa) were predicted as membrane proteins which belong to the protein families *NADHdh* (PF00146) including NADH dehydrogenase, and *Oxidored_q2* (PF00420) including NADH-ubiquinone/plastoquinone oxidoreductase chain 4L, respectively. The proposed function of the two proteins was oxidoreductase activity.

Vt-HyfG (66.0 kDa) corresponding to the large subunit of the [NiFe]-hydrogenase was identified. The amino acid sequence alignment of the large subunits of the [NiFe]-hydrogenases belonging to group 4 revealed that two CxxC motifs coordinating [NiFe] center at the active site were included at the N- and C-terminal regions of *Vt*-HyfG (Fig. 2-3A). The CxxC motif at the C-terminal region is a part of the DPCxxCxxR motif (Fig. 2-3A) followed by the C-terminal extension, which is usually cut down by a protease [Rossmann *et al*., 1994; Rossmann *et al*., 1995]. As a feature of the gene, the translation start of *Vt-hyfG* gene was ATG codon, nevertheless *Ec-hyfG* gene uses GTG as the start codon [Andrews *et al*., 1997].

Vt-HyfH (21.6 kDa) contained two CxxCxxCxxxCP motifs which are also found in *Ec*-HycF, *Ec*-HyfH, and *Vf*-HyfH (Fig. 2-4). Therefore, *Vt*-HyfH possesses the two [4Fe4S] clusters and the proposed function of this is to play a role in electron transport. In addition, $CxxCx_nCPxC$ (n=29-36) motif was also found in *Vt*-HyfH and CooX of *Carboxydothermus hydrogenoformans* and *Rhodospirillum rubrum*, suggesting the presence of a third iron site.

Vt-HyfI (29.6 kDa) had a $CxxCx_nGxCxxxGx_mGCPP$ (n=61-106, m=24-61) motif typically

found in the small subunits of the [NiFe] hydrogenase (Fig. S2). In addition, CHGC sequence, which might relate to the active site, was observed at the C-terminal region of HyfI of *V. tritonius* and *V. furnissii* but not at those of HycE and HyfG of *E. coli*, and CooH of *C. hydrogenoformans* and *R. rubrum* (Fig. 2-3B).

Vt-HyfJ (16.5 kDa) shared 48% amino acid identity with *Ec*-HycH, which might be responsible for the maturation of the large subunit of hydrogenase-3 [Casalot *et al*., 2001]. *Ec*-HyfJ is also known as the only homologue of *Ec*-HycH, sharing 47% identity [Andrews *et al*., 1997]. The function of HycH and HyfJ remains unknown but might be involvement in the maturation of hydrogenase.

Vt-HycI (16.8 kDa) shared 53% homology against *Ec*-HycI (Table 2-1), which might play an important role of the maturation of HycE corresponding to the large subunit of hydrogenase-3 [Casalot *et al*., 2001]. *Vt-hycI* gene is located in the downstream of the *Vt-hyfJ* gene, and the CDSs of the two genes overlapped (Fig. 2-1A).

Effects of pH of the medium on H_2 production and hyfG expression in *Vibrio tritonius*

The pH dependency of H_2 production and expression level of *Vt-hyfG* gene which encodes the large subunit of the [NiFe]-hydrogenase of *V. tritonius*, were examined in the pH range of 5.5-7 in the batch culture (Fig. 2-5). In the batch culture after 12 hours, the H_2 production per DSW increased along with acidification of pH of the medium, and the H_2 production at pH 5.5, 6 and 6.5 were 35, 23 and 8-fold higher than that at pH 7.0 (Fig. 2-5A). In the 12 hour-batch culture at pH 7, H_2 production was not detected. *Vt-hyfG* gene expression showed similar tendency to the pH dependency of the H_2 production, the expression fold at pH 5.5, 6.0, and 6.5 were 1.7, 1.5 and 1.2 folds than that at pH 7 (Fig. 2-5B).

Transcriptional unit analysis of FHL-Hyp gene cluster during glucose fermentation

The FHL-Hyp gene cluster of *V. tritonius* consists of 21 genes in total, of which orientations were the same on the positive strand, on the 24 kb region of the Chr. 1 (Fig. 2-1A). In order to determine the largest transcription unit of the FHL-Hyp gene cluster, RT-PCR experiments were performed with primer pairs capable of amplifying various regions of the FHL-Hyp gene cluster as the first strand cDNA synthesized by a primer targeting on 3’ end of the FHL-Hyp gene cluster (corresponding to the 3’ end of *Vt-hypB* gene) template. In the preliminary *in silico* analysis to predict possible transcriptional unit base on the GC skew change it was found that the 24 kb cluster could be transcribed as a single unit (data not shown). The electrophoretic profile showed that at least the 24 kb of transcript covering all 21 genes consisted of *Vt*-FHL-Hyp gene

cluster (Fig. 2-1B). However, two terminator regions were predicted at the back of 3' end of *Vt-fdhF* and *Vt-hypB* genes as a hairpin-loop forming palindrom by ARNold finding terminators [Naville *et al*., 2011].

DISCUSSION

Since Andrews *et al*. discovered the *hyf* operon in the *E. coli* genome sequence in 1997, many hydrogenases assigned to group 4 share similarities with the Hyf-type proteins in *E. coli* [Vignais *et al*., 2007; Andrews *et al*., 1997; Marreiros *et al*., 2013]. Several proteins, however, could not be identified as the [NiFe]-hydrogenases due to the lack of the two conserved CxxC motifs located at the N- and C-terminal regions of the large subunits, which are residues acting as ligands for the [NiFe] center at the active site. The four gene products of *hyf*-like operon in *Mycobacterium tuberculosis* (Orf2, 3, 4 and 5) share amino acid sequence similarities with HyfC (34%), HyfE (24%), HyfBDF (24, 21 and 36%, respectively) and HyfG (31%) of *E. coli*, respectively, but these proteins do not correspond to the [NiFe]-hydrogenase components due to the absence of the CxxC motifs in Orf5 [Andrews *et al*., 1997]. Likewise, Coppi (2005) indicated that the Ech homologue cluster of *Geobacter sulfurreducens* does not encode the [NiFe]-hydrogenase, and thus designated it to Ehr (Ech-hydrogenase-related) [Coppi, 2005]. Presence of *hyf*-operons with co-occurrence of *fdhH* gene in the genome of vent species of chemolithoautotrophic epsilonproteobacteria [Marreiros *et al*., 2013, Zhang and Sievert, 2014] suggests an unexpected link of formate-spilitting pathway to CO_2 and H_2 in deep-sea chemolithotrophs and shallow water atypical vibrio species. However, simple genome sequence comparison against annotated data could not cover the presence of active bacterial enzymes belonging to *hyf* related group 4 hydrogenases.

Using a marine vibrio, *V. tritonius* AM2, we first identified an effective Hyf complex-driven H_2 production among bacteria using a H_2 production assay, complete genome analysis and a gene transcriptional experiment (Figs. 2-1 and 2-5). The *Vt*-FHL-Hyp gene cluster found here consisted of three parts: FHL, Fdh and activator, and Hyp regions with the length of total gene cluster up to 24 kb. The first 10 genes (*Vt-hyfABCDEFGHIJ*) formed the *hyf*-like operon. The middle four genes encode formatted dehydrogenase and an activator, *fhlA*, which controls in a formate regulon of *E. coli*. The last 6 genes may be involved in hydrogenase maturation and processing. As functions and regulations of *Ec-hyf* operon (*Ec-hyfABCDEFGHIJ*) have not elucidated yet due to the insignificant activities and expressions in the wild-type *E. coli* strain [Andrews *et al*., 1997; Skibinski *et al*., 2002; Self *et al*., 2004], the findings *hyf* gene cluster expressed in the marine vibrio could contribute to the understanding of *hyf* regulation and

evolution. The complete genome analysis of the strain AM2 revealed that 1) the *hyf* gene cluster is the only gene responsible for fermentative hydrogen evolution, 2) the hydrogenase is classified as [NiFe]-hydrogenase possesses two CxxC motifs on the *Vt-hyfG* gene. The genetic features are likely to be common among *V. tritonius* strains (unpublished data). On the basis of the gene structure of the *Vt*-FHL-Hyp gene cluster, we could also conduct gene expression studies, and these suggest that 1) the *Vt-hyfG* is up-regulated under slightly acidic conditions of the medium, and 2) the longest transcriptional unit may cover all genes consisting of *Vt*-FHL-Hyp. The *V. tritonius* Hyf also plays a key role in the H_2 production.

For biosynthesis of active [NiFe]-hydrogenases, several proteins related to maturation are required [Casalot and Rousset, 2001]. In the maturation process proposed in *E. coli*, a precursor of the large subunit (pre-HycE) containing the C-terminal extension is formed by six Hyp proteins (HypABCDEF). The extension site coordinated by the DPCxxCxxR motif is usually removed at the final stage of the maturation process [Sawers *et al*., 2004]. The last 6 genes of the *Vt*-FHL-Hyp gene cluster are identified as *hyp* genes (*Vt-hypFCDEAB*) (Fig. 2-1A and Table 2-1). *Vt*-HyfG also possesses the DPCxxCxxR motif followed by the C-terminal extension (Fig. 2-3A), which is usually cut down by an endopeptidase, such as HycI and HupD in *E. coli* and *Rhodobacter capsulatus*, respectively [Rossmann *et al*., 1995; Casalot and Rousset, 2001]. The presence of *Vt-hycI* gene and the DPCxxCxxR motif in *Vt*-HyfG suggests that it is reasonable to consider that *Vt*-HycI may also be involved in the maturation process of *Vt*-HyfG.

Compared to the Hyf proteins in *E. coli*, *Vt*-HyfBDF are predicted to be the transmembrane proteins related to NADH-ubiquinone oxidoreductase (complex I), and *Vt*-HyfCD might show oxidoreductase activity related to proton translocation [Treberg and Brand, 2011] according to the results of InterPro Scan search [Hunter *et al*., 2011]. Therefore, the FHL consisting of the Hyf-type proteins and FdhF in *V. tritonius* was thought to form the homologous complex of FHL-2, which was proposed as an energy-conserving FHL coupled to proton translocation in *E. coli* [Andrews *et al*., 1997]. On the contrary, *V. furnissii* type strain shows very low hydrogen emission activity, and the gene structure of the FHL obtained from the complete genome sequence of *V. furnissii* differs from those of *V. tritonius*; only 7 genes (*hyfABCGHIJ*) homologues to Hyc subunits of hydrogenase-3 which is part of the non-energy-conserving FHL (FHL-1). Hydrogenases driving H_2 production and energy-conservation has been well described in the [NiFe]-hydrogenases belonging to group 4 found in Mbh of *Pyrococcus furiosus* [Ma *et al*., 1993; Sapra *et al*., 2000], and Ech of *Methanosarcina barkeri* [Künkel *et al*., 1998; Meuer *et al*., 1999]. Coo of *R. rubrum* and *C. hydrogenoformans* is also energy-conserving [Fox *et al*., 1996; Soboh *et al*., 2002]. The study using the membrane vesicles of *P. furiosus* shows that Mbh played

a role of proton reduction (H_2 production) coupled to proton translocation [Sapra *et al*., 2003]. Until now, however, there has been no direct proof of how energy-conservation by the [NiFe]-hydrogenases contribute to the growth or maintenance of cells. Moreover, the vibrio Hyf consists of 12 proteins including formate dehydrogenase, which has been long discussed regarding the structural similarity of complex I, of which 14 proteins are present [Marreiros *et al*., 2013]. As vibrios are fast growing microbes, these *V. tritonius* strains could be promising materials for providing much information on physicochemical features of the *V. tritonius* FHL machinery, bioenergetics of the group of marine microbes, and evolutional linkage to complex I.

At least two genes, one from Chr. 1 and the other from Chr. 2, may encode the proteins with Fdh activities in the *V. tritonius* genome sequences. The gene on the Chr. 2 contains molydopterin dinucleotide binding domain like the catalytic subunits of Fdh-N and Fdh-O of *E. coli*. However, the gene product is predicted to be located in the cytoplasm (localization scores is 9.97) by PSORTb 3.0 [Yu *et al*., 2010], whereas the catalytic subunits of the *E. coli* Fdh-N and Fdh-O are located on the periplasm (localization scores are 10) in *E. coli*. On the other hand, the protein on the Chr. 1 might be a homologue of the NAD(P)-dependent formate dehydrogenase because of the domain of pyridine nucleotide-disulphide oxidoreductase responsible for NADH binding [Popov *et al*., 1994]. The gene product is also predicted to be located on the periplasmic side (localization scores is 9.97). Formate metabolism in the marine vibrio might differ from those of enterobacteria. In enterobacteria, formate contributes to their energy metabolism by the workings of various enzymes rather than being simply excreted. The knowledge of physiological functions and mechanisms of FocA has rapidly increased due to the successful crystal structure analysis of FocA of *E. coli* [Wang *et al*., 2009] and *V. cholerae* [Waight *et al*., 2010]. The volume of H_2 production and the expression of the *hyfG* gene of *V. tritonius* were higher under slightly acidic conditions than at pH 7 (Fig. 2-5B), whereas the cell growth of *V. tritonius* showed a countertrend [Matsumura *et al*., 2014]. These results suggest that the FHL of *V. tritonius* might contribute to the disposal of the cytoplasmic formate in order to avoid not only the critical acidification of the cytoplasm but also energy-conservation in unfavorable environments, such as acidic conditions where cell growth is repressed compared to a neutral pH of the medium.

Compared to formate regulon in *E. coli*, the FHL-Hyp gene cluster is likely to form a simpler structure (Fig. 2-1A). RT-PCR experiments revealed that the total length of 24 kb of the FHL-Hyp gene cluster forms a single transcript during the mid-logarithmic phase of *V. tritonius* (Fig. 2-1A), whereas the terminator region was predicted to be 43 bp upstream of the 5' end of *Vt-fhl*A gene, which was predicted to be a transcriptional activator of formate regulon (Fig. 2-1). Simple sequence similarity search using *E. coli* sequence failed to identify the UAS (universal

activating sequence) [Sawers *et al*., 2004] (data not shown). Absence of homologue gene to *hycA* gene which is a negative regulator of the formate regulon is also indicated so far [Skibinski *et al*., 2002]. Currently we conducted global transcriptome analyses for the bacterium, which help us to elucidate the genome-wide transcriptional control of the FHL-Hyp gene cluster. Along with details of the genome feature of *V. tritonius* and the other H_2 producing marine vibrios, these omics-analysis are in progress.

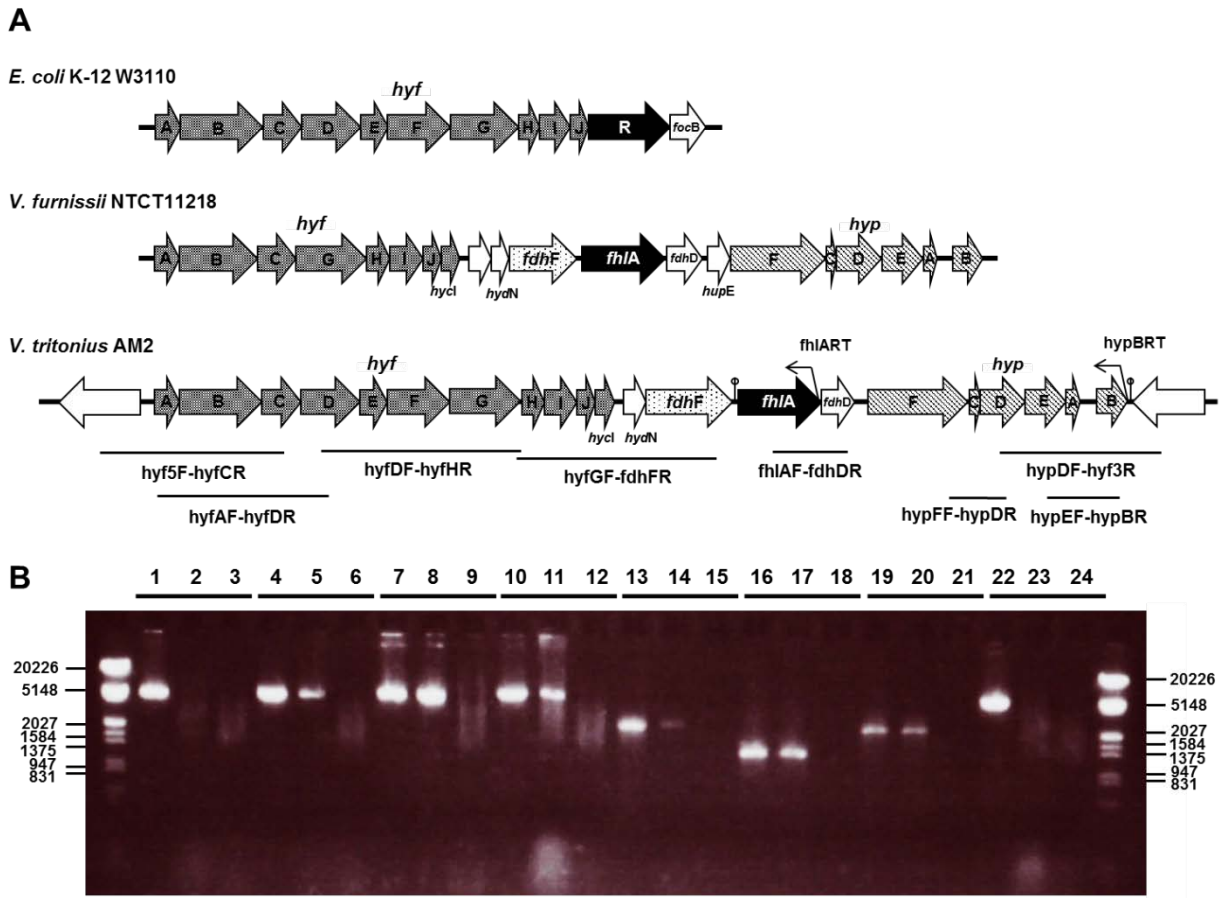

Fig. 2-1. Genomic architecture and the transcription of *Vibrio tritonius* FHL-Hyp gene cluster. The gene arrangement of *Escherichia coli hyf* operon, *Vibrio furnissii* and *Vibrio tritonius* FHL-Hyp gene cluster (A): Symbols: ○, predicted terminator region. The PCR products derived from *V. tritonius* FHL-Hyp gene cluster and its transcript (B): The cDNA synthesized by fhlART was amprified by hyf5F and hyfCR (lane 1, 2, and 3), hyfAF and hyfDR (lane 4, 5, and 6), hyfDF and hyfHR (lane 7, 8, and 9), hyfGF and fdhFR (lane 10, 11, and 12), respectively. The cDNA synthesized by hypBRT was amprified by fhlAF and fdhDR (lane 13, 14, and 15), hypFF and hypDR (lane 16, 17, and 18), hypEF and hypBR (lane 19, 20, and 21), hypDF and hyf3R (lane 22, 23, and 24), respectively. Genome DNA template: lane 1, 4, 7, 10, 13, 16, 19 and 22, RT (+) experiments: lane 2, 5, 8, 11, 14, 17, 20 and 23, and RT (-) experiments: lane 3, 6, 9, 12, 15, 18, 21 and 24. PCR cycle was defined as 40 cycles at lane 13-21. Before apply samples, each samples was diluted in the following ratios: lane 1, 4, 7, 10 and 22, 1/15; lane 5, 8 and 11, 1/3; lane 13, 16, 17, 19 and 20, 1/20; lane 14, 1/25.

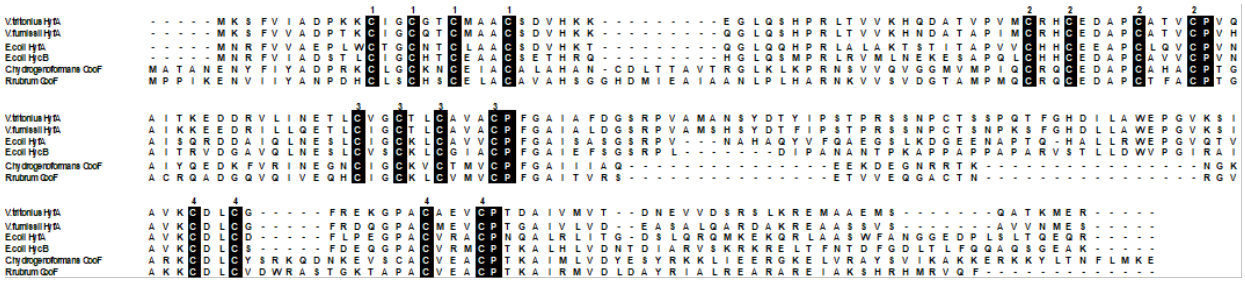

Fig. 2-2. Multiple amino acid sequence alignment of *Vt*-HyfA encoding four [4Fe4S] clusters subunits of the [NiFe]-hydrogenases with representative related sequences. Numbers 1, 2, 3 and 4 indicates [4Fe4S] ligands. The amino acid sequences used in the alignment are as follows: *Vibrio furnissii* HyfA (ADT87211), iron-sulfur subunit of hydrogenase complex; *Escherichia coli* HycB (BAE76801), iron-sulfur subunit of Hyc complex; *E. coli* HyfA (BAA16359), iron-sulfur subunit of Hyf complex; *Carboxydothermus hydrogenoformans* CooF (ABB15805), iron-sulfur cluster-binding protein of CO-induced hydrogenase; *Rhodospirillum rubrum* CooF (AAC45122), iron-sulfur cluster-binding protein of CO-induced hydrogenase.

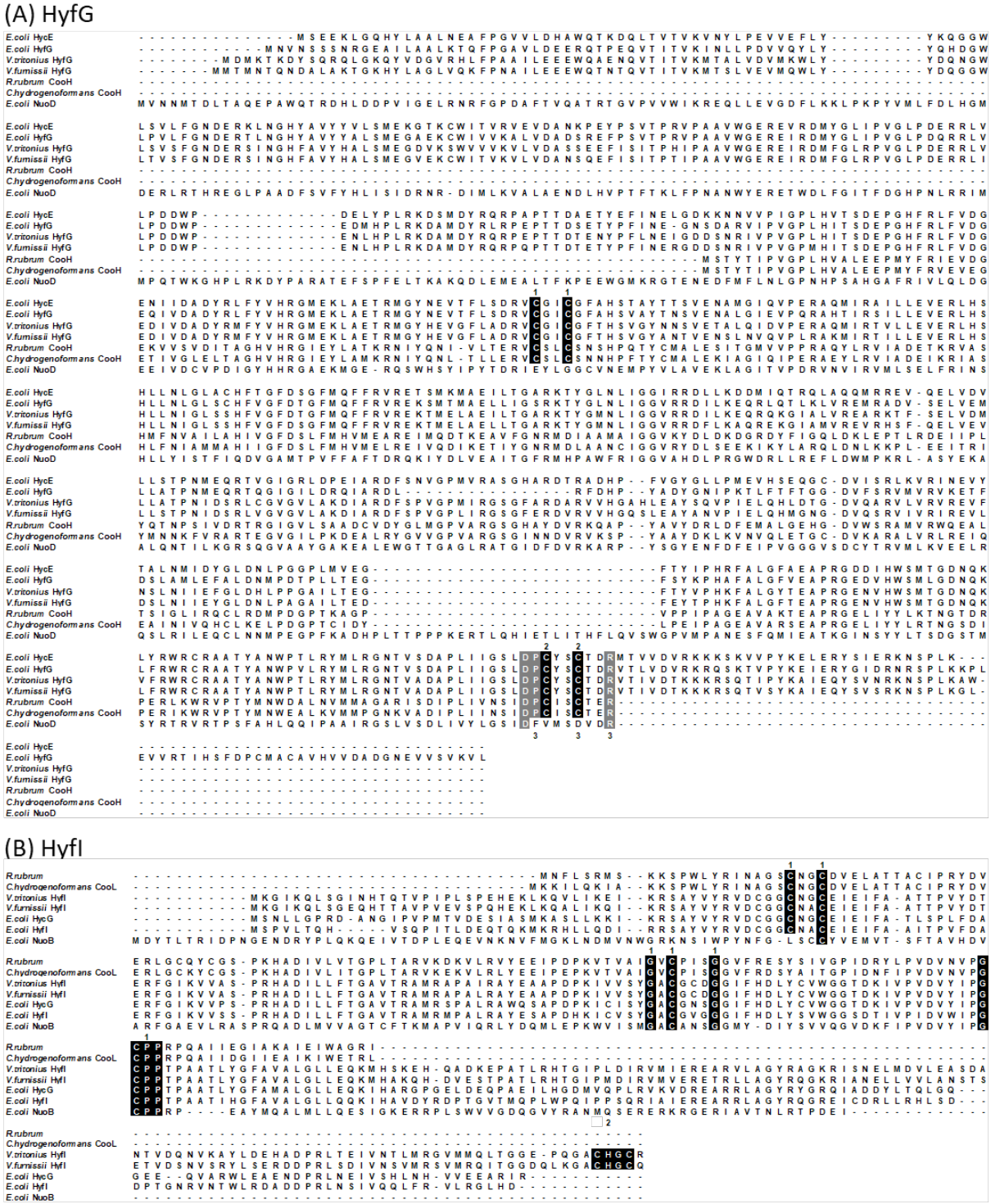

Fig. 2-3. Multiple amino acid sequence alignment of the large and small subunit of the [NiFe]-hydrogenases with representative related sequences. *Vt*-HyfG (A) Number 1 and 2 indicate [NiFe(CO)$(CN)_2$] cluster; and 3 indicates C-terminal cleavage site. The amino acid sequences used in the alignment are as follows: *Vibrio furnissii* HyfG (ADT87208, large subunits of hydrogenase complex; *Escherichia coli* HycE (P16431), large subunit of Hyc complex; *E. coli* HyfG (P77329), large subunit of Hyf complex; *Carboxydothermus hydrogenoformans* CooH (ABB14885), CO-induced hydrogenase large subunits; *Rhodospirillum rubrum* CooH

(AAC45121), CO-induced hydrogenase large subunits; *E. coli* NuoD (BAA16115), NuoD subunit of Nuo complex. *Vt*-HyfI (B) Number 1 and 2 indicate [4Fe4S] ligands possible additional iron site, respectively. The amino acid sequences used in the alignment are as follows: *V. furnissii* HyfI (ADT87206), small subunits of hydrogenase complex; *E. coli* HycG (P16433), small subunit of Hyc complex; *E. coli* HyfI (P77668), small subunit of Hyf complex; *C. hydrogenoformans* CooL (Q3AB34), CO-induced hydrogenase small subunits; *R. rubrum* CooL (AAC45118), CO-induced hydrogenase small subunits; *E. coli* NuoB (BAA16121), Nuo subunit of Nuo complex.

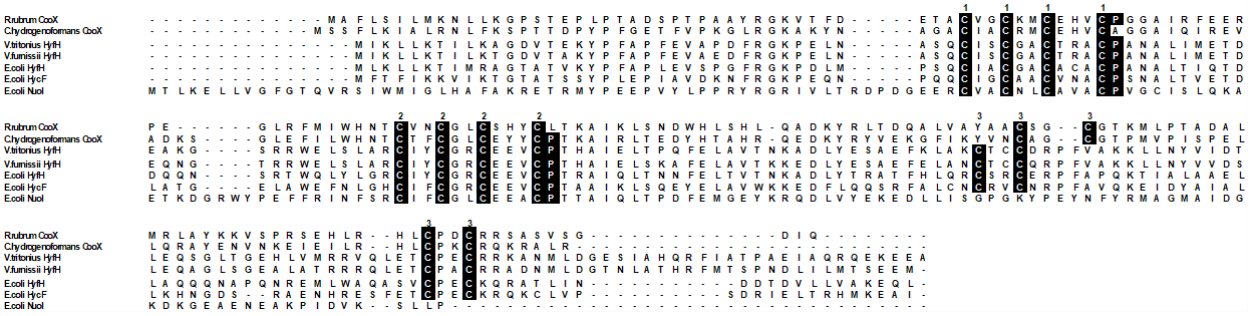

Fig. 2-4. Multiple amino acid sequence alignment of *Vt*-HyfH encoding two [4Fe4S] clusters subunits of the [NiFe]-hydrogenases with representative related sequences. Numbers 1 and 2 indicate [4Fe4S] ligands, and 3 indicates possible third iron site. The amino acid sequences used in the alignment are as follows: *Vibrio furnissii* HyfH (ADT87207), iron-sulfur subunit of hydrogenase complex; *Escherichia coli* HycF (BAE76797), iron-sulfur subunit of Hyc complex; *E. coli* HyfH (BAA16376), iron-sulfur subunit of Hyf complex; *Carboxydothermus hydrogenoformans* CooX (ABB14138), iron-sulfur cluster-binding protein of CO-induced hydrogenase; *Rhodospirillum rubrum* CooX (AAC45119), iron-sulfur cluster-binding protein of CO-induced hydrogenase.

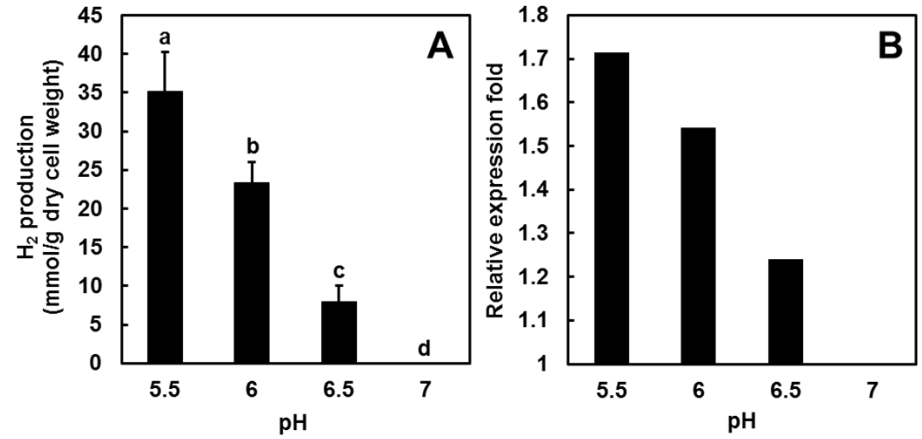

Fig. 2-5. Effects of pH of the medium on hydrogen production and expression of *hyf*G gene of *Vibrio tritonius* AM2. Culture condition: *Vbrio tritonius* AM2 was batch cultured at 37°C for 12 hour. (A) hydrogen production was measured after 12 hour culture, error bars represent SD, n=3. Statistically significance (P<0.05) is indicated by letters; (B) Expression levels were normalized to the pH 7. n=1.

Table 2-1. Predicted function and characteristics of gene products encoded by FHL-Hyp gene cluster of *Vibrio tritonius*

Gene product	Molecular Mass	Predicted function	Predicted membrane helices	Amino acid sequence identity		Predicted localization
Vt	*Vt* / E*c* (kDa)		*Vt* / *Ec*	*Vt* / *Ec*	*Vt* /*Vf* (%)	*Vt* /*Ec*
HyfA	21.6 / 22.2	Electron carrier activity	nd	50	78	Ct / Ct
HyfB	72.6 / 72.6	ATP synthesis coupled electron transport	17 / 16	53	50	CM / CM
HyfC	34.4 / 34.4	Oxidoreductase activity	8 / 8	57	69	CM / CM
HyfD	51.2 / 51.8	ATP synthesis coupled electron transport	12 / 13	62	nd	CM / CM
HyfE	23.7 / 23.4	Oxidoreductase activity	5 / 6	52	nd	CM / CM
HyfF	56.6 / 56.8	ATP synthesis coupled electron transport	13 / 12	53	nd	CM / CM
HyfG	66.0 / 63.4	Hydrogenase activity (Large subunit)	nd	68	84	Ct / Ct
HyfH	21.6 / 20.1	Electron carrier activity	nd	55	80	Ct / CM
HyfI	29.6 / 28.1	Hydrogenase activity (Small subunit)	nd	64	82	- / -
HyfJ	16.5 / 15.6	Formate hydrogenlyase maturation protein	nd	45	74	- / CM
HycI	16.8 / 17.1	Processing of C-terminal end of HycE (and HyfG?*)	nd	53	70	- / -
HydN	19.3 / 19.0	Electron transport protein***	nd	54	78	CM / Ct
FdhH	79.6 / 79.4	Foemate dehydrogenase	nd	66	78	Ct /
FhlA	76.0 / 78.5	Transcriptional activator	nd	41	58	Ct / Ct
FdhD	30.5 / 30.6	Required for formate dehydrogenase activity	nd	52	59	Ct / Ct
HypF	92.0 / 82.1	CN/CO delivery**	nd	38	55	CM / Ct
HypC	9.3 / 9.7	Chaperone/maturation**	nd	35	64	- / -
HypD	41.4 / 41.4	Ni incorporation/maturation**	nd	46	74	Ct / Ct
HypE	35.5 / 33.7	Purine derivative binding ? **	nd	46	67	Ct / Ct
HypA	12.2 / 13.2	Ni incorporation/maturation**	nd	32	60	Ct / Ct
HypB	43.3 / 31.6	Nickelin/Ni insertion**	nd	67	79	Ct / Ct

Vt: *Vibrio tritonius*, *Ec*: *Escherichia coli*, *Vf*: *Vibrio furnissii*. Methods for predictions of protein function and characteristics are described in Materials and Methods.

Table 2-2. Nucleotide sequence of the primers used for the reverse transcriptional studies

Primers	Sequence
hypBRT	GTGAGCGAGTTGATGCTGCT
fhlART	TTAGTGAGCGAGTTGATGCTGC
hyf5F	TAGGCAAGTTCTTGTCCTGC
hyfCR	AGACCTAACTTGACCATCGC
hyfAF	ATGAAGAGCTTTGTGATTGCAG
hyfDR	CGCCAGTTGAGTAATGGTTGAG
hyfDF	GGTCAGTGCTTATTTGCACG
hyfHR	TTGAGCTCAGGTTTACCACG
hyfGF	CGATTGAGCAATACAGCGTG
fdhFR	TTATGCCTGTTCAACGTGTGATC
fhlAF	ATGAGTGTTGAGTTGTCACCC
fdhDR	ATCAACCGGTTCAAACCCTG
hypFF	ATCGATTAACGATACCGCTGAC
hypDR	AAGATAACGCATGCGAGGTGC
hypEF	AACACATCACTGGTGTACGTGG
hypBR	TTGTTCTGCCATCTCCACC
hypDF	TGTTTAGTTCGACATGCCG
hyf3R	AGATGGGATCGATAGCCTC
hyfG1F	CGTGCGGCGACTTATGC
hyfG1R	CATCGGCCACTGTGTTACCA

CHAPTER IV

Comparative physiology and genomics of hydrogen-producing vibrios

ABSTRACT

Occurrence of Hyf-type FHL complex was first proposed in *E. coli* in 1994 based on sequence comparisons. The FHL is estimated to be a proton-translocating energy-conserving [NiFe]-hydrogenase. Although the structure of FHL is similar to that of complex I, silent gene expression in *E. coli* have caused delays in unveiling genetic and biochemical features of FHL complex. Recently, the full set of genes required for Hyf-type FHL synthesis has been found in *V. tritonius*, which is a higher H_2 producer than *E. coli*. Here we investigated the physiological characteristics, genome comparisons, and gene expressions to elucidate the genetic backgrounds and how Hyf-type FHL correlates with the high H_2 production of *V. tritonius*. Physiological comparisons among seven H_2-producing vibrios revealed that *V. porteresiae* and *V. tritonius*, grouped as the Porteresiae clade, showed greater abilities in H_2 production than the other species. The structures of FHL-Hyp gene clusters were closely related in both Porteresiae species, but differentiated from those of the others with the presence of *hupE*, a possible nickel permease gene. Interestingly, deeper genome comparisons revealed co-presence of nickel ABC transporter genes (*nik*) with the Hyf-type FHL gene only on the genome of the Porteresieae clade species. Active primary Ni transport might be one of the key factors characterizing higher H_2 production in *V. tritonius*. The first global transcriptome of *V. tritonius* cells after being stimulated with formate showed significant up-regulation of the FHL gene cluster. Formate is likely to be a gene expression control factor in the gene clusters of *V. tritonius* with some similarity to the formate regulon of the *E. coli* Hyc-type FHL gene cluster.

INTRODUCTION

Vibrios are *Gammaproteobacterium* living in a wide range of aquatic environments, and often associated with plant and animal hosts [Thompson *et al*., 2005; Sawabe *et al*., 2007; Sawabe *et al*., 2013]. The family *Vibrionaceae* is recognized as one of the most diverse bacterial groups both genotypically and phenotypically. Currently, more than 170 species with valid nomenclature are assigned to the family *Vibrionaceae* [Association of Vibrio Biologists website, http://www.vibriobiology.net/] showing various unique physiological findings in nitrogen (N_2) fixation, phototrophy, and H_2 production machinery [Gomez-Gil *et al*., 2014].

The family *Vibrionaceae* consisting of at least eight polyphyletic lineages, and metabolically versatile species/strains [Thompson *et al*., 2005]. Until now, the H_2 production

phenotype has been experimentally confirmed in at least 10 species of vibrios belonging to five clades; *Vibrio fluvialis* [Lee *et al*., 1981] and *Vibrio furnissii* [Brenner *et al*., 1983] (Cholerae clade), *Vibrio gazogenes* [Harwood, 1978; Baumann *et al*., 1984], *Vibrio aerogenes* [Shieh *et al*., 2000], *Vibrio ruber* [Shieh *et al*., 2003], and *Vibrio rhizosphaerae* [Kumar *et al*., 2007] (Gazogenes clade), *Vibrio mytili* [Pujalte *et al*., 1993] (Harveyi clade), *Vibrio aphrogenes* [Tanaka *et al*., 2017] (Rumoiensis clade), and *Vibrio porteresiae* [Rameshkumar *et al*., 2008] and *Vibrio tritonius* [Sawabe *et al*., 2013] (Porteresieae clade). *V. tritonius* was described as an AM2 as a type strain isolated from gut of a sea hare Aplysiomorpha [Sawabe *et al*., 2013; Gomez-Gil *et al*., 2014]. The Multilocus sequence analysis (MLSA) with 8-housekeeping genes phylogeny revealed that *V. tritonius* shares a common ancestry with *V. porteresiae*, which was isolated from wild rice collected from the Pichavaram mangroves in India [Rameshkumar *et al*., 2008]. Interestingly, *V. tritonius* exhibited high H_2-producing ability during mixed acid fermentation where the maximum H_2 molar yield corresponded to approximately 85% of the theoretical yield even under saline conditions [Matsumura *et al*., 2014]. The discovery of *V. tritonius* provided better clues to direct the genetical, ecophysiological and evolutionary studies of H_2 producing *Vibrio* species.

H_2 production was achieved by H_2-evolving enzymes, hydrogenase and nitrogenase. Hydrogenases catalyze the simple reaction; $2H^+ + 2e^- \rightleftarrows H_2$. On the other hand, nitrogenases catalyze the reduction of N_2 to NH_3 followed by the chemical reaction; $N_2 + 8H^+ + 8e^- \rightarrow 2NH_3 + H_2$. Hydrogenases can be classified into [NiFe]-hydrogenases, [FeFe]-hydrogenases, and [Fe]-hydrogenases based on the distinctive functional core containing catalytic metal centers [Vignais *et al*., 2004; Nicolet and Lemon, 2000]. [NiFe]-hydrogenases, which are widespread in the domain of *Bacteria* and *Archaea*, can ecologically contribute to the H_2 metabolism either aerobically or anaerobically [Vignais *et al*., 2007] and also in adaptation to critical acidic environments [Mnatsakanyan *et al*., 2004; Noguchi *et al*., 2010]. Facultative anaerobes produce H_2 via the [NiFe]-hydrogenase assigning group 4 [Vignais *et al*., 2001, Vignais and Billoud, 2007; Schmidt *et al*., 2011]. *E. coli* possesses two kinds of group 4 [NiFe]-hydrogenase; hydrogenase-3 (Hyc) complex encoded by the *hycABCDEFGHI* operon and hydrogenasea-4 (Hyf) complex encoded by *hyfABCDEFGHIJ-hyfR-focB* operon [Vignais *et al*., 2001, Vignais and Billoud, 2007]. Hyc complex and formate dehydrogenase (Fdh-H) form FHL which is capable of catalyzing the cleavage of formate to H_2 and carbon dioxide during the mixed acid fermentation. On the other hand, Hyf complex has the integral-membrane subunits (HyfDEF), which have no direct counterparts in the Hyc complex, and was proposed to constitute a proton-translocating FHL with Fdh-H [Andrew *et al*., 1997]. The biosynthesis, regulation, and

ecophysiological of Hyc-type FHL have been well described [Sawers, 1994; Sawers, 2005; Casalot and Rousset, 2001; Vignais *et al*., 2001, Vignais and Billoud, 2007], but we have been less able to understand those of Hyf complex. In *E. coli*, Hyc complex mainly achieved H_2 production at acidic pH levels or in the presence of extracellular formate, whereas Hyf complex is believed to be silent [Self *et al*., 2004]. The other studies proposed that Hyf complex catalyzes the H_2 production and ion transport across the membrane at a slightly alkaline pH, and Fdh-H activity was partially dependent on Hyf complex and FoF1-ATPase [Bagramyan *et al*., 2002].

As in *E. coli*, *Vibrio s*pecies can perform mixed acid fermentation. The major reducing equivalents for H_2 production is also pyruvate, which is cleaved to acetyl coenzyme A and formate, and FHL converts formate to H_2 and CO_2 [Böck and Sawers, 1996; Matsumura *et al*., 2014; Gomez-Gil *et al*., 2014]. Our previous gene mining and quantitative RT-PCR analysis revealed that *V. tritonius* [NiFe]-hydrogenase is assigned to the Hyf complex, and this enzyme complex mainly contributes to the H_2 production under acidic conditions [Matsumura *et al*., 2015]. However, the lack of their genome sequences has resulted in limited understanding of the regulation and ecophysiological roles of their H_2 production abilities. To better understand the regulation and ecophysiological role of H_2 production in vibrios, we need further investigation into the H_2-producing ability from genomic and transcriptomic insights.

In this study, we performed the comparative genomics between the gap-closed *V. tritonius* genome and the draft genomes of the other H_2-producing species belonging to the Porteresieae, Gazogenes, and Cholerae clade, and transcriptomic profiling of *V. tritonius* to elucidate the key genetic factor related to effective H_2 production achieved by Hyf-type FHL of *V. tritonius*. Furthermore, genome analysis provided us with the evolutional and physiological understanding of Hyf-type FHL in vibrios. We expected that vibrios, which are one of the largest and most diverse bacterial groups distributed in a wide range of aquatic environments, would provide us with a better understanding of the ecophysiological role of H_2 metabolism and gene evolution.

MATERIALS AND METHODS

Bacterial strains and culture condition

Bacterial strains used in this study were *V. tritonius* AM2 (=JCM 16456^T), *V. porteresiae* MSSRF30^T, *V. gazogenes* ATCC 29988, *V. rhizosphaerae* MSSRF3^T, *V. ruber* LMG 23124^T and *V. aerogenes* LMG 19650^T. These strains were precultured aerobically in marine broth (0.5% (w/v) polypeptone, 0.1% (w/v) yeast extract and 75% (w/v) artificial seawater composed of 3% (w/v) NaCl, 0.07% (w/v) KCl, 0.53% (w/v) $MgSO_4 \cdot 7H_2O$, 1.08% (w/v) $MgCl_2 \cdot 6H_2O$, and 0.13% (w/v) $CaSO_4 \cdot 2H_2O$) with shacking of 130 rpm at 30°C overnight. Batch culture

experiments were conducted using an addition of 1 mL of the preculture solution to 100 mL of marine broth containing 5% (w/v) mannitol and 100 mM 3-morpholinopropanesulfonic acid (MOPS) (Dojindo, Kumamoto, Japan) in silicon rubber-capped glass bottles, which were stirred with a magnetic stirrer (RO 10 power IKAMAG, IKA, Staufensee, Germany). The temperature was maintained at 30°C and the pH of the medium was adjusted to 6.0 using pH controller system (DT-1023P, ABLE, Tokyo, Japan) with an electrode (FermProbe pH electrodes, Broadly-James Corp., Branford, USA) by adding 5 M NaOH.

Hydrogen and formate producing ability measurements

The fermentative gas was collected in an aluminum bag (GL Sciences Inc., Tokyo, Japan) connected by a silicon cap via the PharMed tube, and was then measured by displacement of water. The volume of H_2 production was determined by analyzing the H_2 composition of the head space of the bottles using gas chromatography (GC2014, Shimadzu, Kyoto, Japan) with a thermal conductivity detector and Shincarbon ST (Shinwa Chemical Industries Ltd., Kyoto, Japan). The operational temperatures of the injection port, oven and detector were 200, 40 and 200ºC, respectively. Formate concentration was measured using a F-kit (Roche Diagnostics, Mannheim, Germany). Mannitol concentration was measured by HPLC with reflective index detector and TSKgel Amide-80 column (TOSOH, Tokyo, Japan) using 75% acetonitrile as a mobile phase. Cell density in the medium was measured with optical density at 620 nm.

Genome analysis

The sequences of chromosome 1 (Chr. 1) and 2 (Chr. 2) of *V. tritonius* AM2 were reported in CHAPTER III (accession numbers are AP014635 and AP014637, respectively). Functions of all predicted CDSs were manually annotated on the basis of the top 30 results of BLASTx search. Functions of all predicted CDSs were manually annotated on the basis of the top 30 results of BLASTx search. Draft genome sequences of *V. porteresiae* MSSRF30 ^{T}, *V. gazogenes* ATCC 29988^{T}, *V. rhizosphaerae* MSSRF3 ^{T}, *V. ruber* LMG 23124 ^{T} and *V. aerogenes* LMG 19650 ^{T} were newly obtained using a 454 GS FLX Titanium sequencer (Roche Diagnostics, Branford, USA), and Newbler software version 2.3 (454 Life Sciences, Branford, USA) was used for sequence reads assembling. Operation of genome analysis was mainly performed using In Silico Molecular Cloning software (In silico biology, Inc., Yokohama, Japan). Comparative genomics of the seven *Vibrio* species was performed on the basis of re-annotated CDSs using RAST version 2.0 (http://rast.nmpdr.org/rast.cgi) [Overbeek *et al*., 2014] with classic RAST annotation scheme. Sequence based comparison was performed using the SEED Viewer version 2.0.

RNA-Sequencing

The expression profiles of *V. tritonius* cells metabolizing mannitol and formate were obtained by RNA-Seq. The fermentation was carried out at 37°C in marine broth; 1) supplemented with 5% (w/v) mannitol, 2) supplemented with 50 mM formate for 1 hour before sampling for RNA extraction, and 3) without supplementation. The pH of medium was maintained at 6.0 using a pH controlling system as described above. Total RNA was extracted using TRIzol LS regent (Life Technologies, Carlsbad, USA) according to the manufacturer's instructions. The extracted total RNA was treated using RNase-free DNase (Promega, Madison, USA) and was then purified using RNeasy Mini kit (Qiagen Hilden, Germany). Depletion of rRNA was conducted using Ribo-Zero™ rRNA Removal Kits (Bacteria) (Epicentre, WI, USA). The cDNA libraries were constructed using TruSeq RNA library preparation kit (Illumina, San Diego, CA). The sequencing was conducted using Illumina HiSeq 2500 (Illumina, Inc., San Diego, CA. USA). The high quality reads, which pathed Q30 filter, were mapped to the reference genomes of *V. tritonius* AM2 using Bowtie2 [Langmead and Salzberg, 2012] and SAMtools [Li *et al*., 2009]. Read counts were calculated using Artemis Entry Edit Release 16.0.0 [Berriman and Rutherford, 2003], and differentially expressed genes (DEGs) were detected on the basis of the read counts by exact tests (P<0.05) and were evaluated using package edgeR [Robinson *et al*., 2010]. FDR <0.05 and log fold change >= 2.0 were used as the thresholds to determine the significance of gene expression difference. Mapping feature was visualized using IGV software [Thorvaldsdóttir *et al*., 2013].

Nitrogenase activity measurements

Nitrogenase activity of *V. tritonius* and *V. porteresieae* was determined by the acetylene reduction assay *in vivo*. The bacterial strains were cultivated by stab culture on a modified N_2-free medium consisting of (l^{-1}): 5 g sucrose; 3 g mannitol; 0.8 g K_2HPO_4; 0.2 g KH_2PO_4; 0.2 g $MgSO_4 \cdot 7H_2O$; 20 g NaCl; 0.02 g $CaCl_2$; 28 mg $Na_2FeEDTA$; 25 mg $Na_2MoO4 \cdot 2H_2O$; 2 g agar and 0.02g yeast extract [Gyaneshwar *et al*., 2001]. The pH of the medium was adjusted to 7.0 by adding NaOH. The acetylene concentration in the head space of the vial was adjusted to 5% (v/v), and the amount of ethylene produced was measured by gas chromatography (GC2014, Shimadzu, Kyoto, Japan) with a flame ionization detector and Shincarbon ST (Shinwa Chemical Industries Ltd., Kyoto, Japan).

RESULTS

Comparison of hydrogen-producing abilities

We compared the H_2-producing abilities of the seven species of vibrios; four (*V. gazogenes*, *V. rhizosphaerae*, *V. ruber* and *V. aerogenes*) in the Gazogenes clade, and one (*V. furnissii*) in the Cholerae clade, and two (*V. porteresiae* and *V. tritonius*) in the Porteresiae clade. The batch culture experiments at pH 6.0 at 30°C confirmed the molar yields of H_2 and formate that are precursors of H_2, when mannitol was supplied as a carbon source (Fig. 3-1). *V. porteresieae* and *V. tritonius* showed higher molar yields of H_2 compared with the other species, which corresponds to 1.59±0.13 and 1.38±0.07 mol/mol mannitol, respectively. The H_2 molar yields of *V. gazogenes*, *V. rhizosphaerae*, and *V. ruber* were lower than those of the Porteresieae clade species (0.72±0.08, 0.48±0.06, and 0.50±0.04 mol/mol mannitol, respectively), but the formate molar yields showed almost similar levels to the Porteresieae clade species. *V. aerogenes* and *V. furnissii* showed significantly lower molar yields of H_2 than the other species, but the formate yields of *V. aerogenes* and *V. furnissii* were higher than other *Vibrio* species, which corresponds to 0.95±0.06 and 0.88±0.05 mol/mol mannitol, respectively.

Comparison of FHL-Hyp gene clusters encoded in *Vibrio* genomes

To investigate the genes responsible for affecting H_2 productivity, genome sequences of the six *Vibrio* species were compared on the basis of *V. tritonius* gap-closed genomes. Through our manual annotation, total 3094 and 1691 CDSs were annotated on the Chr. 1 and the Chr. 2, respectively, and 39% of the total CDSs were determined as hypothetical proteins. Subsequently, we newly obtained the draft genome sequences of the other six H_2-producing species by 454 pyrosequencing (Table 3-1). We identified the gene set related to FHL biosynthesis in the genomes of the seven H_2-producing vibrios (Fig. 3-2). The other H_2-evolving hydrogenase genes were not encoded in the drat genome sequences of the six *Vibrio* species in common with *V. tritonius*. The total length of the gene sets encoded in genomes of Porteresieae and Gazogenes clade species were approximately 24 kb, but the *V. furnissii* FHL-Hyp gene cluster corresponded to approximately 20 kb length. The gene order was also closely similar in the Porteresieae clade and Gazogenes clade species, except for *V. aerogenes* and *V. furnissii*, which exhibited lower activity of H_2 production. The FHL-Hyp gene cluster of *V. aerogenes* and *V. furnissii* exhibited significant differences to those of other vibrios. *V. aerogenes* FHL-Hyp gene cluster was separately located on two contigs; contig 1 (*hyfABCDEFGHIJ* and *hycI*) and the contig 4 (*hydN*, *fdhF*, *fhlA*, *fdhD* and *hypFCDEAB*). We confirmed that *V. furnissi* FHL-Hyp gene cluster did not possess the three genes homologous to the *hyfDEF* encoding integral membrane subunits,

indicating that the hydrogenase complex does not have proton-translocation properties, as in the *E. coli* Hyc complex [Matsumura *et al*., 2015]. Furthermore, no apparent mobile elements were present in the flanking region of the FHL-Hyp gene cluster of *V. tritonius*. In addition, the codon usage patterns of the FHL-Hyp gene cluster and the whole genomes were closely similar (Fig. 3-3).

Furthermore, we found that the hydrogenase/urease accessory protein gene (*hupE*/*ureJ*) was located between the *fdhD* gene and *hypF* gene in the genome of the Gazogenes and Cholerae clade species (Fig. 3-2 and Table 3-1). The *hupE*/*ureJ* gene encodes transmembrane nickel permease, and is often encoded within [NiFe]-hydrogenase gene cluster [Rowe *et al*., 2005; Rodionov *et al*., 2006]. Any homologues of *hupE*/*ureJ* genes were not identified in the two Porteresieae clade species (Table 3-1). On the other hand, CDSs comparison using the SEED Viewer indicated that intact *nikR-nikABCDE* (*V. tritonius*, vtAM2_cI_1277-1282; *V. porteresieae*, gene_738-743 at contig 3) encoding nickel-responsive regulator and nickel ABC-transporter, and nickel/cobalt transporter (NiCoT permease) genes (*V. tritonius*, vtAM2_c1_1622; *V. porteresieae*, gene_1130 at contig 5) were annotated in the genomes of the two Porteresieae clade species. The gene order in the *nik* operon of Porteresieae clade species was also the same as *E. coli*'s (Fig. 3-4). *V. gazogenes*, *V. ruber*, *V. rhizosphaerae*, and *V. furnissii* draft genomes did not encode the Nik and NiCoT genes. On the genome of *V. aerogenes*, *nikABCD* genes were annotated, but the adjacent gene was annotated as *oppF* gene encoding oligopeptide transport ATP-binding protein. Both nickel and oligopeptide ABC transporter belongs to the Opp/Dpp/Nik family of proteins, all components of ABC transporter show amino acid sequence similarity [Remy *et al*., 2013]. In addition, the *nikR* gene encoding repressor of *nik* operon was not encoded in the genome of the Gazogenes and Cholerae clade species (Table 3-1). Therefore, *V. aerogenes* do not have the complete set of genes responsible for the nickel ABC transporter system as with other Gazogenes clade species.

Transcriptional profiling of mannitol and formate-supplemented *Vibrio tritonius*

To understand the genome-wide transcriptional profile of *V. tritonius* AM2 during H_2 production, RNA-Seq was performed using the cells metabolizing mannitol and formate as substrates, respectively. The cDNA libraries were also derived using RNA prepared form logarithmic growth cells, which consumed 50% of the mannitol. To select the formate concentration for transcriptomic analysis, formate effect against *V. tritonius* was tested. The efficient consumption of formate was observed in the medium containing 25 mM and 50 mM formate (Fig. 3-5A). The 50 mM formate-supplemented cultivation demonstrated the more

effective H_2 production of *V. tritonius* AM2 than the 25 mM formate-supplemented cultivation through the 96-hour cultivation (Fig. 3-5B). Using these results, 50 mM formate-supplemented condition was chosen for RNA-Seq analysis. To investigate the formate effects on transcriptional profiles, the cDNA library was prepared from the exponentially grown-cells supplemented in 50 mM formate for 1 hour before sampling for RNA extraction, and also without supplementation (Fig. 3-6). Through HiSeq sequencing, approximately 23.3 to 24.1 million high quality reads per sample were obtained, and 77.6-81.8% and 16.3-20.8% were mapped to Chr. 1 and Chr. 2, respectively. The variance analysis of package edgeR was used to systematically search DEGs in formate- and mannitol-supplemented conditions on the basis of the criteria of FDR <0.05 and fold change >= 2.0. A total of 147 and 71 genes were detected as

DEGs in mannitol- and formate-supplemented test conditions, respectively, and 26 genes were common in both conditions (Table 3-2 and 3-3). Among the identified DEGs, 62 and 21 genes were upregulated by mannitol and formate supplementation, respectively.

First, the genes which showed differential expression by addition of mannitol were described. As expected, three genes composed of *mlt* operon (vtAM2_cII_1648-1650), and sugar transporter protein gene (vtAM2_cI_1391) were significantly overexpressed by >7.4-fold, indicating the activation of mannitol transporting. On the other hand, the genes encoding several substrate uptake systems were significantly down-regulated in mannitol metabolism; TRAP-type C_4-dicarboxylate transport system (vtAM2_cI_2103-2105), L-arabinose ABC transporter (vtAM2_cI_3030-3033), amino acid transporter and metabolism-related genes (vtAM2_cI_1964-1966, vtAM2_cII_0365, 1321, 1324, 1325, 1679), glycerol uptake-related genes (vtAM2_cII_1239 and 1240), and putative sodium/sulfate symporter (vtAM2_cI_2764), suggesting that carbon catabolite repression regulates the transcription of the genes.

By mannitol supplementation, the genes consisted of the FHL-Hyp gene cluster except for *fdhD* and *hypB* were upregulated by >2.8-fold, and the 11 genes (vtAM2_c1_0416-0425, and vtAM2_c1_0431) encoding hydrogenase structural and maturation protein were determined to be DEGs. In addition, the *nikBCDE* genes (vtAM2_cI_1279-1282) and NiCoT genes (vtAM2_cI_1622) were more than 2.0-3.4-fold upregulated in mannitol metabolism relative to the control, although these genes were not predicted as DEGs.

Respiratory chain-related genes, such as three succinate dehydrogenase genes (vtAM2_cI_0802-0804), and cytochrome *o* ubiquinol oxidase genes (vtAM2_cII_0009-0012) were significantly downregulated due to anaerobic fermentative conditions, but FoF1 ATP synthase genes (vtAM2_cII_0680-0685) and Na^+/H^+ antiporter (NhaD type) (vtAM2_cII_1637) were significantly upregulated in mannitol metabolism. The genes (vtAM2_cII_1668-1669)

encoding the components of the Fe^{3+}-siderophores transport system were upregulated >7.8-fold in mannitol metabolism. Iron is an essential element for bacterial growth. Actually, the genes (vtAM2_cI_0873) encoding bifunctional acetaldehyde-CoA/alcohol dehydrogenase, which were iron containing enzyme were expressed significantly higher in mannitol metabolism.

Subsequently, the transcriptional profile when formate was added is described here (Table 3-3). In the FHL-Hyp gene cluster, the *hyfABCD* (vtAM2_cI_0416-0419) and *hydN* genes (vtAM2_cI_0427) in the FHL-Hyp gene cluster were also upregulated by 28.5, 15.3, 8.2, 2.9, and 5.3-fold, respectively, compared to the control conditions. Especially, the *hyfAB* genes located at the 5' side of FHL-Hyp gene cluster and the *hydN* genes which might share transcriptional units with the *fdhF* gene were significantly overexpressed by adding extracellular formate. These results indicate that the expression of the FHL-Hyp gene cluster is regulated by formate. The transcriptional expression change of nickel transporter (Nik and NiCoT) genes were not observed in these test conditions.

Furthermore, the mapping feature provided the transcriptional units images, that might be composed of at least four transcriptional units; *hyfABCDEFGHIJ-hycI*, *hydN-fdhF*, *fhlA-fdhD*, and *hypFCDEAB* (Fig. 3-7). Formate supplementation induced significant upregulation of the *mntH* gene (vtAM2_cI_1059), which encodes manganese transporters.

Nitrogenase genes and its activity in hydrogen-producing vibrios

V. tritonius, *V. porteresieae*, and *V. aerogenes* genomes encode *nif* genes for biosynthesis of nitrogenase. In *V. aerogenes* draft genome sequences, *nifHDKTX* genes were encoded on the contig 1 and *nifENXUSVZMQFBAL* genes and *rnfABCDGE* genes were encoded on the contig 4. In addition, *rnfABCDGE* genes encoding Rnf proteins are located near to the *nif* regulon (*nifQFBAL*) in the Chr. 2. To confirm the *in vivo* N_2 fixation potential of *V. tritonius*, the acetylene reduction activity was tested. *V. tritonius* was able to reduce acetylene to ethylene, indicating the nitrogenases were active under the N_2-limited conditions. The ethylene production rates of *V. porteresieae* and *V. tritonius* were 8.5 and 4.2 nmol/mL/h, respectively.

DISCUSSION

Many accessory genes related to synthesis and maturation of the [NiFe]-hydrogenases. Nickel uptake genes play an important role in the anaerobic biosynthesis of nickel-dependent enzymes such as [NiFe]-hydrogenases [Eitinger and Mandrand-Berthelot, 2000; Rowe *et al*., 2005]. Uptake of Nickel across the cytoplasmic membrane is mainly mediated by high-affinity nickel transporters which are classified into two broad groups, single-component nickel

permeases assigned to the NiCoT families and HupE/UreJ families, and nickel ABC-transporter (Nik system) [Rodionov *et al*., 2005; Brito *et al*., 2010]. The nickel permeases, HoxN and HupE, contribute to biosynthesis of the [NiFe]-hydrogenases in *Ralstonia eutropha* [Eitinger and Mandrand-Berthelot, 2000] and *Rhizobium leguminosarum* [Brito *et al*., 2010], respectively. Nickel ABC-transporter is required for the biosynthesis of [NiFe]-hydrogenases in *E. coli* [Rossmann *et al*., 1994]. Compared to the Gazogenes and Cholerae clade species, the Gazogenes clade species exhibited higher H_2 production. Interestingly, the Porteresieae clade species possess the Nik system and NiCoT which were not present in the Gazogenes and Cholerae clade species. Recently, genome sequencing of *Vibrio aphrogenes* which is a H_2-producer belonging to Rumoiensis clade revealed that the FHL-Hyp gene cluster also involved the *hupE/ureJ* gene [Tanaka *et al*., 2017]. The H_2 producing ability of *V. aphrogenes* is lower than those of Porteresieae clade species (unpublished data). Our study suggested that three types of nickel transporter contributed to the hydrogenase activities of vibrios, and the difference might relate to their H_2 production ability. The two Porteresieae clade species possessed a more efficient extracellular nickel transporting system for hydrogenase biosynthesis than the Gazogenes and the Cholerae clade species. The transcriptional profiling of *V. tritonius* did not detect the significant upregulation of the Nik and NiCoT genes with both mannitol and formate addition. Because *V. tritonius* cultured in marine broth with mannitol exhibited high H_2 producing ability, the medium contained enough amounts of nickel for biosynthesis of the [NiFi]-hydrogenases. In order to gain a deeper understanding of the link between H_2-producing ability and nickel transporter systems, gene engineering approaches were needed for *V. tritonius*.

Andrews *et al*. proposed the schematic model of the respiratory-linked proton translocating formate oxidation pathway by Hyf-type FHL, which differs from the non-energy conserving FHL (Hyc-type FHL) in *E. coli* [Andrews *et al*., 1997]. Later, Bagramyan *et al*. reported a possibility of the physiological link between Hyf complex and FoF1-ATP synthase in H_2 production of *E. coli* at slightly alkaline pH [Bagramyan *et al*., 2002]. The transcriptomic profiling of *V. tritonius* revealed that the expression of the genes encoding each subunit of the FoF1 ATP synthase, Na^+/H^+ antiporter and Hyf complex were significantly upregulated during fermentation of mannitol, although the genes responsible for respiratory chain complexs were significantly downregulated (Table 3-2). The transcriptional profile of *V. tritonius* also supported the energy-conserving model of Hyf-type FHL that the proton motive force generated by proton-translocating activities of Hyf complex might achieve energy conservation during mannitol fermentation. *V. tritonius* converted H_2 from mannitol more efficiently than *E. coli* [Matsumura *et al*., 2014]. Theoretically, high conversion ratio of H_2 corresponding to 1.4-1.7

mol/mol hexose observed in *V. tritonius* [Matsumura *et al*., 2014] (Fig. 3-1) indicates that translocation ratio of proton is also high because the proton translocation is thought to couple with H_2 production via Hyf-type FHL. Considering the theoretical yields of ATP generated by substrate-level phosphorylation (2.0 mol ATP/mol hexose), the significant activity of Hyf-type FHL might contribute to the energy metabolism of *V. tritonius* under anaerobic conditions.

The previous our study revealed that *V. tritonius* genomes encoded an intact gene set responsible for the biosynthesis of energy conserving hydrogenase complex sharing homology with the *E. coli* Hyf complex [Matsumura *et al*., 2015]. We confirmed that hydrogenase assigned to H_2-evolving, proton-translocating and energy-coupling [NiFe]-hydrogenase (group 4) is only spread in the H_2-producing *Vibrio* species assigned to the Porteresieae and Gazogenes Clade. [NiFe]-hydrogenases (group 4) are thought to share common ancestor with the NADH:quinone oxidoreductase (respiratory complex I) [Moparthi and Hägerhäll, 2011; Marreiros *et al*., 2013; McDowall *et al*., 2014]. In many halophilic and pathogenic bacteria, Na^+-NQR which is associated with aerobic respiratory metabolism exhibits no homology with the subunits of Nuo and complex I [Baradaran *et al*., 2013; Barquera, 2014]. *Vibrio cholerae* use Na^+-NQR as the sole energy-conserving NADH dehydrogenase [Barquera *et al*., 2002; Barquera, 2014]. Therefore, H_2-producing vibrios belonging to the Porteresieae and Gazogenes clade have two phylogenetically distinct respiratory chain complex systems; Na^+-NQR for aerobic respiration and proton-translocating hydrogenase which might contribute to energy conservation during fermentation.

One of the important aspects of this study is the evolutionally position of Hyf-type FHL genes in vibrios. Recent study reported that the *V. aphrogene* 66-kb genome region containing the FHL-Hyp gene cluster was replaced by RIO1 family protein gene in non H_2-producing species in Rumoiensis clade species [Tanaka *et al*., 2017]. This replacement might have occurred as a comparatively recent event. Codon usage pattern, however, showed that the Hyf-type FHL genes of *V. tritonius* might not be acquired as a recent horizontal transfer event. We consider that the Hyf-type FHL and its formation machinery might be common in ancient H_2-producing vibrios.

RNA-Seq provided the transcriptional profiling of the FHL-Hyp gene cluster of *V. tritonius*, which metabolize mannitol and formate. The FHL-Hyp gene cluster corresponding to 24-kb is formate regulon, which is composed of at least four transcriptional units. This is the first study on the expression profiling of the energy-conserving FHL genes. We previously predicted two possible terminators on the downstream of the 3' end of *fdhF* and *hypB* in the FHL-Hyp gene cluster [Matsumura *et al*., 2015]. These terminator positions were likely to be supported by the

expression profiles. In addition, the transcriptional prolife predicted that the terminator site might be located at 3’ end of the *hycI* and *fdhF* genes. In *E. coli* FHL-1, formate regulon include three transcriptional units; *hyc* operon, *hyp-fhlA* operon, and *fdhF* gene [Sawers, 1994; Skibinski *et al*., 2002]. Therefore, the predicted formate regulon of *V. tritonius* were regulated in a different manner from the *E. coli* formate regulon.

V. porteresiae is able to fix N_2 [Rameshkumar *et al*., 2008]. In this study, we succeeded in detecting nitrogenase activity of *V. tritonius* by acetylene reduction assay, indicating the nitrogenase genes were actively regulated under N_2 limited conditions. In N_2 fixer, uptake [NiFe]-hydrogenases (Group I) are induced when nitrogenase is synthesized and produces H_2. Because N_2 fixation by nitrogenase is a reaction to consuming a large amount of ATP, the uptake [NiFe]-hydrogenases oxidize H_2 produced by nitrogenases is used for for energy recycling. However, the genomes of Porteresieae clade species do not encode any H_2 uptake hydrogenase genes. Therefore, other energy supporting system may contribute to the N_2 fixation of the Porteresieae clade species.

V. tritonius was isolated from the gut of marine invertebrate (*Aplysia kurodai*) [Sawabe *et al*., 2013]. Our previous study showed that *V. tritonius* directly consumed mannitol contained in brown algae and produced H_2 with a 70% conversion ratio [Matsumura *et al*., 2014]. Presumably, the powerful H_2 production activity coupling with energy conservation might contribute to the niche of *V. tritonius i*n the gastrointestinal environment of *A. kurodai*. In addition, the genome of Porteresieae clade species encodes nitrogenase genes. Associations of host organisms with N_2-fixing bacteria occur in many environments [Kneip *et al*., 2007]. Zehr *et al*. reported that copepod gut microflora contain microorganisms with potential for N_2 fixation [Zehr *et al*., 1998]. They suggested that the invertebrate gut may provide an unexpected refuge with suitable conditions for anaerobic nitrogen fixation [Zehr *et al*., 1998]. Considering the presence of FHL (pH homeostasis) and nitrogenase encoded in *V. tritonius* and their ecological background, we currently predict the symbiotic-like relationship between *A. kurodai* and *V. tritonius*. To determine the ecophysiological roles of *Vibrio* FHL and nitrogenase in their niche, further metagenomics and metatranscriptomic survey are needed.

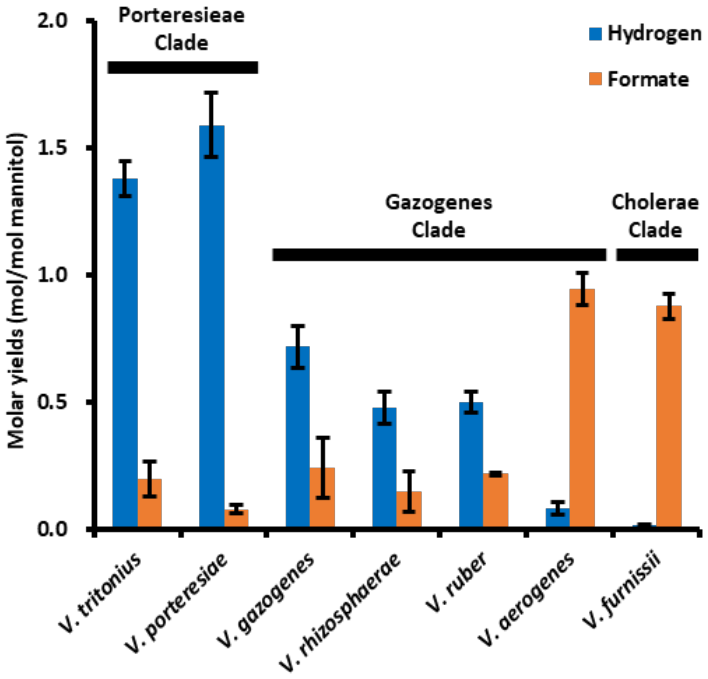

Fig. 3-1. Comparison of molar yields of hydrogen and formate. Hydrogen and formate molar yields in batch culture at pH 6.0 and 30ºC. n=3, error bars represent S.D.

Table 3-1. Summary of the genome sequences of seven hydrogen-producing vibrios

Strains	Total contig size (Mbp)	Number of contigs	Number of predicted CDSs	Nickel uptake systems		
				NikABCED and NikR	HupE	NiCoT
Vibrio tritonius AM2^T (= LMG25401^T)	3.43 (Chr. 1) 1.78 (Chr. 2)	2	3094 (Chr. 1) 1691 (Chr. 2)	intact	-	+
Vibrio porteresiae MSSRF30^T	5.45	8	4863	intact	-	+
Vibrio gazogenes ATCC29988	4.65	9	4074	-	+	-
Vibrio rhizosphaerae MSSRF3^T	4.53	5	3867	-	+	-
Vibrio ruber LMG23124^T	4.66	11	3926	-	+	-
Vibrio aerogenes LMG19650^T	5.34	5	4620	-	+	-
Vibrio furnissii LMG 7910^T	4.96	8	4535	-	+	-

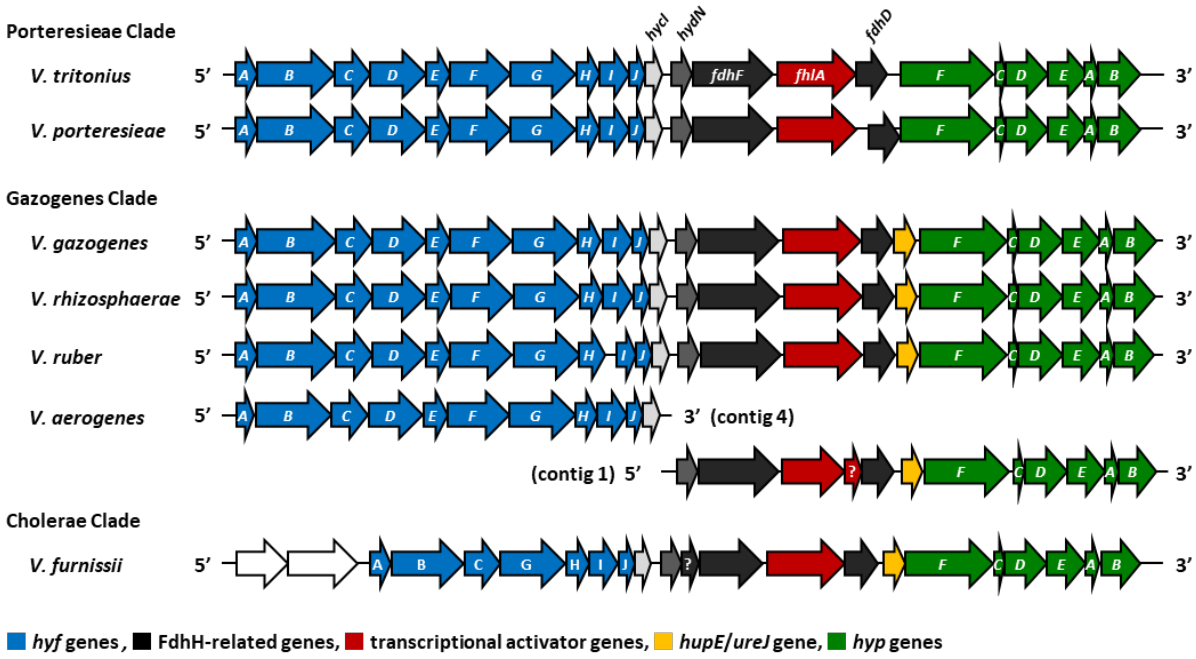

Fig. 3-2. Genomic architecture of FHL-Hyp gene cluster from vibrios.

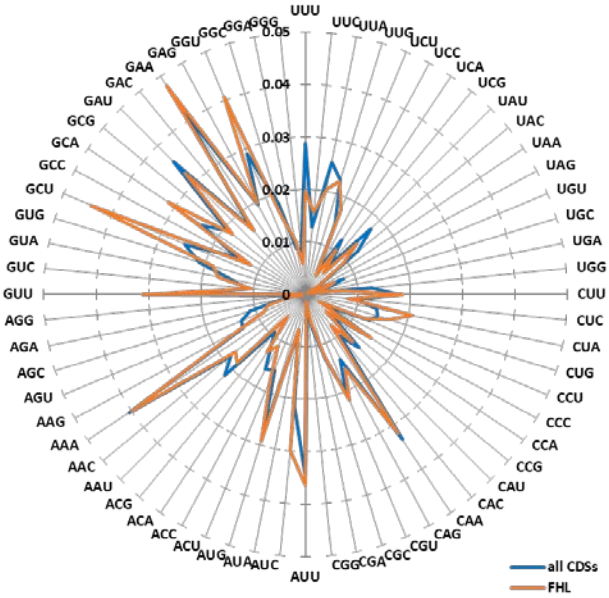

Fig. 3-3. Comparison of codon usage of CDSs on FHL-Hyp gene cluster and chromosome 1 of *Vibrio tritonius* AM2.

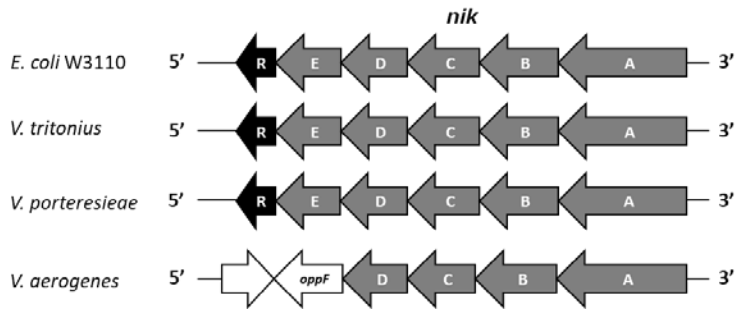

Fig. 3-4. Identification of *nikABCDE* and *nikR* genes in vibrios. Relationship of genes responsible for nickel ABC transporter identified in genome sequences of hydrogen-producing vibrios.

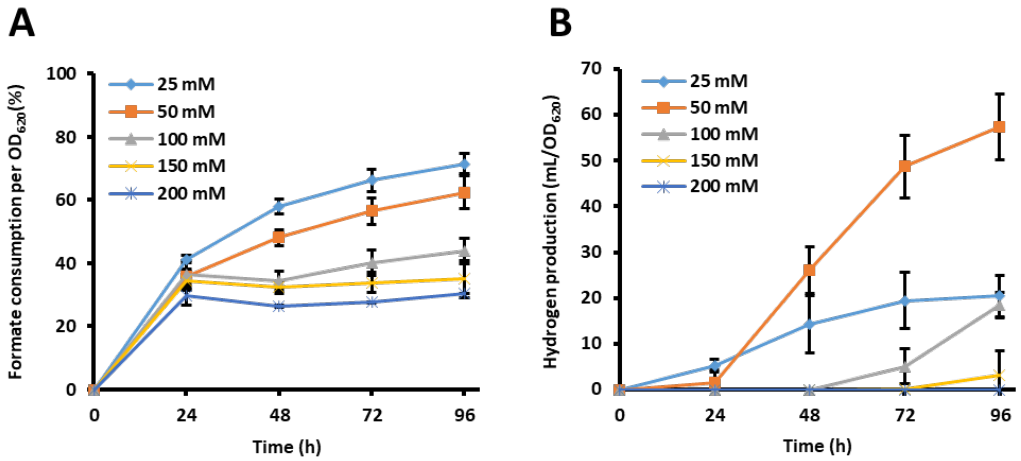

Fig. 3-5. Effect of extracellular formate on hydrogen production of *Vibrio tritonius* AM2. (A) hydrogen production carves in the marine broth containing differential concentration of formate. (B) hydrogen molar yield estimated from the values of hydrogen production and formate consumption during 96 hour. Culture conditions were set at pH 6.0 and 37ºC. n=3, error bars represent S.D.

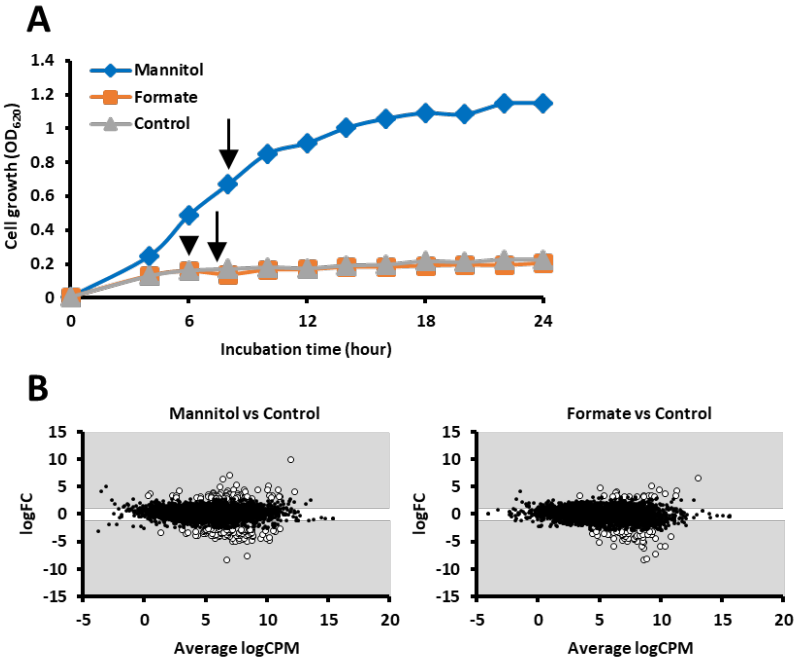

Fig. 3-6. RNA-Seq data of *Vibrio tritonius* AM2. (A) Growth carves and the sampling condition of *V. tritonius* AM2 for RNA-Seq. Arrows: the sampling points of bacterial cells for total RNA extraction at each test condition. Arrow head: the addition point of formate; (B) Relative expression profiling of all genes. White plots indicate DEGs predicted at the basis of FDR<0.05 and log fold change >= 2.0.

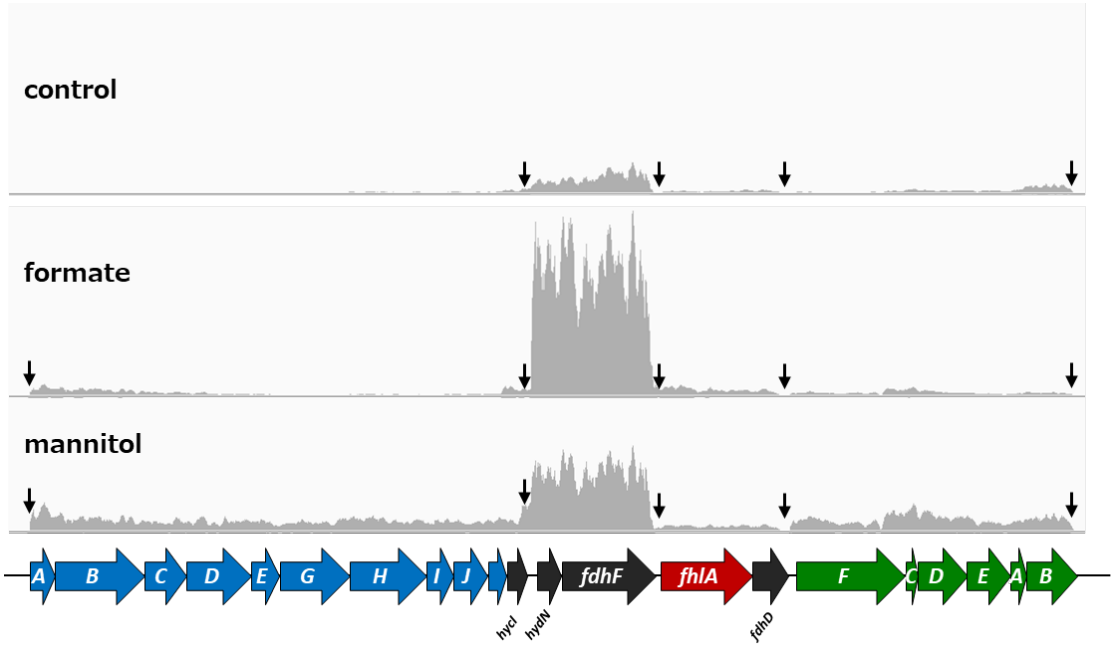

Fig. 3-7. Coverage of RNA-Seq reads mapping to FHL-Hyp gene cluster in *Vibrio tritonius* AM2. Arrows indicate the predicted discontinuity sites of transcripts of FHL-Hyp gene cluster.

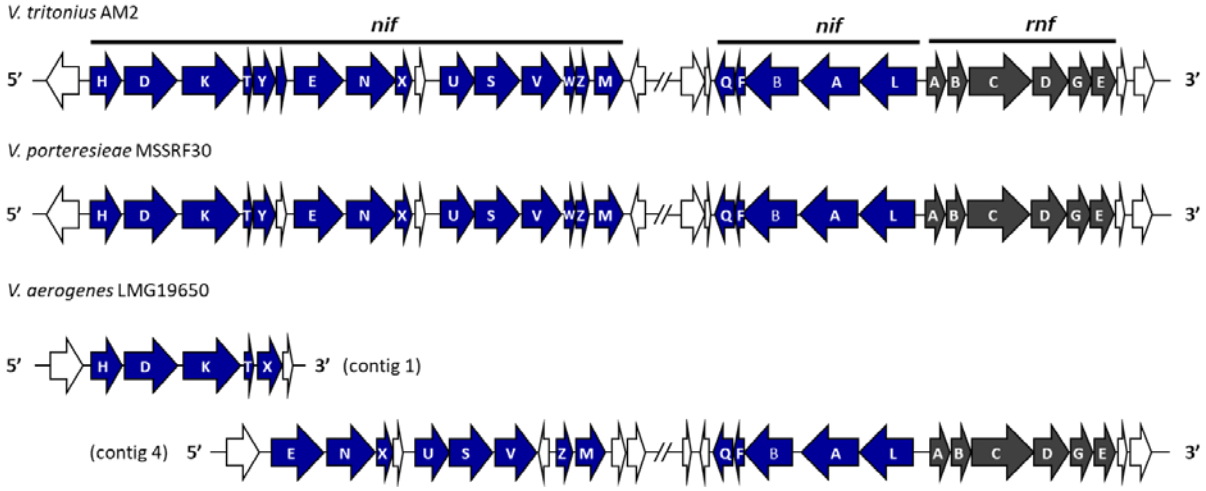

Fig. 3-8. Genomic architecture of *nif* gene cluster from *Vibrio tritonius, Vibrio porteresieae, and Vibrio aerogenes*.

Table 3-2. The genes showing differential expression by mannitol supplementation

Locus	Products	log Fold change	FDR
vtAM2_cI_0024	hypothetical protein	-3.829601094	0.002127499
vtAM2_cI_0025	hypothetical protein	-3.904070048	0.00197567
vtAM2_cI_0176	periplasmic protein	-2.935461882	0.028501237
vtAM2_cI_0189	arabinose-5-phosphate isomerase	-2.842739752	0.041448612
vtAM2_cI_0292	bacterioferritin-associated ferredoxin	-3.32391727	0.01046661
vtAM2_cI_0310	phosphoadenosine phosphosulfate reductase	-2.843572939	0.033752712
vtAM2_cI_0324	hypothetical protein	3.660558675	0.003407743
vtAM2_cI_0396	phosphoglycerate kinase	3.135086549	0.015180713
vtAM2_cI_0416	hydrogenase-4 component A	6.340581296	4.12744E-07
vtAM2_cI_0417	hydrogenase-4 component B	5.245943023	3.66292E-05
vtAM2_cI_0418	hydrogenase-4 component C	4.929193728	8.5476E-05
vtAM2_cI_0419	Hydrogenase-4 component D	4.238817334	0.000653373
vtAM2_cI_0420	Hydrogenase-4 component E	3.836924649	0.002127499
vtAM2_cI_0421	hydrogenase-4 component F	3.958273346	0.001423742
vtAM2_cI_0422	hydrogenase 4, large subunit	3.530667397	0.005066201
vtAM2_cI_0423	4Fe-4S binding domain protein	3.679442133	0.003380354
vtAM2_cI_0424	hydrogenase 3 and formate hydrogenlyase complex, HycG subunit	3.142428822	0.015261039
vtAM2_cI_0425	formate hydrogenlyase maturation HycH family protein	3.127827164	0.015858113
vtAM2_cI_0431	hydrogenase maturation protein HypF	3.405918675	0.007272022
vtAM2_cI_0558	autonomous glycyl radical cofactor GrcA	4.156644187	0.000807664
vtAM2_cI_0600	N-acetylglutamate synthase	-4.44461527	0.000322148
vtAM2_cI_0689	conserved hypothetical protein	-3.313705493	0.009134672
vtAM2_cI_0746	hypothetical protein	2.883735486	0.03021605
vtAM2_cI_0802	succinate dehydrogenase cytochrome b556 largemembrane subunit	-3.4061353	0.007272022
vtAM2_cI_0803	succinate dehydrogenase hydrophobic membraneanchor protein	-3.863690754	0.001871562
vtAM2_cI_0804	succinate dehydrogenase flavoprotein subunit	-3.743358696	0.002479687
vtAM2_cI_0846	hypothetical protein	3.369509769	0.00791204
vtAM2_cI_0873	bifunctional acetaldehyde-CoA/alcoholdehydrogenase	3.250516402	0.010588625
vtAM2_cI_0895	hypothetical protein	-3.61732535	0.004959967
vtAM2_cI_0929	hypothetical protein	3.318204866	0.009134672
vtAM2_cI_0982	predicted metal dependent hydrolase/sulfatase	-2.730199057	0.048589793
vtAM2_cI_0996	hypothetical protein	-3.53533599	0.005358599
vtAM2_cI_1158	adenosylmethionine--8-amino-7-oxononanoatetransaminase	-3.502690845	0.005425406
vtAM2_cI_1166	hypothetical protein	-4.895226752	8.5476E-05
vtAM2_cI_1167	hypothetical protein	-4.883078629	8.5476E-05
vtAM2_cI_1209	TorCAD operon transcriptional regulatory protein TorR	2.765024104	0.043290135
vtAM2_cI_1289	hypothetical protein	-3.850742807	0.002052479
vtAM2_cI_1324	hypothetical protein	-2.908771017	0.028972009
vtAM2_cI_1338	methyl-accepting chemotaxis protein	-3.217422102	0.011740926
vtAM2_cI_1355	transcriptional regulator AraC N-terminal domain protein	-3.394635683	0.00747921
vtAM2_cI_1356	major facilitator transporter	-4.002527914	0.0012872
vtAM2_cI_1389	hypothetical protein	3.341665613	0.034664867
vtAM2_cI_1391	sugar transporter	3.793721049	0.002132914
vtAM2_cI_1453	nitroreductase family protein	-2.899112441	0.029709415
vtAM2_cI_1519	hypothetical protein	4.431138449	0.000322148
vtAM2_cI_1532	putative NAD-glutamate dehydrogenase	-4.202762288	0.000689384
vtAM2_cI_1621	Acid phosphatase lipoprotein	2.742606017	0.045892672
vtAM2_cI_1695	hypothetical protein	-2.906796608	0.030135864
vtAM2_cI_1726	outer membrane protein	-2.875158805	0.031059814
vtAM2_cI_1727	membrane-fusion protein	-3.813022092	0.002132914
vtAM2_cI_1728	ABC-type multidrug transport system permease component	-3.0858716	0.017963569

vtAM2_cI_1729	ABC-type multidrug transport system permease compo□nen	-3.539859029	0.005108491
vtAM2_cI_1749	hypothetical protein	-2.76628467	0.042179717
vtAM2_cI_1872	hypothetical protein	3.400213496	0.00747921
vtAM2_cI_1958	methyl-accepting chemotaxis protein	3.413225437	0.007273431
vtAM2_cI_1959	glutamate decarboxylase	2.840185813	0.034664867
vtAM2_cI_2103	TRAP-type C4-dicarboxylate transport system large□permease	-4.838293272	0.000100149
vtAM2_cI_2104	TRAP-type C4-dicarboxylate transport system, small□permease compon	-8.271730666	2.92237E-10
vtAM2_cI_2105	TRAP-type C4-dicarboxylate transport system compo□nent	-7.711148702	1.15895E-09
vtAM2_cI_2149	hypothetical protein	2.95166846	0.026082408
vtAM2_cI_2298	NADP-dependent formate dehydrogenase alpha subunit	3.213715768	0.011748856
vtAM2_cI_2342	hypothetical protein	-2.760097182	0.044054837
vtAM2_cI_2393	polar amino acid ABC transporter, inner membrane□subunit	-3.150030765	0.015261039
vtAM2_cI_2395	xylose isomerase	-4.52341854	0.000310142
vtAM2_cI_2396	hypothetical protein	-3.173899641	0.015135848
vtAM2_cI_2717	ornithine carbamoyltransferase	-3.942511719	0.001439198
vtAM2_cI_2763	adenylylsulfate kinase	-3.930010085	0.001510916
vtAM2_cI_2764	putative sodium/sulfate symporter	-3.539760656	0.004952829
vtAM2_cI_2765	sulfate adenylyltransferase subunit 1	-4.516179134	0.000310142
vtAM2_cI_2766	sulfate adenylyltransferase subunit 2	-3.961200491	0.001408357
vtAM2_cI_2767	uroporphyrin-III C-methyltransferase	-3.48911053	0.005425406
vtAM2_cI_2847	argininosuccinate synthase	-3.805745866	0.002127499
vtAM2_cI_2848	acetylglutamate kinase	-4.092245488	0.001007292
vtAM2_cI_2849	N-acetyl-gamma-glutamyl-phosphate reductase	-4.642899038	0.000201294
vtAM2_cI_2941	phosphoenolpyruvate carboxykinase	-2.70441293	0.049725194
vtAM2_cI_3030	L-arabinose-binding periplasmic protein	-5.067339667	5.44803E-05
vtAM2_cI_3031	L-arabinose transporter ATP-binding protein	-2.815910074	0.037552658
vtAM2_cI_3032	L-arabinose transporter permease	-3.017622481	0.022706137
vtAM2_cI_3033	ABC-type sugar transporter, periplasmic binding p□otein	-3.840228289	0.002209656
vtAM2_cII_0009	cytochrome o ubiquinol oxidase subunit II	-2.96783934	0.024601652
vtAM2_cII_0010	cytochrome o ubiquinol oxidase, subunit I	-3.003046918	0.022329431
vtAM2_cII_0011	cytochrome o ubiquinol oxidase subunit III	-2.808804613	0.037468563
vtAM2_cII_0012	CytOchrome o ubiquinol oxidase subunit IV	-2.775744288	0.041448612
vtAM2_cII_0030	transporter, NadC family	-2.907653955	0.028972009
vtAM2_cII_0037	phosphatidylglycerophosphatase B	-2.714492724	0.049625485
vtAM2_cII_0044	membrane protein, GtrA family protein	-3.034694325	0.020301003
vtAM2_cII_0045	Glycosyltransferase	-3.594545414	0.004116389
vtAM2_cII_0109	methionine synthase putative	3.335285516	0.008911187
vtAM2_cII_0167	peptidase T	2.981132749	0.023785484
vtAM2_cII_0284	hypothetical protein	-2.931644529	0.028299015
vtAM2_cII_0365	cationic amino acid ABC transporter, periplasmic□binding protein	-4.509458502	0.000310142
vtAM2_cII_0405	outer membrane lipoprotein	-3.99372524	0.001344935
vtAM2_cII_0460	hypothetical protein	3.127293836	0.016419035
vtAM2_cII_0481	chaperonin GroEL	3.361934212	0.00791204
vtAM2_cII_0482	heat shock protein 60 family co-chaperone GroES	4.124186349	0.000903954
vtAM2_cII_0483	hypothetical protein	7.100399992	1.72389E-08
vtAM2_cII_0565	hypothetical protein	4.171254956	0.0012872
vtAM2_cII_0581	hypothetical protein	3.232931113	0.011542539
vtAM2_cII_0582	hypothetical protein	3.707757948	0.015547912
vtAM2_cII_0627	putative resistance protein, yhjX	10.00795936	6.93756E-14
vtAM2_cII_0666	ABC transporter, quaternary amine uptaketransporter□r (QAT) family, subs	3.306090632	0.009134672
vtAM2_cII_0680	F0F1 ATP synthase subunit A	3.231241197	0.011740926
vtAM2_cII_0681	ATP synthase F0, C subunit	3.47742563	0.006214474
vtAM2_cII_0682	ATP synthase B chain	3.804115135	0.002132914

vtAM2_cII_0683	ATP synthase delta chain	3.611027887	0.004116389
vtAM2_cII_0684	F0F1 ATP synthase subunit alpha	3.497504034	0.005425406
vtAM2_cII_0685	F0F1 ATP synthase subunit gamma	3.616436364	0.003977417
vtAM2_cII_0699	acetate kinase	5.114234364	5.25581E-05
vtAM2_cII_0882	hypothetical protein	3.444617297	0.009375641
vtAM2_cII_1047	hypothetical protein	-3.437711921	0.015647496
vtAM2_cII_1107	hypothetical protein	3.408888456	0.009496709
vtAM2_cII_1128	hypothetical protein	2.73990737	0.048589793
vtAM2_cII_1222	hypothetical protein	-3.31474105	0.009134672
vtAM2_cII_1239	glycerol kinase	-4.441119045	0.000322148
vtAM2_cII_1240	glycerol uptake facilitator protein	-4.031266431	0.001174326
vtAM2_cII_1268	outer membrane protein OmpA	-2.783747503	0.041648174
vtAM2_cII_1270	sodium:citrate symporter	-2.893992181	0.03021605
vtAM2_cII_1280	hypothetical protein	-3.572245497	0.004952829
vtAM2_cII_1281	aldehyde dehydrogenase	-3.325828871	0.008988444
vtAM2_cII_1309	hypothetical protein	2.753789572	0.043494713
vtAM2_cII_1321	glycine cleavage system T protein	-2.918974054	0.02833355
vtAM2_cII_1323	hypothetical protein	-3.290541131	0.009496709
vtAM2_cII_1324	glycine cleavage system protein H	-2.990435399	0.023080812
vtAM2_cII_1325	glycine dehydrogenase	-3.150379595	0.014618433
vtAM2_cII_1383	outer membrane protein W	3.070602857	0.017963569
vtAM2_cII_1399	aldehyde dehydrogenase (NAD) family protein	-5.065809496	5.44803E-05
vtAM2_cII_1400	sigma-54 dependent transcriptional regulator	-3.9512892	0.001423742
vtAM2_cII_1416	Methyl-accepting chemotaxis protein	4.427704254	0.000322148
vtAM2_cII_1511	hypothetical protein	-4.106589575	0.001007292
vtAM2_cII_1529	hypothetical protein	2.938249912	0.027988089
vtAM2_cII_1530	cyclopropane-fatty-acyl-phospholipid synthase	3.306194903	0.009134672
vtAM2_cII_1537	acyl-CoA synthetase	-3.043439088	0.01993294
vtAM2_cII_1599	hypothetical protein	-3.403258014	0.007273431
vtAM2_cII_1600	hypothetical protein	-3.668158404	0.003380354
vtAM2_cII_1601	hypothetical protein	-4.063279423	0.001111057
vtAM2_cII_1625	hypothetical protein	2.995194902	0.030301076
vtAM2_cII_1634	pyruvate dehydrogenase	4.423830611	0.000322148
vtAM2_cII_1637	Na+/H+ antiporter NhaD type	2.892579735	0.030135864
vtAM2_cII_1648	phosphotransferase system mannitol-specific	4.479893348	0.000310142
vtAM2_cII_1649	mannitol-1-phosphate 5-dehydrogenase	4.340030497	0.000414823
vtAM2_cII_1650	mannitol operon represso	2.89878985	0.029888981
vtAM2_cII_1668	iron complex transport system permease	2.966201136	0.027510201
vtAM2_cII_1669	Fe3+-siderophores ABC superfamily ATP binding cassette transporter, I	3.206104136	0.012826547
vtAM2_cII_1673	3,4-dihydroxy-2-butanone 4-phosphate synthase	-2.852385257	0.032943729
vtAM2_cII_1679	sodium/proline symporter	-3.021477152	0.021096805
vtAM2_cII_1680	delta 1-pyrroline-5-carboxylate dehydrogenase domain protein	-4.372986262	0.000382751
vtAM2_cII_1681	bifunctional prolinedehydrogenase/pyrroline-5-carboxylate dehydrogena	-4.762020071	0.000123804

Table 3-3. The genes showing differential expression by formate supplementation

Locus	Products	log Fold change	FDR
vtAM2_cI_0014	hypothetical protein	4.021205803	0.004455689
vtAM2_cI_0015	heat shock protein A	4.401158909	0.001338344
vtAM2_cI_0308	sulfite reductase [NADPH] flavoprotein,alpha-component	-5.860501382	1.14015E-05
vtAM2_cI_0309	sulfite reductase subunit beta	-5.957746029	1.02588E-05
vtAM2_cI_0310	phosphoadenosine phosphosulfate reductase	-5.781925712	1.45101E-05
vtAM2_cI_0406	glucosamine--fructose-6-phosphateaminotransferase (isomerizing)	-3.724189655	0.009334523
vtAM2_cI_0416	hydrogenase-4 component A	4.835697036	0.000418074
vtAM2_cI_0417	hydrogenase-4 component B	3.937240546	0.005913304
vtAM2_cI_0427	putative electron transport protein HydN	3.369940393	0.024555298
vtAM2_cI_0534	carbamoyl phosphate synthase large subunit	-3.284313634	0.032058822
vtAM2_cI_0600	N-acetylglutamate synthase	-3.507578775	0.017810584
vtAM2_cI_1059	metal ion transporter Nramp family	3.441114674	0.021431636
vtAM2_cI_1158	adenosylmethionine--8-amino-7-oxononanoatetransaminase	-3.137801986	0.046812043
vtAM2_cI_1159	biotin synthase	-3.169182828	0.044323482
vtAM2_cI_1338	methyl-accepting chemotaxis protein	-3.877816102	0.006429656
vtAM2_cI_1519	hypothetical protein	3.105792003	0.049349
vtAM2_cI_1588	hypothetical protein	3.188339787	0.042926365
vtAM2_cI_1758	hypothetical protein	3.447836859	0.020117801
vtAM2_cI_1964	arginine ABC transporter	-3.683359672	0.010810272
vtAM2_cI_1965	arginine ABC transporterperiplasmicarginine-binding protein ArtI	-4.401345984	0.001338344
vtAM2_cI_1966	arginine transporter permease subunit ArtQ	-3.460858046	0.020117801
vtAM2_cI_2103	TRAP-type C4-dicarboxylate transport system large permease	-4.376776506	0.001394389
vtAM2_cI_2104	TRAP-type C4-dicarboxylate transport system, small permease compon	-4.796061814	0.000418074
vtAM2_cI_2105	TRAP-type C4-dicarboxylate transport system component	-3.737570458	0.00911974
vtAM2_cI_2187	LuxO repressor protein	3.166836593	0.044323482
vtAM2_cI_2234	cysteine synthase	-4.135897517	0.003038761
vtAM2_cI_2356	DNA sulfur modification protein DndE	-3.667788281	0.011640793
vtAM2_cI_2393	polar amino acid ABC transporter, inner membrane subunit	-3.912745977	0.006429656
vtAM2_cI_2513	clpB protein	3.446076279	0.020117801
vtAM2_cI_2763	adenylylsulfate kinase	-3.842389383	0.007252094
vtAM2_cI_2764	putative sodium/sulfate symporter	-3.896756138	0.006339428
vtAM2_cI_2765	sulfate adenylyltransferase subunit 1	-7.218682022	1.23113E-07
vtAM2_cI_2766	sulfate adenylyltransferase subunit 2	-8.158893266	4.30705E-09
vtAM2_cI_2767	uroporphyrin-III C-methyltransferase	-8.35772355	3.91934E-09
vtAM2_cI_2847	argininosuccinate synthase	-4.243090925	0.002109952
vtAM2_cI_2848	acetylglutamate kinase	-4.440078454	0.001269724
vtAM2_cI_2849	N-acetyl-gamma-glutamyl-phosphate reductase	-4.933496237	0.000257428
vtAM2_cI_2885	malic enzyme	-3.117234698	0.048431936
vtAM2_cI_3057	choline dehydrogenase	-3.787852126	0.008175981
vtAM2_cI_3058	putative glycine betaine-binding ABCtransporter	-4.081809003	0.003497801
vtAM2_cI_3059	ABC transporter: transmembrane protein	-3.644114172	0.011891316
vtAM2_cI_3060	hypothetical ATP-binding component of ABC transporter	-3.239197633	0.037206906
vtAM2_cI_3084	F0F1 ATP synthase subunit gamma	-3.204081761	0.041036051
vtAM2_cII_0090	NADH-dependent flavin oxidoreductase Oye family	3.15721514	0.044589472
vtAM2_cII_0226	N-formimino-L-glutamate deiminase	3.153623475	0.044589472
vtAM2_cII_0228	histidine ammonia-lyase	3.801015221	0.007992879
vtAM2_cII_0229	imidazolonepropionase	3.393002833	0.023473308
vtAM2_cII_0280	sulfate ABC transporter periplasmicsulfate-binding protein	-6.144043661	6.06489E-06
vtAM2_cII_0281	sulfate ABC transporter inner membrane subunit CysT	-5.955180697	1.08392E-05
vtAM2_cII_0282	sulfate ABC transporter inner membrane subunit CysW	-4.529174141	0.001030197
vtAM2_cII_0283	sulfate ABC transporter, ATP-binding protein	-4.111025884	0.003325545

vtAM2_cII_0365	cationic amino acid ABC transporter, periplasmic binding protein	-4.578320295	0.000860345
vtAM2_cII_0481	chaperonin GroEL	4.261502818	0.002034481
vtAM2_cII_0482	heat shock protein 60 family co-chaperone GroES	5.073989526	0.000179224
vtAM2_cII_0483	hypothetical protein	3.380231074	0.029930913
vtAM2_cII_0646	diaminobutyrate--2-oxoglutarateaminotransferase	-3.782398389	0.008671362
vtAM2_cII_0647	L-ectoine synthase	-3.542120959	0.017810584
vtAM2_cII_0648	aspartokinase associated with ectoin biosynthesis	-3.160618817	0.046573618
vtAM2_cII_0662	Transcriptional regulator, MarR family	-3.635829333	0.012749187
vtAM2_cII_0663	glycine betaine transporter periplasmic subunit	-5.223214782	0.000121388
vtAM2_cII_0664	glycine betaine ABC transporter, binding protein inner membrane compo	-4.994858128	0.000230243
vtAM2_cII_0665	glycine/betaine/proline ABC transporter	-4.438338973	0.001269724
vtAM2_cII_1247	choline-glycine betaine transporter	-3.739094965	0.00911974
vtAM2_cII_1280	hypothetical protein	-5.187341772	0.000166078
vtAM2_cII_1281	aldehyde dehydrogenase	-4.945669734	0.000257428
vtAM2_cII_1282	ThiJ/PfpI domain-containing protein	-3.458101479	0.020117801
vtAM2_cII_1374	3-oxoacyl-ACP synthase II	-3.578448653	0.014325445
vtAM2_cII_1384	hypothetical protein	6.593173509	1.14609E-06
vtAM2_cII_1472	SM-20-related protein	3.185918407	0.043759423
vtAM2_cII_1644	conserved hypothetical protein	3.392330286	0.023867676
vtAM2_cII_1680	delta 1-pyrroline-5-carboxylate dehydrogenase domain protein	-3.102565796	0.049349

CHAPTER V

General discussion

To overcome increasing demands for global energy, accumulation of GHG, and the depletion of fossil fuels, renewable energy is becoming an essential sector in the development of a sustainable energy cycle [Friedlingstein and Solomon, 2005; Nigam and Singh, 2010]. Biomass can serve as an excellent alternative source for providing renewable energy using microbial metabolism. Studies focusing on marine vibrio utilization in developing bioenergy conversion techniques from marine biomass, have been undertaken in our laboratory [Matsumura *et al*., 2014]. In this study, I focused on the utilization of *Vibrio* species with the aim of producing H_2 from seaweed biomass. Coincidentally, in the process of investigating efficient energy production from seaweed biomass, I have described unique H_2 producing vibrios. In this chapter, I discuss the prospects and challenges of vibrio utilization in biological H_2 production, evolutionary aspects of Hyf-type FHL comparing to Complex I, and the ecophysiological role of the FHL in *V. tritonius*.

Prospects and challenges of hydrogen production from seaweed biomass

In CHAPTER II, I described the H_2 production ability of *V. tritonius* AM2. Sodium (Na^+) tolerance is recognized as one of the advantages of vibrio utilization in H_2 production from marine biomass. *V. tritonius* AM2 can achieve high-yields of H_2 production (1.7 mol H_2/mol mannitol) even in the presence of 2.25% (v/w) NaCl. In general, high Na^+ concentration inhibits H_2 production of bacteria, such as *Enterobacter* spp. and *E. coli* [Kim *et al*., 2009]. The H_2 production of *En. aerogenes* which reaches 1.6 mol H_2/mol mannitol in non-saline condition, however it decreases dramatically in the presence of over 2% (v/w) NaCl [Tanisho, 2011]. The higher H_2 production under saline conditinon is one of the superior features in the use of marine biomass which contains high salt concentrations. Currently, other study in our laboratory has revealed that *V. tritonius* AM2 is capable of producing H_2 under a wide range of salt concentrations and the addition of 1.0% (w/v) NaCl resulted in a relatively higher value in hydrogen production rates, molar H_2 yields, and substrate conversion efficiency (unpublished data).

For commercially valuable H_2 production, it is necessary to overcome two main limiting factors; low H_2 yield from raw seaweed materials and low volumetric H_2 production rate [Yoshida *et al*., 2005]. When mannitol was used as a carbon source, *V. tritonius* showed the high molar yields of H_2 corresponding to 75% of the theoretical value [Matsumura *et al*., 2014].

However, to achieve efficient biological conversion of seaweed biomass to H_2, I still face challenges. Brown algae consist of two major carbohydrate components, mannitol and alginate [Obluchinskaya, 2008]. Many bacteria can use mannitol as the sole carbon source during fermentation in the H_2 production. Alginate, which is oxidized polysaccharide composed of β-D-mannuronate and α-L-guluronate, is easy to be depolymerized by microbes, but is not the preferred substrate in biofuel production [Hashimoto *et al*., 2010]. Unfortunately, *V. tritonius* does not possess alginate degradation and assimilation features. Using only by the single use of the *V. tritonius* cells it was not possible to achieve alginate-H_2 conversion. So with the aim of efficient H_2 production using a variety of seaweed carbohydrates, 1) the cascading of formate, and 2) the metabolic engineering are both major challenges.

Formate performs roles in both the end-point product in the mixed acid fermentation and as a precursor of H_2 produced by FHL. To prevent critical cytoplasmic acidification, *E. coli* export formate across the cytoplasmic membrane by FocA (formate channel encoded by *focA* gene) [Sawers, 1994; Sawers, 2005; Waight *et al*., 2010]. Once the pH of the growth medium drops below 6.8, formate is rapidly and completely reimported via FocA into the cells where it is oxidized by FHL [Sawers, 2005]. Shin *et al*. reported that supplemented extracellular formate enhanced the H_2 productivity of *E. coli* [Shin *et al*., 2010]. Our study also confirmed that *V. tritonius* was able to reimport the extracellular formate and convert it to H_2. Using the unique feature of reimporting formate by *V. tritonius* could help us succeed in developing a two-step system, consisting of alginate to formate conversion by alginate assimilating vibrios, such as *Vibrio halioticoli*, *Vibrio inusitatus*, and *Vibrio gallicus*, and then the formate to H_2 conversion using *V. tritonius* (unpabulished data).

Metabolic engineering is also an effective way to achieve H_2 production from alginate. In bioenergy production from seaweed biomass, many researchers reported high productivity of ethanol from alginate using metabolically engineered bacteria [Hashimoto *et al*., 2010; Wargacki *et al*., 2012; Enquist-Newman *et al*., 2014]. Redox balance is the key factor in ethanol fermentation. The reason is considered to be that excess reducing equivalent stored in NAD(P)H is generated for conversion mannitol to glyceraldehyde 3-phosphate in the mannitol metabolism whereas NAD(P)H is consumed by the reaction of short-chain dehydrogenase in alginate metabolism resulting in NADH-dependent ethanol synthesis which is an energetically unfavorable reaction. Previous report demonstrated that the alginate-catabolizing bacterium *Sphingomonas* sp. strain A1 has been metabolically engineered to install homo-ethanol fermentation from alginate [Hashimoto *et al*., 2010]. *E. coli* has also been engineered to harbor alginate-metabolizing genes to produce bioethanol from alginate [Wargacki *et al*., 2012]. On the

other hand, facultative anaerobes, such as *E. coli* and *Vibrio* species produce H_2 via the FHL pathway in which NADH is unlikely to be used, indicating that oxidation potential of alginate might not directly affect H_2 production.

Cloning of the gene clusters responsible for alginate transport and metabolism is still a major challenge even in *E. coli* [Wargacki *et al*., 2012]. It is effective and efficient to use native bacteria possessing gene clusters responsible for alginate degradation and metabolism for constructing metabolically engineered homoethanologenic strains. Recent studies in our laboratory have succeeded in isolating a novel H_2 producer assigned to the genus *Vibrio*, *V. aphrogenes*. Additionally, the strain was capable of producing H_2 from alginate during the fermentation [Tanaka *et al*., 2017]. To our knowledge, this is the first report of H_2 production from alginate using a single strain. The genome sequencing showed that *V. aphrogenes* also has a FHL pathway, but its genes organization is the Gazogenes type possessing *hupE* on the FHL-Hyp cluster [Tanaka *et al*., 2017].

The nickel and iron metal center is located in the large subunit of hydrogenase, and nickel is required for the activation of hydrogenase [Sawers *et al*., 2004]. Comparative genomics demonstrate that the nickel ABC transporter (and/or nickel cobalt permease) might be one of the key factors contributing to the efficient H_2 productivity of *V. tritonius*. This indicates that extracellular nickel concentration could be one of the important factors affecting the H_2 producing ability of *V. tritonius*. I also designed the synthetic medium containing $NiCl_2$, ferric citrate, $Na_2Mo_4 \cdot 2H_2O$, and Na_2SeO_3 as trace metals for [NiFe]-hydrogenase activity [Matsumura *et al*., 2015]. Optimization of these trace metal contents in the medium for enhancing H_2 production is now in progress. Such physiological studies show the minimum requirement in constructing an active FHL complex in marine vibrios.

Evolutional aspects of the Hyf-type FHL of vibrios

Complex I is the first component of the respiratory chains in microorganisms and mitochondria [Marreiros *et al*., 2013; Baradaran *et al*., 2013]. In domain of *Bacteria*, complex I is composed of 14 subunits; NuoA-N for NADH: ubiquinone oxidoreductase and Nqo1-14 for NADH: quinone oxidoreductase [Marreiros *et al*., 2013]. On the bais of amino acid sequences and structural simiralities, an evolutional relationship between Complex I and membrane-bound [NiFe]-hydrogenases (group 4) has been assumed for long time [McDowall *et al*., 2014; Baradaran *et al*., 2013]. In CHAPTER III and IV, the genome analyses of H_2-producing vibrios revealed that the Porteresieae and Gazogenes clade species have Hyf-type FHL (predicted energy-conserving FHL) and *V. furnissii* belonging to the Cholerae clade have Hyc-type FHL

(non-energy-conserving FHL) as H_2 producing machinery. In general, vibrios have Na^+-NQR not Nuo and Nqo complex as respiratory chain complex. The H_2-producing *Vibrio* species have two phylogenetically distinct respiratory chain complex systems; Na^+-NQR for aerobic respiration and FHL for anaerobic respiration. More interestingly, the codon usage pattern comparison shows that the Hyf-type FHL genes of *V. tritonius* might not have been acquired as a recent horizontal transfer event, considering that the Hyf-type FHL might be common in ancient H_2-producing vibrios.

On the other hands, the H_2 production phenotype was experimentally confirmed in only ten species of vibrios [Gomez-Gil *et al*., 2014]. Sawabe *et al*. proposed the 17 taxonomical clades in the genus *Vibrio* on the basis of 8-gene MLSA [Sawabe *et al*., 2013]. Among them, H_2-producing phenotype was described in species belonging to only the four clades; Porteresieae, Gazogenes, Cholerae, and Rumoiensis clade [Sawabe *et al*., 2013; Tanaka *et al*., 2017]. Why do not many vibrios have H_2-producing propeties? Recently, Tanaka *et al*. reported that the recent replacement of FHL-Hyp gene cluste was occurred in the Rumoiensis clade [Tanaka *et al*., 2017]. However, the acquisition and/or missing of FHL-Hyp gene cluster at long term level was not described. *Vibrionaceae* is phylogenetically related to *Enterobacteriaceae* [Ruimy *et al*., 1994; Gomez-Gil *et al*., 2014]. Compared to *E. coli* formate regulone, the *Vibrio* formate regulone (FHL-Hyp gene cluster) is likely to form a simpler structure because all genes are encoded in the same strand, suggesting that *Vibrio* formate regulone may be origin. The group 4 [NiFe]-hydrogenases which is defined as H_2-evolving, energy-conserving, and membrane-associated hydrogenase, plays an important role in the disposal of excess reducing equivalents [Nakashimada *et al*., 2002], acidic resistance [Noguchi *et al*., 2008], and energy-conservation [Andrews *et al*., 1997; Sapra *et al*., 2003; Kulkarni *et al*., 2009]. These roles of Hyf-type FHL may confer an advantage in the life cycles of vibrios. To understand how these vibrios acquired and/or lost the Hyf-type FHL during their evolutionally process, further genome information, deep sequence analysis, and understanding their ecosystem were needed.

Predicted ecophysiology of *Vibrio tritonius*

After comparative physiology and genetics and a transcriptome of marine H_2 producing vibrios described in CHAPTER III and IV, I propose that the proton-translocating, energy-conserving hydrogenases might be widespread, particularly in ancient H_2-producing vibrios. The energy-conserving [NiFe]-hydrogenase have been well studied in Archaea, such as Mbh of *P. furiosus* [Ma *et al*., 1993; Sapra *et al*., 2003], Mfh2 of *Thermococcus onnurineus* [Lim *et al*., 2014] and Ech of *M. barkeri* [Künkel *et al*., 1998; Meuer *et al*., 1999]. Lim *et al*. reported

that hyperthermophilic archaea, *T. onnurineus* NA1 was able to grow by chemiosmotic energy conservation coupled to formate oxidation to CO_2 and H_2 via Mfh2 hydrogenase with Na^+/H^+ antiporter [Lim *et al*., 2014]. Until now, however, experimental evidence that Hyf-type FHL contribute to cell activity has not been reported. Theoretically, high conversion ratio of H_2 corresponding to 1.5-1.7 mol/mol hexose indicate that translocation ratio of proton is also high because the proton translocation is thought to couple with H_2 production via Hyf type FHL. Our transcriptional profiling shows that hydrogenase genes and FoF1 ATP synthase genes are overexpressed, although the expression of respiratory chain-related genes was downregulated in mannitol fermentation, suggesting that *V. tritonius* Hyf-type FHL might achieve energy conservation during fermentation. Thus, our study also supports its energy conserving properties. As with *V. portereseiae*, *V. tritonius* belonging to the Porteresieae clade also exhibited higher productivity of H_2 from mannitol than other known H_2-producing vibrios. *V. tritonius* AM2 was isolated from the gut of sea hare (*Aplysia kurodai*) [Sawabe *et al*., 2013]. The gut of sea hare forms an anaerobic microenvironment where seaweed carbohydrates were stably supplied. Formate is a common end product of fermentation, and is often exported to out of cells due to the critical acidification effects. I hypothesize that *V. tritonius* has an advantage to survive in the gut environment of *A. kurodai* due to the efficient detoxification coupled with energy conservation by Hyf-type FHL.

Subsequently, the author discusses the advantages for *A. kurodai* which might sustain the predicted symbiotic, *V. tritonius* in their gut. Various animals and plants maintain a symbiotic relationship with microorganisms that contribute to nutrition and defense against predators or danger [Douglas, 1998]. The genus *Vibrio* also includes several species that are pathogenic to humans and marine animals and some that are facultatively symbiotic. Many studies report that nitrogen fixers are associated with marine invertebrates [Kneip *et al*., 2007; König *et al*., 2016; Petersen *et al*., 2016]. Recent research has reported that chemosynthetic symbionts of marine invertebrates encode nitrogenases, which are capable of nitrogen fixation [Petersen *et al*., 2016]. Suprisingly, *V. porteresieae* and *V. tritonius* genome encodes nitrogenase genes. Very high structural similarity was observed between the nitrogense machinery of *V. porteresieae* and *V. tritonius*. Nitrogen fixation of *V. porteresieae* activity was experimentally detected by acetylene reduction assay [Rameshkumar *et al*., 2008]. More recently, nitrogenase activities have also been detected in *V. tritonius* cells by acetylene reduction assay, indicating the nitrogenase genes are active under nitrogen limited conditions.

Zehr *et al*. stated that copepod gut microflora contains microorganisms with potential in nitrogen fixation [Zehr *et al*., 1998]. They further suggested that the invertebrate gut may

provide an unexpected refuge for suitable conditions for anaerobic nitrogen fixation [Zehr *et al*., 1998]. Judging from the Hyf-type FHL and nitrogenase encoded in *V. tritonius* and their ecological background, I propose the hypothesis of symbiotic-like relationship between *A. kurodai* and *V. tritonius*. The predicted host, *A. kurodai* provides stable seaweed carbohydrate to *V. tritonius* in the gut. In contrast, *V. tritonius* fixes nitrogen to ammonia for *A. kurodai*. Anoxic conditions in the gut environment could protect hydrogenase and nitrogenase from oxygen inactivation. Energy conservation by Hyf-type FHL might contribute to nitrogen fixation of *V. tritonius* because a lot of ATP is needed to fix nitrogen. In addition, *V. tritonius* genomes encode secretion system (ex. type IV pilus) genes, suggesting their relationship with the host (unpublished data). In addition, 16S rRNA sequences (97% identity threshold) survey using MetaMetaDB [Yang and Iwasaki, 2014] provided that *V. tritonius* have habitability on freshwater (26.39%), symbiont (22.43%), aquatic (18.56%), food (16.83%), and fish (15.78%). To determine the ecophysiological roles of *Vibrio* FHL and nitrogenase in their niche, further metagenomics and metatranscriptomic surveys are needed.

REFERENCES

Abánades A, Rubbia C, Salmieri D. Thermal cracking of methane into hydrogen for a CO_2-free utilization of natural gas. Int J Hydrogen Energy. 2013;38:8491-8496.

Alam KY, Clark DP. Anaerobic fermentation balance of *Escherichia coli* as observed by *in vivo* nuclear magnetic resonance spectroscopy. J Bacteriol. 1989;171:6213-6217.

Andrews SC, Berks BC, McClay J, Ambler A, Quail MA, Golby P, Guest JR. A 12-cistron *Escherichia coli* operon (*hyf*) encoding a putative proton-translocating formate hydrogenlyase system. Microbiol. 1997;143:3633-3647.

Armor JN. The multiple roles for catalysis in the production of H_2. Appl Catal A: Gen. 1999;176:159-176.

Axley MJ, Grahame DA, Stadtman TC. *Escherichia coli* formate-hydrogen lyase. J Biol Chem. 1990;265:18213-18218.

Bagramyan K, Mnatsakanyan N, Poladian A, Vassilian A, Trchounian A. The roles of hydrogenases 3 and 4, and the F_0F_1-ATPase, in H_2 production by *Escherichia coli* at alkaline and acidic pH. FEBS Lett. 2002;516:172-178.

Baradaran R, Berrisford JM, Minhas GS, Sazanov L. Crystal structure of the entire respiratory complex I. Nature. 2013;494:443-448.

Barquera B, Hellwig P, Zhou W, Morgan JE, Häse CC, Gosink KK, Nilges M, Bruesehoff PJ, Roth A, Lancaster CR, Gennis RB, Purification and Characterization of the Recombinant Na^+-Translocating NADH:Quinone Oxidoreductase from *Vibrio cholerae*. Biochemistry. 2002;41:3781-3789.

Barquera B. The sodium pumping NADH:quinone oxidoreductase (Na^+-NQR), a unique redox-driven ion pump. J Bioenerg Biomembr. 2014;46:289-298.

Baumann P, Furniss AL, Lee JV. Genus I. *Vibrio Pacini* 1854, 411 AL. In Bergey's Manual of

Systematic Bacteriology, 1984, vol. 1, pp. 518–538. Edited by Krieg NR, J. G. Holt. Baltimore: Williams & Wilkins.

Berriman M, Rutherford K, Viewing and annotating sequence data with Artemis. Brief Bioinform. 2003;4:124-132.

Böck A, Sawers G. Fermentation. in *Escherichia coli* and *Salmonella*: cellular and molecular biology, eds Neidhardt FC, Curtiss III R, Ingraham JL, Lin ECC, Low KB, Magasanik B, Reznikoff WS, Riley M, Schaechter M, Umbarger HE. (American Society for Microbiology, Washington, D.C), 2nd ed. 1996;262-282.

Brenner DJ, Hickman-Brenner FW, Lee JV, Steigerwalt AG, Fanning GR, Hollis DG, Farmer JJ. 3rd, Weaver RE, Joseph SW, Seidler RJ. *Vibrio furnissii* (formerly aerogenic biogroup of *Vibrio fluvialis*), a new species isolated from human feces and the environment. J Clin Microbiol. 1983;18:816-824.

Brito B, Prieto RI, Cabrera E, Mandrand-Berthelot MA, Imperial J, Ruiz-Argüeso T, Palacios JM, *Rhizobium leguminosarum hupE* Encodes a Nickel Transporter Required for Hydrogenase Activity. J Bacteriol. 2010;192:925-935.

Casalot L, Rousset M. Maturation of the [NiFe] hydrogenases. Trends Microbiol. 2001;9:228-237.

Cornell NW, Veech RL. Enzymatic measurement of ethanol or NAD in acid extracts of biological samples. Anal Chem. 1983;132:418-423.

Coppi MV. The hydrogenases of *Geobacter sulfurreducens*: a comparative genomic perspective. Microbiol. 2005;151:1239-1254.

Das D. Advances in biohydrogen production processes: an approach towards commercialization. Int J Hydrogen Energy. 2009;34:7349-7357.

Delcher AL, Harmon D, Kasif S, White O, Salzberg SL. Improved microbial gene identification with GLIMMER. Nucl Acids Res. 1999;27:4636-4641.

Douglas AE. Host benefit and the evolution of specialization in symbiosis. Heredity. 1998;81:599-603.

Dubois M, Gilles KA, Hamilton JK, Rebers PA, Smith F. Colorimetric method for determination of sugar and related substances. Anal Chem. 1956;28:350-356.

Egan ES, Waldor MK. Distinct replication requirements for the two *Vibrio cholerae* chromosomes. Cell. 2003;114:521-530.

Eitinger T, Mandrand-Berthelot MA. Nickel transport systems in microorganisms. Arch Microbiol 2000;173:1-9.

Enquist-Newman M, Faust AME, Bravo DD, S. Santos CN, Raisner RM, Sarvabhowman P, Le C, Regitsky DD, Cooper SR, Peereboom L, Clark A, Goldsmith J, Cho MY, Donohoue PD, Luo L, Lamberson B, Tamrakar P, Villari JL, Gill A, Tripathi SA, Karamchedu P, Paredes CJ, Kotlar HK, Bailey RB, Miller DJ, Ohler NL, Hane A, Martinez Y, Kim EJ, Rajgarhia V, Swimmer C, Yoshikuni Y. Efficient ethanol production from brown macroalgae sugars by a synthetic yeast platform. Nature. 2013;505:239-243.

Fox JD, Kerby RL, Roberts GP, Ludden PW. Characterization of the CO-induced, CO-tolerant hydrogenase from *Rhodospirillum rubrum* and the gene encoding the large subunit of the enzyme. J Bacteriol. 1996;178:1515-1524.

Friedlingstein P, Solomon S. Contributions of past and present human generations to committed warming caused by carbon dioxide. Proc Natl Acad Sci U S A. 2005;102:10832-10836

Gao F, Zhang C-T. Ori-Finder: a web-based system for finding *oriC*s in unannotated bacterial genomes. BMC Bioinformatics. 2008;9:79.

Gasparatos A, Stromberg P, Takeuchi K. Sustainability impacts of first-generation biofuels. Animal frontier. 2013;3:12-26.

Gomez-Gil B, Thompson CC, Vicente A, Matsumura Y, Sawabe T, Iida T, Christen R, Sawabe T.

(2014). “FAMLILY VIBRIONACEAE”. In: Rosenberg E, DeLong EF, Thompson FL, Lory S, Stachebrandt E. eds. The Prokaryotes, 4th ed. New York, Springer: 2014. In press.

Gyaneshwar P, James EK, Mathan N, Reddy PM, Reinhold-Hurek B, Ladha JK. Endophytic colonization of rice by a diazotrophic strain of *Serratia marcescens*. J Bacteriol. 2001;183:2634-2645.

Hallenbeck PC. Fermentative hydrogen production: Principles, progress, and prognosis. Int J Hydrogen Energy. 2009;34:7379–7389.

Harwood CS. *Beneckea gazogenes* sp. nov., a red, facultatively anaerobic marine bacterium. Curr Microbiol. 1978;1:233–238.

Hashimoto W, Kawai S, Murata K. Bacterial supersystem for alginate import/metabolism and its environmental and bioenergy applications. Bioeng Bugs. 2010;1:97-109.

Heidelberg JF, Eisen AJ, Nelson WC, Clayton RA, Gwinn ML, Dodson RJ, Haft DH, Hickey EK, Peterson JD, Umayam L, Gill SR, Nelson KE, Read TD, Tettelin H , Richardson D, Ermolaeva MD, Vamathevan J, Bass S, Qin H, Dragoi I, Sellers P, McDonald L, Utterback T, Fleishmann RD, Nierman WC, White O, Salzberg SL, Smith HO, Colwell RR, Mekalanos JJ, Venter JC, Fraser CM. DNA sequence of both chromosomes of the cholera pathogen *Vibrio cholera*. Nature. 2000;406:477-484.

Hirokawa T, Chieng SB, Mitaku S. SOSUI: classification and secondary structure prediction system for membrane proteins. Bioinformatics. 1998;14:378-379.

Horn SJ, Aasen IM, Østgaard K. Ethanol production from seaweed extract. J Ind Microbiol Biot. 2000a;25:249-254.

Horn SJ, Aasen IM, Østgaard K. Production of ethanol from mannitol by *Zymobacter palmae*. J Ind Microbiol Biot. 2000b;24:51-57.

Hunter S, Jones P, Mitchell A, Apweiler R, Attwood TK, Bateman A, Bernard T, Binns D, Bork P, Burge S, Castro E, Coggill P, Corbett M, Das U, Daugherty L, Duquenne L, Finn RD, Fraser M,

Gough J, Haft D, Hulo N, Kahn D, Kelly E, Letunic I, Lonsdale D, Lopez R, Madera M, Maslen J, McAnulla C, McDowall J, McMenamin C, Mi H, Muellenet PM, Mulder N, Natale D, Orengo C, Pesseat S, Punta M, Quinn AF, Rivoire C, Vegas AS, Selengut JD, Sigrist CJA, Scheremetjew M, Tate J, Thimmajanarthanan M, Thomas PD, Wu CH, Yeats C, Yong SY. InterPro in 2011: new developments in the family and domain prediction database. Nucleic Acids Res. 2011;40:306-312.

Kapdan IK, Kargi F. Bio-hydrogen production from waste materials. Enzyme Microbiol Thechnol. 2006;38:569-582.

Kim DH, Kim SH, Shin HS. Sodium inhibition of fermentative hydrogen production. Int J Hydrogen Energy. 2009;34:3295-3304.

Kim HY. A low cost production of hydrogen from carbonaceous wastes. Int J Hydrogen Energy. 2003;28:1179–1186.

Kneip C, Lockhart P, Voß C, Maier UG. Nitrogen fixation in eukaryotes - New models for symbiosis. BMC Evol Biol. 2007;7:55.

König S, Gros O, Heiden SE, Hinzke T, Thürmer A, Poehlein A, Meyer S, Vatin M, Mbéguié-A-Mbéguié D, Tocny J, Ponnudurai R, Daniel R, Becher D, Schweder T, Markert S. Nitrogen fixation in a chemoautotrophic lucinid symbiosis. Nat Microbiol. 2016;2:16193.

Kotay SM, Das D. Biohydrogen as a renewable energy resource-Prospects and potentials. Int J Hydrogen Energy. 2008;33:258-263.

Kraan S. Mass-cultivation of carbohydrate rich macroalgae, a possible solution for sustainable biofuel production. Mitig Adapt Strateg Glob Change. 2013;18:27-46.

Kumar NR, Sudha N. *Vibrio rhizosphaerae* sp. nov., a red-pigmented bacterium that antagonizes phytopathogenic bacteria. Int J Syst Evol Microbiol. 2007;57:2241-2246.

Künkel A, Vorholt JA, Thauer RK, Hedderich R. An *Escherichia coli* hydrogenase-3-type hydrogenase in methanogenic archaea. Eur J Biochem. 1998;252:467-476.

Kulkarni G, Kridelbaugh DM, Guss AM, Metcalf WW. Hydrogen is a preferred intermediate in the energy-conserving electron transport chain of *Methanosarcina barkeri*. Proc Natl Acad Sci USA. 2009;106:15915-15920.

Langmead B, Salzberg SL. Fast gapped-read alignment with Bowtie 2. Nat Methods. 2012;4;9:357-359.

Larkin MA, Blackshields G, Brown NP, Chenna R, McGettigan PA, McWilliam H, Valentin F, Wallace IM, Wilm A, Lopez R, Thompson JD, Gibson TJ, Higgins DG. Clustal W and Clustal X version 2.0. Bioinformatics. 2007;23:2947-2948.

Lee JV, Shread P, Furniss AL, Bryant TN, Taxonomy and Description of *Vibrio fluvialis* sp. nov. (Synonym Group F Vibrios, Group EF6). J Appl Bacteriol. 1981;50:73-94.

Lee JH, Lee DG, Park JI, Kim JY. Bio-hydrogen production from a marine brown algae and its bacterial diversity. Korean J Chem Eng. 2010;27:187-192.

Lee MJ, Kim TH, Min B, Hwang SJ. Sodium (Na^+) concentration effects on metabolic pathway and estimation of ATP use in dark fermentation hydrogen production through stoichiometric analysis. J Environ Mang. 2012;108:22-26.

Levin DB, Islam R, Cicel N. Sparling R. Hydrogen production by *Clostridium thermocellum* 27405 fom cellulosic biomass substrates. Int J Hydrogen Energy. 2006:31:1496-1503.

Li H, Handsaker B, Wysoker A, Fennell T, Ruan J, Homer N, Marth G, Abecasis G, Durbin R. The sequence alignment/map format and SAMtools. Bioinformatics. 2009;25:2078-2079.

Lim JK, Mayer F, Kang SG, Müller V. Energy conservation by oxidation of formate to carbon dioxide and hydrogen via a sodium ion current in a hyperthermophilic archaeon. Proc Natl Acad Sci U S A. 2014;111:11497–11502.

Liu H, Wang G. Hydrogen production of a salt tolerant strain *Bacillus* sp. B2 from marine intertidal sludge. World J Microbiol Biotechnol. 2012;28:31-37.

Lux TM, Lee R, Love J. Complete genome sequence of a free-living *Vibrio furnissii* sp. nov. strain (NCTC 11218). J Bacteriol. 2011;193:1487-1488.

Ma K, Schicho RN, Kelly RM, Adams MWW. Hydrogenase of the hyperthermophile *Pyrococcus furiosus* is an elemental sulfur reductase or sulfhydrogenase: evidence for a sulfur-reducing hydrogenase ancestor. Proc Natl Acad Sci USA. 1993;90:5341-5344.

Maeda T, Sanchez-Torres V, Wood TK. Enhanced hydrogen production from glucose by metabolically engineered *Escherichia coli*. Appl Microbiol Biotechnol. 2007;77:879-890.

Marreiros BC, Batista AP, Duarte AM, Pereira MM. A missing link between complex I and group 4 membrane-bound [NiFe] hydrogenases. Biochim Biophys Acta. 2013;1827:198-209.

Matsumura Y, Sato K, Al-saari H, Nakagawa S, Sawabe T, Enhanced hydrogen production by a newly described heterotrophic marine bacterium, *Vibrio tritonius* strain AM2, using seaweed as the feedstock. Int J Hydrog Energy. 2014;39:7270-7277.

Matsumura Y, Al-saari H, Mino M, Nakagawa S, Maruyama F, Ogura Y, Hayashi T, Kurokawa K, Sawabe T, Sawabe T, Identification of a gene cluster responsible for hydrogen evolution in *Vibrio tritonius* strain AM2 with transcriptional analyses. Int J Hydrog Energy. 2015;40:9137-9146.

McDowall JS, Murphy BJ, Haumann M, Palmer T, Armstrong FA, Sargent F. Bacterial formate hydrogenlyase complex. Proc Natl Acad Sci U S A. 2014;111:E3948-3956.

Meuer J, Bartoschek S, Koch J, Künkel A, Hedderich R. Purification and catalytic properties of Ech hydrogenase from *Methanosarcina barkeri*. Eur J Biochem. 1999;265:325-335.

Mnatsakanyan N, Bagramyan K, Trchounian A. Hydrogenase 3 but not hydrogenase 4 is major in hydrogen gas production by *Escherichia coli* formate hydrogenlyase at acidic pH and in the presence of external formate. Cell Biochem Biophys. 2004;41:357-66.

Moparthi VK, Hägerhäll C. The Evolution of respiratory chain complex I from a smaller last

common ancestor consisting of 11 protein subunits. J Mol Evol. 2011;72:484-497.

Nakashimada Y, Rachman MA, Kakizono T, Nishio N. Hydrogen production of *Enterobacter aerogenes* altered by extracellular and interacellular redox states. Int J Hydrogen Energy. 2002;27:1399-1405.

Naville M, Ghuillot-Gaudeffroy A, Marchais A, Gautheret D. ARNold: a web tool for the prediction of Rho-independent transcription terminators. RNA Biol. 2011;8:11-13.

Nicolet Y, Lemon BJ, Fontecilla-Camps JC, Peters JW. A novel FeS cluster in Fe-only hydrogenases. Trends Biochm Sci. 2000;25:138-143.

Nigam P, Singh A. Production of liquid biofuels from renewable resources. Prog Energy Combust Sci. 2011;37:52-68.

Noguchi H, Taniguchi T, Itoh T. MetaGeneAnnotator: detecting species-specific patterns of ribosomal binding site for precise gene prediction in anonymous prokaryotic and phage genomes. DNA Res. 2008;15:387-396.

Noguchi K, Riggins DP, Eldahan KC, Kitko RD, Slonczewski JL. Hydrogenase-3 contributes to anaerobic acid resistance of *Escherichia coli*. PLoS One. 2010;5:e10132.

Obluchinskaya ED. Comparative chemical composition of the Barents Sea Brown Algae. Appl. Biochem Microbiol. 2008;44:305-309.

Overbeek R, Olson R, Pusch GD, Olsen GJ, Davis JJ, Disz T, Edwards RA, Gerdes S, Parrello B, Shukla M, Vonstein V, Wattam AR, Xia F, Stevens R. The SEED and the Rapid Annotation of microbial genomes using Subsystems Technology (RAST). Nucleic Acids Res. 2014;42:D206–D214.

Petersen JM, Kemper A, Gruber-Vodicka H, Cardini U, van der Geest M, Kleiner M, Bulgheresi S, Mußmann M, Herbold C, Seah BK, Antony CP, Liu D, Belitz A, Weber M. Chemosynthetic symbionts of marine invertebrate animals are capable of nitrogen fixation. Nat Microbiol. 2016;2:16195.

Pierra M, Godon ETJ-J, Bernet N. Fermentative hydrogen production under moderate halophilic conditions. Int J Hydrogen Energy. 2014;39:7508-7517.

Popov VO, Lamzin VS. NAD^+-dependent formate dehydrogenase. Biochem J. 1994;301:625-643.

Pujalte MJ, Ortigosa M, Urdaci MC, Garay E, Grimont PAD, *Vibrio mytili* sp. nov., from Mussels. Int J Syst Bacteriol. 1993;43:358-362.

Rachman MA, Furutani Y, Nakashimada Y, Kakizono T, Nishio N. Enhanced hydrogen production in altered mixed acid fermentation of glucose by *Enterobacter aerogenes*. J Ferment Bioeng. 1997;83:358-363.

Rameshkumar N, Fukui Y, Sawabe T, Nair S. *Vibrio porteresiae* sp. nov., a diazotrophic bacterium isolated from a mangrove-associated wild rice (Porteresia coarctata Tateoka) Int J Syst Evol Microbiol. 2008;58:1608-1615.

Remy L, Carrière M, Derré-Bobillot A, Martini C, Sanguinetti M, Borezée-Durant E. The *Staphylococcus aureus* Opp1 ABC transporter imports nickel and cobalt in zinc-depleted conditions and contributes to virulence. Mol Microbiol. 2013;87:730-743.

Rittmann BE. The membrane biofilm reactor is a versatile platform for water and wastewater treatment. Environ Eng Res. 2007;12:157-175.

Robinson MD, McCarthy DJ, Smyth GK. edgeR: a Bioconductor package for differential expression analysis of digital gene expression data. Bioinformatics. 2010;26:139-140.

Rodionov DA, Hebbeln P, Gelfand MS, Eitinger T. Comparative and Functional Genomic analysis of Prokarytic Nickel and Cobalt Uptake Transporters: Evidence for a Novel Group of ATP-binding Cassette Transporters. J Bacteriol. 2006;188:317-327.

Rossmann R, Sauter M, Lottspeich F, Böck A. Maturation of the large subunit (HYCE) of *Escherichia coli* hydrogenase 3 requires nickel incorporation followed by C-terminal processing

at Arg537. Eur J Biochem. 1994;220:377-384.

Rossmann R, Maier T, Lottspeich F, Böck A. Characterisation of a protease from *Escherichia coli* involved in hydrogenase maturation. Eur J Biochem. 1995;227:545-550.

Rousvoal S, Groisillier A, Dittami SM, Michel G, Boyen C, Tonon T. Mannitol-1-phosphate dehydrogenase activity in *Ectocarpus siliculosus*, a key role for mannitol synthesis in brown algae. Planta. 2011;233:261-273.

Rowe JL, Starnes GL, Chivers PT. Complex Transcriptional Control Links NikABCDE-Dependent Nickel transport with hydrogenase expression in *Escherichia coli*. J Bacteriol. 2005;187:6317-6323

Ruimy R, Breittmayer V, Elbaze P, Lafay B, Boussemart O, Gauthier M, Christen R. Phylogenetic analysis and assessment of the genera *Vibrio*, *Photobacterium*, *Aeromonas*, and *Plesiomonas* deduced from small-subunit rRNA sequences. Int J Syst Bacteriol. 1994;44:416-426.

Sauter M, Böhm R, Böck A. Mutational analysis of the operon (*hyc*) determining hydrogenase 3 formation in *Escherichia coli*. Mol Microbiol. 1992;6:1523-1532.

Sapra R, Bagramyan K, Adams MWW. A simple energy-conserving system: proton reduction coupled to proton translocation. Proc Natl Acad Sci USA. 2003;100:7545-7550.

Sawabe T, Kita-Tsukamoto K, Thompson FL. Inferring the evolutionary history of vibrios by means of multilocus sequence analysis. J Bacteriol. 2007;189:7932-7936.

Sawabe T, Ogura Y, Matsumura Y, Feng G, Amin AR, Mino S, Nakagawa S, Sawabe T, Kumar R, Fukui Y, Satomi M, Matsushima R, Thompson FL, Gomez-Gil B, Christen R, Maruyama F, Kurokawa K, Hayashi T. Updating the Vibrio clades defined by multilocus sequence phylogeny: proposal of eight new clades, and the description of *Vibrio tritonius* sp. nov. Front Microbiol. 2013;4:414.

Sawers G. The hydrogenases and formate dehydrogenases of *Escherichia coli*. Antonie van

Leeuwenhoek. 1994;66:57-88.

Sawers RG. Formate and its role in hydrogen production in *Escherichia coli*. Biochem Soc Trans. 2005;33:42-46.

Sawers RG, Blokesch M, Böck A. Anaerobic formate and hydrogen metabolism. In Curtiss R, III, Kaper JB, Squires CL, Karp PD, Neidhardt FC, Slauch JM, eds. *Escherichia coli* and *Salmonella*. ASM Press, Washington DC. www.ecosal.org. doi: 10.1128/ecosal.3.5.4. ASM Press. 2004.

Schmidt O, Wüst PK, Hellmuth S, Borst K, Horn MA, Drake HL. Novel [NiFe]- and [FeFe]-Hydrogenase Gene Transcripts Indicative of Active Facultative Aerobes and Obligate Anaerobes in Earthworm Gut Contents. Appl Environ Microbiol. 2011;77:5842-5850.

Self WT, Hasona A, Shanmugam KT. Expression and Regulation of a Silent Operon, hyf, Coding for Hydrogenase 4 Isoenzyme in *Escherichia coli*. J Bacteriol. 2004;186:580-587.

Shieh WY, Chen AL, Chiu HH. *Vibrio aerogenes* sp. nov., a facultatively anaerobic marine bacterium that ferments glucose with gas production. Int J Syst Evol Microbiol. 2000;50:321-329.

Shieh WY, Chen YW, Chaw SM, Chiu HH. *Vibrio ruber* sp. nov., a red, facultatively anaerobic, marine bacterium isolated from sea water. Int J Syst Evol Microbiol. 2003;53:479-484.

Shin JH, Yoon JH, Lee SH, Park TH. Hydrogen production from formic acid in pH-stat fed-batch operation for direct supply to fuel cell. Bioresour Technol. 2010;101:S53-S58.

Sinha P, Pandey A. An evaluative report and challenges for fermentative biohydrogen production. Int J Hydrogen Energy. 2011;36:7460-7478.

Skibinski DA, Golby P, Chang YS, Sargent F, Hoffman R, Harper R, Guest JR, Attwood MM, Berks BC, Andrews SC. Regulation of the Hydrogenase-4 Operon of *Escherichia coli* by the σ^{54}-Dependent Transcriptional Activators FhlA and HyfR. J Bacteriol. 2002;184:6642-6653.

Soboh B, Linder D, Hedderich R. Purification and catalytic properties of a

CO-oxidizing:H_2-evolving enzyme complex from *Carboxydothermus hydrogenoformans*. Eur J Biochem. 2002;269:5712-5721.

Somerville C, Taylor C, Davis SC, Youngs H, Long SP. Feedstocks for lignocellulosic biofuels. Science. 2010;329:790-792.

Sugawara H, Ohyama A, Mori H, Kurokawa K. Microbial Genome Annotation Pipeline (MiGAP) for diverse users. Abstr. 20th Int Conf Genome Inf abstr. 2009;S001:1-2

Taguchi F, Yamada K, Hasegawa K, Taki-Saito T, Hara K. Continuous hydrogen production by *Clostridium* sp. strain no. 2 from cellulose hydrolysate in an aqueous two-phase system. J Ferment Bioeng. 1996;82:80-83.

Takeda H, Yoneyama F, Kawai S, Hashimoto W, Murata K. Bioethanol production from marine biomass alginate by genetically engineered bacteria. Energy Environ Sci. 2011;4:2575-2581.

Tanaka M, Endo S, Kotake F, Al-Saari N, Amin AKMR, Gao F, Mino S, Doi H, Ogura Y, Hayashi T, Suda W, Hattori M, Yumoto I, Sawabe T, Sawabe T, Araki T. *Vibrio aphrogenes* sp. nov., in the Rumoiensis clade isolated from a seaweed. PLoS One. 2017;12:e0180053.

Tanisho S. Bio-hydrogen production technology. In: Notoya M, ed. Seaweed Biofuel. Tokyo: 2011;177-204. In Japanese.

Thompson FL, Gevers D, Thompson CC, Dawyndt P, Hoste B, Munn CB. Phylogeny and molecular identification of vibrios on the basis of multilocus sequence analysis. Appl Environ Microbiol. 2005;71:5107–5115.

Thompson JD, Higgins DG, Gibson TJ. CLUSTAL W: improving the sensitivity of progressive multiple sequence alignment through sequence weighting, position-specific gap penaltiesand weight matrix choice. Nucleic Acids Res. 1994;22:4673-4680.

Thorvaldsdóttir H, Robinson JT, Mesirov JP. Integrative Genomics Viewer (IGV): high-performance genomics data visualization and exploration. Brief Bioinform. 2013;14:178-192.

Treberg JR, Brand MD. A model of the proton translocation mechanism of complex I. J Biol Chem. 2011;286:17579-17584.

Vignais PM, Billoud B, Meyer J. Classification and phylogeny of hydrogenase. FEMS Microbiol Rev. 2001;25:455-501.

Vignais PM, Colbeau A. Molecular biology of microbial hydrogenases. Mol Biol. 2004;6:159-188.

Vignais PM, Billoud B, Occurrence, classification, and biological function of hydrogenases: an overview. Chem Rev. 2007;107:4206-4272.

Waight AB, Love J, Wang DN. Structure and mechanism of a pentameric formate channel. Nat Struct Mol Biol. 2010;17:31-37.

Wang J, Kim YM, Rhee HS, Lee MW, Park JM. Bioethanol production from mannitol by a newly isolated bacterium, *Enterobacter* sp. JMP3. Bioresour Technol. 2013;135:199-206.

Wang Y, Huang Y, Wang J, Cheng C, Huang W, Lu P, Xu YN, Wang P, Yan N, Shi Y. Structure of the formate transporter FocA reveals a pentameric aquaporin-like channel. Nature. 2009;462:467-472.

Wargacki AJ, Leonard E, Win MN, Regitsky DD, Santos CNS, Kim PB, Cooper SR, Raisner RM, Herman A, Sivitz AB, Lakshmanaswamy A, Kashiyama Y, Baker D, Yoshikuni Y. An engineered microbial platform for direct biofuel production from brown macroalgae. Science. 2012;335:308-313.

Yang CC, Iwasaki W. MetaMetaDB: A Database and Analytic System for Investigating Microbial Habitability. PLoS One. 2014;9:e87126.

Yoshida A, Nishimura T, Kawaguchi H, Inui M, Yukawa H. Enhanced hydrogen production from formic acid by formate hydrogen lyase-overexpressing *Escherichia coli* strains. Appl Environ Microbiol. 2005;71:6762-6768.

Yoshida A, Nishimura T, Kawaguchi H, Inui M, Yukawa H. Enhanced hydrogen production from glucose using *ldh*- and *frd*-inactivated *Escherichia coli* strains. Appl Microbiol Biotechnol. 2006;73:67-72.

Yu NY, Wagner JR, Laird MR, Melli G, Rey S, Lo R, Dao P, Sahinalp SC, Ester M, Foster LJ, Brinkman FSL. PSORTb 3.0: improved protein subcellular localization prediction with refined localization subcategories and predictive capabilities for all prokaryotes. Bioinformatics. 2010;26:1608-1615.

Zehr JP, Mellon MT, Zani S. New nitrogen-fixing microorganisms detected in oligotrophic oceans by amplification of Nitrogenase (*nifH*) genes. Appl Environ Microbiol. 1998;64:3444-3450.

Zhang Y, Sievert SM. Pan-genome analyses identify lineage- and niche-specific markers of evolution and adaptation in *Epsilonproteobacteria*. Frontier Microbiol. 2014;5:110.

Zubia M, Payri C, Deslandes E. Alginate, mannitol, phenolic compounds and biological activities of two range-extending brown algae, *Sargassum mangarevense* and *Turbinaria ornata* (Phaeophyta: Fucales), from Tahiti (French Polynesia). J Appl Phycol. 2008;20:1033-1043.

ACKNOWLEDGEMENTS

I would like to express my sincere appreciation to Dr. Tomoo Sawabe, Professor of the Laboratory of Marine Microbiology, Hokkaido University, and Dr. Sayaka Mino, Assistant Professor of the Laboratory of Marine Microbiology, Hokkaido University for their heartfelt guidance and encouragement. I wish to thank Dr. Takao Ojima, Professor of the Laboratory of Marine Molecular Biology, Hokkaido University for his critical review and constructive criticism of this study which has improved this report greatly. I am also thankful to the members of our laboratory, especially Ms. Yoshiko Kawahara, Mr. Kazumichi Satoh, Mr. Sota Mizukoshi Ms. Yuri Amada for their cooperation and successful advice.